Open research issues on
Multi-models for Complex Technological Systems

C. Ciufudean
Dept. of Computers, Automatics and Electronics
University Stefan cel Mare of Suceava
Romania
calin@eed.usv.ro

F. Neri
Dept. of Computer Science
University of Naples "Federico II"
Naples, Italy
nerifil@gmail.com

Abstract - We are going to report here about state of the art works on multi-models for complex technological systems both from the theoretical and practical point of view. A variety of algorithmic approaches (k-mean, dss, etc.) and applicative domains (wind farms, neurological diseases, etc.) are reported to illustrate the extension of the research area.

Keywords: - multi models, control systems, complex technological systems

Introduction

The format of special issues hosted in WSEAS Transactions on Systems is well proved and continues to develop over time [1-15]. The main aim of this special issue "Multi models for complex technological systems" is the presentation of state of the art contributions in the field originating from our community of authors. Despite conventional approaches, Multi-models for Complex Technological Systems are not guided by rigid control algorithms but by flexible event adaptable ones that makes them more vivace and available. All these allow a new design of technological systems dotted with intelligence, autonomous decision making capabilities, and self-diagnosing properties. Heuristics techniques, data mining planning activities, scheduling algorithms, automatic data identification, processing and control represent as many trumps for these new systems` analyzing formalism. This special issue deals with the following issues [16-21]:

- An improved *K*-means algorithm-based aggregation modeling method is proposed for large wind farms. A model is built for a 300 MW wind farm typical of the northern Jiangsu Province in China and simulations performed. The results are compared with simulation results obtained using a single-fan aggregation model and a detailed model. The aggregation method proposed in this study proves to be accurate, fast, and capable of meeting the requirements for output simulation.

- An analysis of the functioning for the heating automation system with hot air blown into an individual dwelling. The structure of the automatic control system for indoor temperature in the dwelling is determined, in which the controller is a thermostat having feature type relay with hysteresis, the conditions related to the evolution of automatic control of the process are specified and the oscillation period of the control system is calculated. The automatic temperature control system model in individual dwelling is established using Simulink and its functioning by simulation in different representative situations is checked.

- Identification of a dynamic behaviour of a through-flow heat exchanger and a design of a self-tuning predictive controller for its control. The designed controller was verified by a real-time control of an experimental laboratory heat exchanger.

- A study on the development and validation un of an Integrated Intelligent System for Parkinson's disease Screening and the system will be extended in the future work for other Neurological Disorders. The system is designed in order to be used by the physician for home monitoring, medical treatment, medical prescriptions, and rehabilitation of the patients. This Decision Support System for Neurological Disorders (NeuroParkinScreen) is among first proposed systems that are cost-efficient and non-invasive.

- New models and concepts for developing smart power grid control systems based on the open standards IEC 61850, IEC 61499 and holonic concepts. Along with the proposed holonic models for different levels of control, we present a simple fault protection application illustrating how the IEC 61499 artifacts can be used for modeling and implementation of IEC 61850 compliant applications.

- A new watermark system for color images which uses the Content Addressable Method. The cover image is divided into a set of clusters which are built using Content Addressable Method. Each cluster is segmented in its turn into a number of portions. In all pixels of a portion a number of bits (3 bits in our study) of the watermark are duplicated. The robustness of our system comes from the fact that it resists to image rotation attacks. The results show that a rotation of any degree does not have any effect on the embedded watermark which can be extracted without any distortion.

Conclusions

We challenge the reader to reveal the development stage of the complex manufacturing systems and to anticipate theirs future evolution in respect to technological and environmental changes. Readers with diverse background like research, academia, industry, etc., can take advantage of this special issue and can shape a new way of analyzing complex technological systems.

Finally before diving into the collected research works [16-21], let us remember the reader that WSEAS Transactions on Systems has broad spectre of Special Issues, e.g. [1-16]. This is has the objective of creating an active and contributing research community around the journal and to present their latest efforts which have achieved wide interest among its members. As a reader of the journal you are invited to take inspiration by the presented papers and to consider to submit your future works to the journal itself.

Enjoy your reading!

References

[1] Volos, C., Neri, F. (2012) An introduction to the special issue: Recent advances in defense systems: Applications, methodology, technology WSEAS Transactions on Systems, 11 (9), pp. 477-478.

[2] Neri, F. (2014) Open research issues on Computational Techniques for Financial Applications. WSEAS Transactions on Systems, 13, in press.

[3] Karthikeyan, P., Neri, F. (2014) Open research issues on Deregulated Electricity Market: Investigation and Solution Methodologies. WSEAS Transactions on Systems, 13, in press.

[4] Panoiu, M., Neri, F. (2014) Open research issues on Modeling, Simulation and Optimization in Electrical Systems. WSEAS Transactions on Systems, 13, in press.

[5] Neri, F. (2014) Open research issues on Advanced Control Methods: Theory and Application. WSEAS Transactions on Systems, 13, in press.

[6] Hájek, P., Neri, F. (2013) An introduction to the special issue on computational techniques for trading systems, time series forecasting, stock market modeling, financial assets modeling WSEAS Transactions on Business and Economics, 10 (4), pp. 201-292.

[7] Azzouzi, M., Neri, F. (2013) An introduction to the special issue on advanced control of energy systems (2013) WSEAS Transactions on Power Systems, 8 (3), p. 103.

[8] Bojkovic, Z., Neri, F.(2013) An introduction to the special issue on advances on interactive multimedia systems. WSEAS Transactions on Systems, 12 (7), pp. 337-338.

[10] Pekař, L., Neri, F. (2013) An introduction to the special issue on advanced control methods: Theory and application (2013) WSEAS Transactions on Systems, 12 (6), pp. 301-303.

[11] Guarnaccia, C., Neri, F. (2013) An introduction to the special issue on recent methods on physical polluting agents and environment modeling and simulation WSEAS Transactions on Systems, 12 (2), pp. 53-54.

[12] Neri, F. (2012) An introduction to the special issue on computational techniques for trading systems, time series forecasting, stock market modeling, and financial assets modeling WSEAS Transactions on Systems, 11 (12), pp. 659-660.

[13] Muntean, M., Neri, F. (2012) Foreword to the special issue on collaborative systems WSEAS Transactions on Systems, 11 (11), p. 617.

[14] Pekař, L., Neri, F. (2012) An introduction to the special issue on time delay systems: Modelling, identification, stability, control and applications. WSEAS Transactions on Systems, 11 (10), pp. 539-540.

[15] Doroshin, A. V., Neri, F. (2014) Open research issues on Nonlinear Dynamics, Dynamical Systems and Processes. WSEAS Transactions on Systems, 13, in press.

[16] Bobal, V., Kubalcik, M., Dostal, P., Novak, J. (2014). Adaptive Predictive Control of Laboratory Heat Exchanger. WSEAS Transactions on Systems, 13, in press.

[17] Tahar Ben Othman, M. (2014). CAM-based Digital Image Watermarking Revisited. WSEAS Transactions on Systems, 13, in press.

[18] Popescu, D. (2014). Specific problems on the operation of the automatic control system of temperature into an individual dwelling. WSEAS Transactions on Systems, 13, in press.

[19] Chiuchisan, I., Geman, O. (2014). An Approach of a Decision Support and Home Monitoring System for Patients with Neurological Disorders using Internet of Things Concepts. WSEAS Transactions on Systems, 13, in press.

[20] Vlad, V., Buzduga, C., Ciufudean, C. (2014). An Approach to Developing Power Grid Control Systems with IEC 61850, IEC 61499 and Holonic Control. WSEAS Transactions on Systems, 13, in press.

[21] Zhang, J., Cheng, H., Tian, S., Yan, D. (2014). Aggregation modeling of large wind farms using an improved K-means algorithm. WSEAS Transactions on Systems, 13, in press.

An Approach of a Decision Support and Home Monitoring System for Patients with Neurological Disorders using Internet of Things Concepts

IULIANA CHIUCHISAN, OANA GEMAN
Faculty of Electrical Engineering and Computer Science
"Stefan cel Mare" Universityof Suceava
13 Universitatii Street, 720229 Suceava, ROMANIA
iulia@eed.usv.ro, geman@eed.usv.ro

Abstract: -The Internet of Things and information and CommunicationTechnologies applied in development of health care systems have reached an evolutionary process. This paper presentsthe development of an integrated intelligent system for Parkinson's disease Screening.The Decision Support and Home Monitoring System aredesigned to assist and support physicians in diagnosis, home monitoring, medical treatment, medical prescriptions, rehabilitation and progress of his patients with Parkinson's disease. The system will be extended in future research for other Neurological Disorders.This paper has an interdisciplinary character and includes areas such as e-Health, Internet of Things, Information and Communication Technologyand Artificial Intelligence with their application in medical domain.

Key-Words: -Health Monitoring, ExpertSystem, Internet of Things, Neurological Disorders, sensors, Artificial Intelligence.

1 Introduction

Worldwide, one billion people are affected by neurological disorders, including 50 million who have epilepsy and 24 million with Alzheimer disease and other neurological diseases [1]. Many neurological disorders affect aperson's functioning resulting in disabilitiesor limited activities.

According to Parkinson disease Foundation [2], in the USA,nearly one million people are living with Parkinson's disease. This disease occurs in approximately 100-250 cases per 100.000 people. In Europe, approximately 1.2 million people with Parkinson's disease have been reported [2].Although there is presently no cureand the cause is still unknown, there are treatment options to manage its symptoms including medication and surgery.Worldwide, it is estimated that four to six million people suffer from the Parkinson's disease and in the USAcomplications from Parkinson's disease are the 14th leading cause of death [3].

Early diagnosis of Neurological Disorders, such as Alzheimer, epilepsy, Parkinson's disease, and other dementias that influence the lives of patients, their families and society, helps them to have a better and healthier life.

As a health-care strategy, screening and rehabilitation of people suffering of neurological disorders aims to achieve optimal functioning, autonomy and self-caring in the interaction with the larger physical, social and economic environments.

The research in the field of information and communication technology has led to the development of a large series of new tools and intelligent devices that can be used inthe field of health services.As the computer-based patient monitoring systemexpands to support medical activities and at-distance monitoring, doctors/medical experts/medical assistantsmust interact with computer systems and use specialized applications in order to assure a better quality of healthservices [4].

Health care applications facilitate exchange of information between doctors and patients or between institutions, reduce costs, extend the scope and reach of medical facilities, and enhance the quality of services.

The new medical devicesare equipped with sensors, actuators, RFID tags, microcontrollers, mobile-communication devices, nano-pumps and more, in order to allow patients, doctors, or other medical specialists to make health monitoring, diagnosis and treatment more personalized, timely and convenient, while also lowering costs of health services.

In this paper we propose a system for monitoring, screening and rehabilitation of patients with Parkinson's disease or other Neurological Disorders, because there is still no reliable screening test for PD early identification.

In section 2, we present some general information aboutheath care systems and their advantages. Section 3 presentsInternet of Things concepts and technologies. In section 4, we describe, in details, the development of the Decision Support and Home Monitoring System for patients with Parkinson's disease andsection 5 provides a conclusion and some future perspectives.

2 Healthcare systems

Advances in computers, telecommunication and network technologiesled to thedevelopment of a revolutionary new paradigm for health care that refers to as *e-Health*, and to the integration of networking capabilities in medical procedures. In the last decades the link between engineering and medicine become closer, and mechanical parts are developed to substitute damaged or missing human parts, micro-devices are used as implants, miniature cameras are utilized to avoid pervasive diagnostic examinations,real-time systems for home monitoring of patients are developed, and intelligent systems are created in order to automatically process medical data and provide support for medical decisions.

Over the past several decades, Information Technology (IT) has produced major breakthroughs in healthcare and has had a great impact on transforming it from in-hospital health services to more advanced at-home healthservices using Internet of Things (IoT) and related technologies (homecare, home monitoring, personal wearable and portable devices etc.).
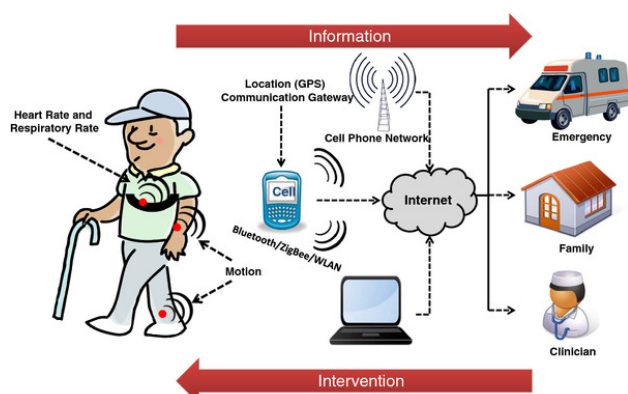

Fig. 1 Health monitoring system

The factors that contribute to the health care transformation include: the nature of new diseases and their treatments; demographic changes; demand for low cost healthcare services; increased availability of complex healthcare medical equipment and services for home monitoring; increased focus on self-care,rehabilitation services and quality of life.

Health care systems are being developed to provide support for medical decisions using health information networks, health portals, tele-health services,electronic health records (EHR), personal wearable and portable communicable systems combined with many other ICT-based tools and applicationsin order to assist physicians/medical experts in disease prevention, diagnosis, treatment, health monitoring and management [4 ÷ 6].

In the case of patient suffering from neurological disorders, such as Alzheimer disease, epilepsy, Parkinson's disease, multiple sclerosis and other dementias influence, the information flow between the patient and doctors is complex and challenging.

In reference [7] is presented a home monitoring that monitor patients with Parkinson's disease who have severe motor fluctuations usinga web-based application and wireless sensors. A web-application was designed in order to provide access to sensor data and that has video conferencing capability to facilitate interaction between patient and physician.

New models for healthmonitoring systems are needed, especially systems that are more patient-centered, not focused primarily on treatment, that assurethe continuity of health services, screening, rehabilitation and prevention on various levels.

3 Internet of Things

Internet of Things canbe viewed „as a global infrastructure for the information society,enabling advanced services by interconnecting (physical and virtual)things based on, existing and evolving, interoperable information andcommunication technologies" [8].

IoT-related healthcare systems are based on the essential definition of IoT as „anetwork of devices that connect directly with each other to capture and share vital data througha secure service layer that connects to a central command and control server in thecloud" [9].

The potential for the convergence of technologies and systems is vast, as can be seen in Figure 2. This development will generate changes in many vertical industries, from health care to manufacturing, from energyto smart buildings and cities [10].

In references [11] ÷ [19] are presented some examples ofcontrol of energy systems such as:

interactive multimedia systems; methods on physical polluting agents and environment modeling and simulation; computational techniques for

trading systems, time series forecasting, stock market modeling, and financial assets modeling;recent advances in defense system.
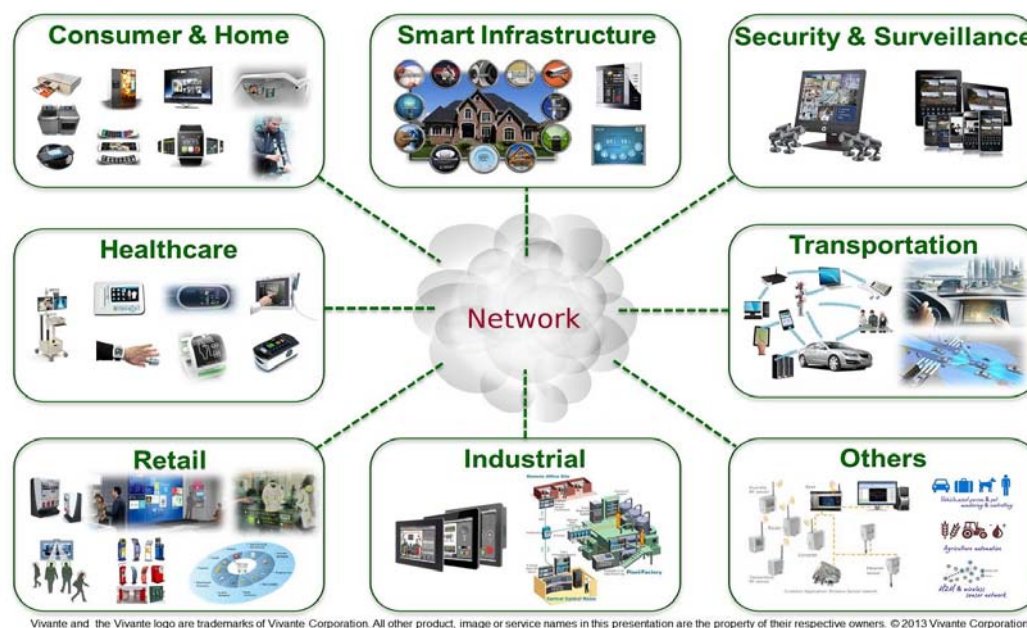

Fig. 2 Internet of Things areas [10]

The IoT offer greater promise in the field of health care, where its principles are already being applied to improve access to healh care services, increase the quality of health services and reduce the cost of thisservices [10].New developments and concepts in ICT lead to innovative smart and portable devices able to identify, locate, sense and connect anytime and anywhere between themselvesleading to a new form of communication and network.

Considering all the medical devices that uses technology for collecting, alaysing, processing, and transmitting data from a system, we can specify that the „Internet of Things" (IoT)concept continues to maturein healthcare domain. Innovative smart devices can collect and share information directly with each other and store it to the cloud, making it possible to collect, record and analyze data faster and more accurately.

In health care field, the possibilities of IoT are so many, because includes systems that facilitate a new concept and support physicians/medical experts/medical assistants and patients in managing the health care process in order to achieve an optimal health status and to avoid a worsening of the illness as long as possible.

4 Decision support and home monitoring system

This paper presentsadecision support system forNeurological Disorders, in particular the Parkinson's disease.This isanexpert system that process tremor data collected from patientswith Parkinson's disease, and alsoassists medical specialists in diagnosis and treatment.

In most cases the estimations are based on the analysis of a large amount of medical history that medical personnel cannot possibly process. Such systems cannot substitute the medical specialist but the information that system provide is extremely useful as an independent source of evidence concerning the correct diagnosis[21].

Although a decision support system is a very complex software system, its operation in the framework of e-Health, as well as the steps typically followed in its design and development, can be generally broken down as illustrated in Figure3.

The information extracted from a patient home monitored and running various medical tests is processed by the doctor in order to reach a conclusion regarding the diagnosis.
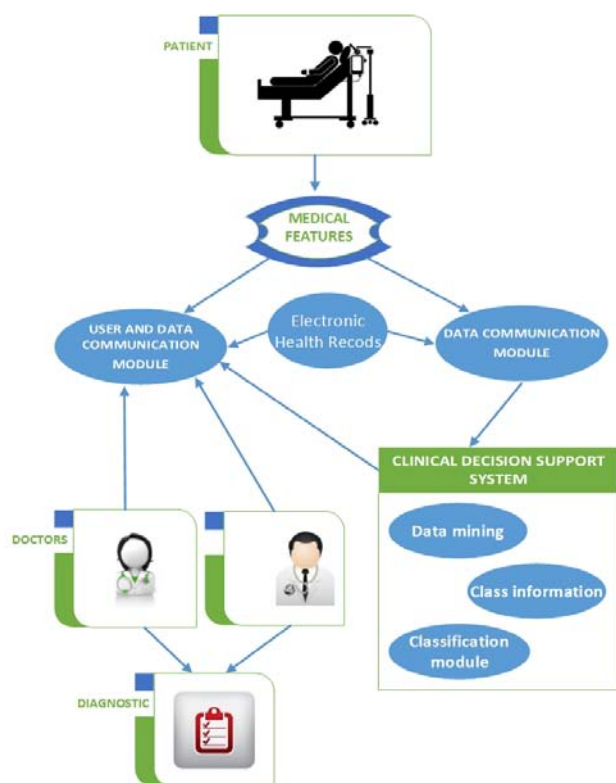
Fig. 3A general architectureof an expertsystem

The collected information could be from a simple body temperature to detailed blood analysis results, MRI images, or, in Parkinson's disease screening, the trajectory of hand movement.

In the process of diagnosis and treatment the doctor may use the networking capabilities offered by the decision support system to retrieve data from distributed electronic health records and/or consult other medical specialists who may be located at different locations [21].

The systemprocess the collected information from patients in order to reach a conclusion regarding a diagnosis and support the medical experts in treatment and home monitoring of patients.The diagnosis is provided by the classification module, which maps available information to one of the known classes of diagnoses. This information about the known classes is either provided manually by human experts or extracted automatically through processing of the medical history contained in the distributed electronic health records by a data mining module.The most important processes in the development of a decision support system arecollecting information regarding the diagnosis classes and classifying of a given case to a diagnosis.

The type of classifier chosen indicates the training methodology.The most applied approaches can be summarized as follows:

- Compare the current case directly to other cases in the medical history, and usesimilarities in order to provide a most probable diagnosis.
- Train different types of Artificial Neural Networks (ANNs), based on medical history, so that data patterns are automatically identified and utilized to provide classification.
- Combine multiple classifiers to minimize the error margin.
- Use a fuzzy system to evaluate the examined case based on information provided by medical experts in the form of simple rules [21].

4.1 Parkinson's disease symptoms

In this paper we present a decision supportsystemfor home monitoring of patients with Parkinson's disease or other Neurological Disorders.

Parkinson's disease is aneurodegenerative brain disorder that progresses slowly, in most cases, and occurs due to loss of a neurotransmitter (dopamine)that induce a slow destruction of neurons responsible for controlling movements.Patients with Parkinson's disease reveal tremor or shaking of a body part, have trouble with moving or walking, postural instability,have rigid and uncontrollable gestures[22], and small handwriting. After many new discoveries and research about the biology of the Parkinson's disease and after almost 200 years since PD was discovered, a diagnosis still depends on identifying the main featuresdescribed by James Parkinson.

The diagnosis of PDrequires a detailed medical history and a physical examination in order to detect the cardinal signs of this disease [23]. The threecardinal signs of Parkinson's disease are resting tremor, rigidity and bradykinesia, from which the first two are essential for PD diagnosis.Thepostural instability is the fourth sign, but occurs late, in disease evolution.

It's a real challenge to develop new methods in order to extract features that can help setting an early diagnosis in case of Parkinson'sdisease or other neurological disorder [22].In Parkinson's disease we can analyze two types of motor symptoms [23]:

- Motor symptoms generated by the diseaseitself and its natural evolution;
- Motorsymptoms generated by complications ofdrugs therapy.

Tremor is usually the first symptom noticed by the patient at rest, although it may be absent in up to 30% of patients. Parkinson's tremor has a regular frequency of 4-6 Hz.The PD tremor has been

observed mainly in the fingers (thumb has a rhythmic movement relative to the index movement associated with "counting money" - "pill rolling") and in the leg movements described as "cycling".

There are two main classifications of tremor:

- Rest tremor that occurs when relevant muscles are not activated
- Actiontremor thatoccurs when relevant muscles are activated,including postural, kinetic, intention and specific tremors.

In 70% of cases, the first symptom isan uncontrollable rhythmic gesture of the hands, head and feetand usually appears at rest when a person's muscles are relaxed, when it is not performing any actions and becomes less evident in progress of the disease [24].

In the research conducted by the Geman O. et al. in [22]÷[26], the physiological information have been combined with time series parameters measured from gait and tremor in order to develop an automatic diagnosis system for Parkinson's disease. The results demonstrate that nonlinear dynamics parameters of gait and tremor signals can be used in PD diagnosis.

4.2System architecture

Our study focuses onthe use of remote tremor measurement devices, data recording, and real-time monitoringin order to help medical specialist in diagnosis. . Remotely located users (physicians and patients) can connect to the database and access information about the patient present condition and his progress, using any device such as PC, laptop, tablets or smartphone. Themeasurements provided by the systemare uploaded and saved on the Internetin order to help medical staff to provide relevant medical counseling and advice to patients according to the measured data

The hardware requirements for the decision support system for home monitoring of patients with Parkinson's disease or other Neurological Disorders can be broken down into three main parts:

1. Smart device that is a special modified mouseequipped with three pressure sensors and an accelerometer sensor;
2. Screening system that includes data acquisition module, tremor data module, feature extraction module using ANN classification algorithms;

this component provides tremor measuring via Bluetooth wireless transmission;
3. Web-based Home Monitoring Portal that allows users access to their personal medical information and medical history andfacilitates interaction betweendoctor and patient.

The general architecture of the decision support system for home monitoring of patients with Parkinson's disease or Neurological Disorder is presented in Figure4.

4.2.1Smartdevice

For the tremor acquisition we propose a low-cost, easy to use, and non-invasive smart device. The main feature of this modified mouse is its motion sensing capability, which allows the users to manipulate items.

This device is a trivial mouse modified for sampling the hand tremor as well as to process the accelerometers signals. This device used for tremor acquisition has mounted, on the bottom ofinside surface, some capacitive sensorsbased on the methodology described in reference [27] and an accelerometer sensor.

The 3-axis accelerometer sensor(ADXL345) [28] collects 3D signalsand acceleration data are transferred via I2C bus to an Acquisition and Processing Unit (APU) that incorporates several registers to set the sensor measurement parameters as the resolution, measurement range, and data rate[27]. The acceleration data are grouped in three 16-bit words and the stream data are acquired by APU, as six 16-bits words and stored in a flash memory. APU was implemented in a microcontroller (ADuC7026)[29] responsible with the managementacquisition.

The results of acquisition and processed data are transferred to a local server via Bluetooth wireless transmission. The convertors (C/N), APU and flash memory are grouped in an Acceleration Sensorial Unit and integrated in our smart device.

The device records both acceleration induced by hand movement and by gravitational force. Therefore, this smart device (modified mouse) is conceived as an intelligent multi-sensors structure dedicated to perform a real time tremor assessment by identifying pathological frequencies of the hand tremor.
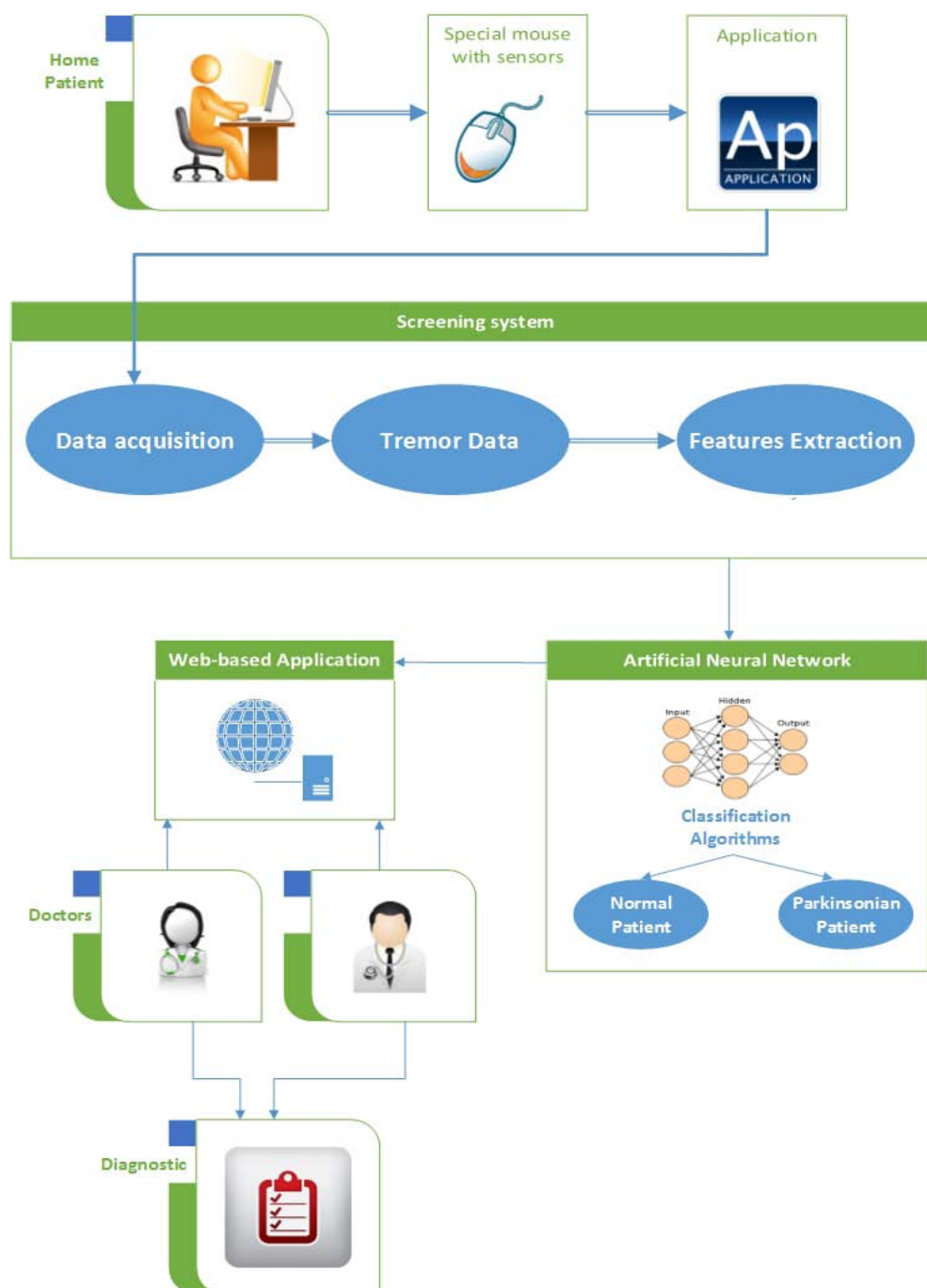
Fig. 4 An overview of architecture of decision support system for home monitoring
of patients with Parkinson's disease

4.2.2 Screening system

In our study, a number of 10 patients with Parkinson's disease (Parkinson's tremor) and 10 normal persons (Normal tremor) were analyzed. All patients are suffering from a moderate or severe postural tremor.

The smart device and PC were connected via Bluetooth™. The application for tremor processing and analysis was developed using Microsoft Visual C, illustrated in Figure5.

The data information was analyzed using nonlinear dynamics tools, and the next steps in our research will consist in feature extraction and classification. We will analyze two types of Artificial Neural Networks (ANN): the Multilayer Perceptron and a Radial Basis Functions Network and the Adaptive Neuro-Fuzzy Classifier, described by O. Geman et al. in references [30]÷[32]. The Artificial Neural Networks can be used to identify a "normal" subject or a "Parkinson" subject (fig. 5).
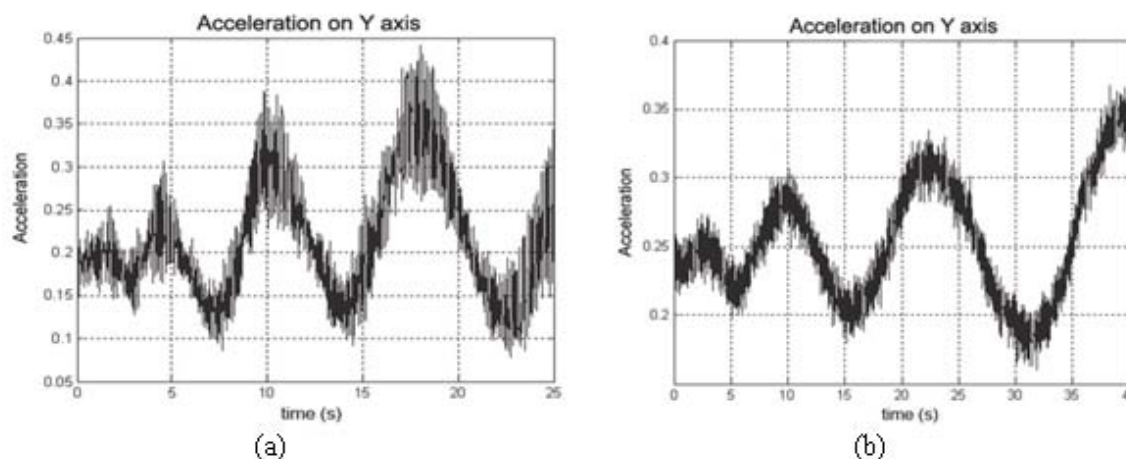
Fig. 5Examples of tremor measurement: (a) Patient with tremor; (b) Normal patient.

More investigations about tremor acquisition and processing techniques in early prediction of Parkinson's disease are presented in references [33] ÷ [35].

4.2.3 Homemonitoring portal

The Web-based Home Monitoring Portal enables the patients to receive health care at home,to stay informed about their current status and progress, to access their own health information, to record the tremor using a smart device, and to contact hisdoctor.PD specialists could access anytime and anywhere the record of the patients' tremor results, increasing the accuracy of diagnosis and improving the quality of healthcare.

Home health monitoring systems of patients with Neurological Disorders has the potential to improve healthcare and provide an efficient and cost effective process. Keeping the patients under observation for a certain period of time in order to evaluate the severity of symptoms helps the differential diagnosis between Parkinson's disease and other similar diseases.

The design of an e-Health portal is a challenging task during to its unique functionality and security requirements. Using HTMLand PHP language, combined with database management with MySQL,wedevelopeda Web-based Home MonitoringPortalwhich includesan expertsystemwhich acquire, analyzeand process data information collected from sensors in orderto support medical specialists in diagnosis and monitoring.

The Home Monitoring Portal facilitates communication in real time between doctor and patients through a friendly User Interface that is accessible at any time and from any device such as PC, tablet or smartphone.

Using this portal, the doctor can analyze and process data received from the patient, and also can prescribe a medical treatment. The patient has access to his personal data and medical history and can communicate with his doctor using text messages or Skype sessions. Users are not required to have sophisticated computer skills in order to use services provided by portal.

Data collected using the above-described system were analyzed, segmented, filtered, and processed using ANN in order to derive features associated with movement characteristics of Parkinson's disease (e.g. the periodic component from 4 to 7 Hz associated with Parkinson's tremor).

Figure 6 presents some screen captures of Home Monitoring Portal for patients with Parkinson's disease or other Neurological Disorders.

5 Conclusions

Combining the Internet of Things and Information and Communication Technology enables the development of health care systems, personalized home management systems. The new methods of collecting patients' assessment and measurement data via wireless transmission, helps the patients to conduct tests on themselves in the comfort of their own homes.

This paper presents the development of an expert system that can be used to gather, analyze, process relevant information for assisting medical specialists in diagnosis of Parkinson's disease. Also a Web-based Home Health Monitoring Portal for patients with Parkinson's disease or other Neurological Disorders is presented.

HOME   ABOUT MD   PATIENTS   NOTES   ACCOUNT

Welcome MD Patrick Guislain!

Doctors

○ **MD Patrick Guislain** - Gent
  ◦ ID card - **Expired on 30.04.2014**
  ◦ Number of patients: **3**
  ◦ Message Sent: **1**
  ◦ Mesage Received: **0**
  ◦ Mesage from board: **1**

List of patients

Search patient in list: [   ]

[1]

No.	Patient name	PIN	Locality	Send message	View message	View patient message	Details
1	Patient 1	1890825030012	Suceava	Send message	Sent message	No received message	Patient details
2	Patient 3	1870508000377	Gent	Send message	No message sent	No received message	Patient details
3	Patient 4	1870508000312	Gent	Send message	No message sent	No received message	Patient details

[1]

Add recipe for Patient 1

Drug name	Quantity	
[ ]	No. quantity	Add drug

Search drug into patient recipe:		Search drug into stock:	

List of patient medication

No.	Name	Quantity	Date	Return
1	Nurofen Forte	1	2014-05-06	Return
2	Paracetamol	2	2014-05-06	Return
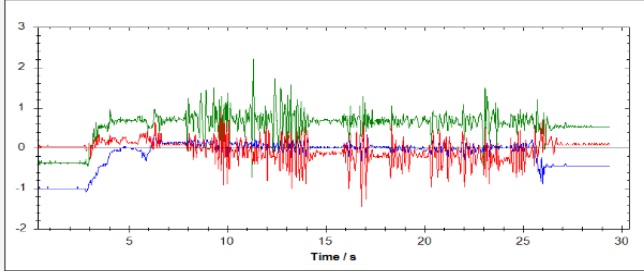
Add medication to patient

No.	Name	Quantity	Add
1	Nurofen Forte	14	Add
2	Paracetamol	8	Add

Export to PDF
Recipe: Print recipe
Medical history: Print medical history

Record tremor

Application	Download application	User manual

ParkinWii - Data collection   DOWNLOAD ▼

Fig. 6 Screen captures ofDecision Support and Home Monitoring System
for patients withParkinson's disease

In the development of the described decision support system we used Information and Communication Technology (ICT) and Internet of Things (IoT) concepts such as: sensors that collect patient data; microcontrollers that process, analyze and wirelessly communicate the data; health care gateways through which sensor data is further analyzed and sent to the Internet.

Acknowledgement

References:
[1] World Health Organization,*Neurological Disorders: Public Health Challenges*, available at http://www.who.int, 2014.
[2] National Parkinson Foundation, available at http://www.parkinson.org, 2014.
[3] Parkinson's Disease Foundation, available at http://www.pdf.org, 2014.
[4] Tan, J., *E-Health Care Information Systems*, Jossey-Bass Press, 2005.
[5] Koch, S., Home telehealth-current state and future trends, *International Journal of Medical Informatics*, 75(8), 2006.
[6] Pepe, G., Frumento, E.,Garlaschelli, A., A service for remote screening of physiological data and follow up of patients using a home gateway and domestic wireless technologies, *Medical and Care Compunetics1*, IOSPress, Amsterdam, 2004.
[7] Patel, S., Borrong, C., et al., Home Monitoring of Patients with Parkinson's Disease via Wearable Technology and a Web-based Application, *International Conference of the IEEE EMBS*, Argentina, 2010.
[8] Vermesan, O.,Friess, P., Furness, A., *The Internet of Things 2012 New Horizons*, ISBN 978-0-9553707-9–3, published in Halifax, UK, 2012, pp. 22-32.
[9] Niewolny, D., How the Internet of Things is revolutionizing healthcare, *FreescaleSemiconductor*, available at http://www.freescale.com/healthcare, 2013.
[10] Vermesan,O., Friess,P., *Internet of Things: Converging Technologies for Smart Environments and Integrated Ecosystems*, River Publishers, Denmark, 2013.
[11] Hajek, P., Neri, F., An introduction to the special issue on computational techniques for trading systems, time series forecasting, stock market modeling, financial assets modeling,*WSEAS Transactions on Business and Economics*, 10 (4), 2013, pp. 201-292.
[12] Azzouzi, M., Neri, F., An introduction to the special issue on advanced control of energy systems,*WSEAS Transactions on Power Systems*, 8 (3), 2013, p. 103.
[13] Bojkovic, Z., Neri, F., An introduction to the special issue on advances on interactive multimedia systems,*WSEAS Transactions on Systems*, 12 (7), 2013, pp. 337-338.
[14] Pekar, L., Neri, F., An introduction to the special issue on advanced control methods: Theory and application,*WSEAS Transactions on Systems*, 12 (6), 2013, pp. 301-303.
[15] Guarnaccia, C., Neri, F. An introduction to the special issue on recent methods on physical polluting agents and environment modeling and simulation,*WSEAS Transactions on Systems*, 12 (2), 2013, pp. 53-54.
[16] Neri, F., An introduction to the special issue on computational techniques for trading systems, time series forecasting, stock market modeling, and financial assets modeling,*WSEAS Transactions on Systems*, 11 (12), 2012, pp. 659-660.
[17] Muntean, M., Neri, F., Foreword to the special issue on collaborative systems WSEAS Transactions on Systems, 11 (11), 2012, p. 617.
[18] Pekar, L., Neri, F., An introduction to the special issue on time delay systems: Modelling, identification, stability, control and applications,*WSEAS Transactions on Systems*, 11 (10), 2012, pp. 539-540.
[19] Volos, C., Neri, F., An introduction to the special issue: Recent advances in defense systems: Applications, methodology, technology,*WSEAS Transactions on Systems*, 11 (9), 2012, pp. 477-478.
[20] Vivante Internet of Things (IoT) Solutions, available at http://bensontao.wordpress.com /2013/10/06/ vivante-internet-of-things, 2014.
[21] Maglogiannis,I. G., Karpouzis,K.,Wallace,M.,*Image and Signal Processing for Networked E-Health*

Applications, Morgan & Claypool Publishers, 2006.

[22] Geman, O., Screening and Rehabilitation System for patients with Parkinson's disease, *Advances in Biomedicine and Health Science Series*, WSEAS Press, Brasov, 2013.

[23] Geman, O., Sanei, S., Chiuchisan, I., Graur, A., Prochazka, A., Vysata, O., Towards an Inclusive Parkinson's Screening System, *17th International Conference on System Theory, Control and Computing*, in press, September, Sinaia, 2014.

[24] Geman, O., Costin, H., Parkinson's Disease Predictionbased on Multistate Markov Models, *International Journal of Computers Communications & Control*, Vol. 8, No. 4, 2013, pp. 525-537.

[25] Geman, O., Costin, H., Tremor and Gait Screening and Rehabilitation System for Patients With Neurodegenerative Disorders, *Automatic Control and Computer Science*, Vol. LIX (LXIII) Issue 2, ISSN 1220-2169, Iasi, 2013.

[26] Geman, O., Turcu, C.O., Partitioning Methods used in DBS Treatments Analysis Results, *ISI Proceedings of the 2011 International JointConference on Neural Networks*, ISSN 2161-4393, California, USA, 2011, pp. 1788-1793.

[27] Hagan, M., Acquisition and Analysis of Tremor Signals using Force and Accelerometer Sensors, *The 20th European Signal Processing Conference (EUSIPCO 2012)*, ISSN 2076-1465, 2012, pp. 1728-1732.

[28] Digital Accelerometer,*ADXL345 datasheet*, available at http://www.analog.com, 2014

[29] Precision Analog Microcontroller,*ADUC7026 Datasheet*, available at http://www.analog.com.

[30] Geman, O., Costin, H., Automatic Assessing of Tremor Severity Using Nonlinear Dynamics, Artificial Neural Networks and Neuro-Fuzzy Classifier, *Advances in Electrical and Computer Engineering*, Vol. 14, No.1, 2014, pp. 133-138.

[31] Geman, O., Turcu, C.O., Graur, A., Parkinson's disease Screening Tools using a Fuzzy Expert System, *Advances in Electrical and Computer Engineering*, Vol. 13, No. 1, ISSN 1582-7445, 2013, pp. 41-46.

[32] Geman, O., Nonlinear Dynamics, Artificial Neural Networks and Neuro-Fuzzy Classifier for Automatic Assessing Tremor Severity, *Proceedings of the IEEE International Conference on E-Health and Bioengineering*, ISBN978-1-4799-2372-4, Iasi, 2013.

[33] Geman, O., Zamfir, C., Using wavelet for early detection of pathological tremor, *The 20th European Signal Processing Conference (EUSIPCO 2012)*, ISSN 2076-1465, Bucharest, 2012, pp. 1723-1727.

[34] Teodorescu, H-N., Chelaru, M., Kandela, A., Tofan, I., Irimia, M., Fuzzy methods in tremor assessment, prediction, and rehabilitation, *Artificial Intelligence in Medicine*, Vol. 21, No. 1-3, 2001, pp. 107-130.

[35] Dobrea, D-M., Teodorescu, H-N., A New Type of Non-Contact 2D Multimodal Interface to Track and Acquire Hand Position and Tremor Signal, *Proceedings of the 8th Baltic Electronics Conference*, 2002, pp. 359-362.

Adaptive Predictive Control of Laboratory Heat Exchanger

VLADIMÍR BOBÁL[1,2], MAREK KUBALČÍK[2], PETR DOSTÁL[1,2], JAKUB NOVÁK[2]
[1]Centre of Polymer Systems, University Institute
[2]Department of Process Control, Faculty of Applied Informatics, Tomas Bata University in Zlín
T. G. Masaryka 5555, 760 01 Zlín
CZECH REPUBLIC
bobal@fai.utb.cz, kubalcik@fai.utb.cz, dostalp@fai.utb.cz, http://web.fai.utb.cz/cs/docs/CV_english.pdf

Abstract: - Heat exchange belongs to the class of basic thermal processes which occur in a range of industrial technologies, particularly in the energetic, chemical, polymer and rubber industry. The process of heat exchange is often implemented by through-flow heat exchangers. It is apparent that for an exact theoretical description of dynamics of heat exchange processes it is necessary to use partial differential equations. Heat exchange is namely a process with distributed parameters. It is also necessary to take into account its nonlinear and stochastic character. In spite of these facts, most of thermal equipment is controlled by digital modifications of PID controllers at present. This paper deals with identification of a dynamic behaviour of a through-flow heat exchanger and a design of a self-tuning predictive controller for its control. The designed controller was verified by a real-time control of an experimental laboratory heat exchanger.

Key-Words: - Model predictive control; Adaptive control; CARIMA model; ARX model; Least squares method; Process identification; Time-delay system; Heat exchanger

1 Introduction

A heat exchanger is a specialized device that exchanges heat between two streams, heating one and cooling the other. Heat exchangers are divided into three basic groups: *direct contact exchangers, recuperators* and *regenerators*. Recuperating (through-flow) heater exchangers are surely used in industrial practice. Their principle consists in following: the hot and cold fluids are separated by a wall and heat is transferred by conduction through the wall. This class includes double pipe (hairpin), shell and tube, and compact (plate and frame, etc.) exchangers. Heat exchangers are typical systems with time-delay (dead-time) and therefore their good function is dependent on the design and implementation of the optimal control system.

The problem of control time-delay processes can be solved by several control methods (e.g. using PID controllers, time-delay compensators, model predictive control techniques). In practice the implementation of the time-delay controllers on analog equipment was difficult. In spite of the fact that all these algorithms are implemented in digital platforms, most of the works analyze only the continuous case (see e.g. [1 - 6]).

When a high performance of the control process is desired or the relative time-delay is very large, a usage of the predictive control strategy is one of possible approaches to control processes with reaching of the good control quality. The predictive control strategy includes a model of the process in the structure of the controller. The first time-delay compensation algorithm was proposed by Smith in 1957 [7]. This control algorithm known as the Smith Predictor (SP) contained a dynamic model of the time-delay process and it can be considered as the first model predictive algorithm. First versions of Smith Predictors were designed in the continuous-time modifications. Because most of modern controllers are implemented on digital platforms, the discrete versions of the time-delay controllers are more suitable for time-delay compensation in industrial practice. Most authors designed the digital time-delay compensators with fixed parameters [8-10]. However, the time-delay compensators are more sensitive to process parameter variations and therefore require an auto-tuning or adaptive (self-tuning) approach in many practical applications. Two adaptive modifications of the digital Smith Predictors are designed in [11, 12] and implemented into MATLAB/SIMULINK Toolbox [13, 15, 16].

One of the possible approaches to control processes with time-delay is Model Predictive Control (MPC) [16-21] method. MPC is becoming

increasingly occurring in industrial process control where time-delays are component parts of the system. However, an accurate appropriate model of the process is required to ensure the benefits of MPC.

The aim of the paper is design of an adaptive predictive controller for control of a laboratory heat exchanger. The second-order model with time-delay was used for the recursive identification and it was also applied in the control part of the GPC (Generalized Predictive Control) algorithm [16, 17].

The paper is organized in the following way. The experimental laboratory heat equipment containing the heat exchanger is described in Section 2. The basic principle of MPC is presented in Section 3. Problems of implementation of GPC method is described in Section 4. The computation of the predictor for time-delay systems is derived in Section 5. The experimental identification of the laboratory heat exchanger is introduced in Section 6. The implementation of the predictive control algorithm for a control of the laboratory heat exchanger in real-time conditions is demonstrated in Section 7. Section 8 concludes the paper.
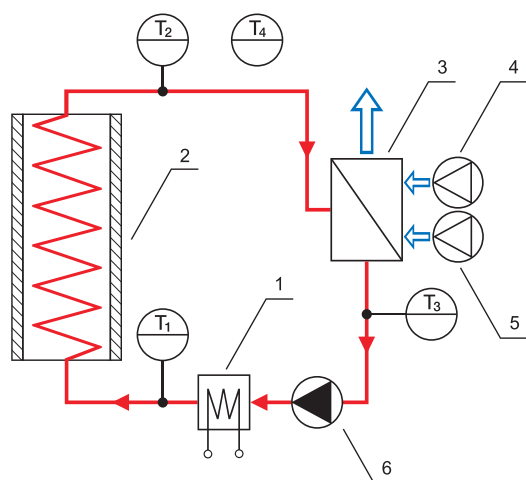
2   Experimental Laboratory Heat Equipment

Fig. 1.Scheme of laboratory heat equipment

A scheme of the laboratory heat equipment [22] is depicted in Fig. 1. The heat transferring fluid (e.g. water) is transported using a continuously controllable DC pump (6) into a flow heater (1) with max. power of 750 W. The temperature of a fluid at the heater output T_1 is measured by a platinum thermometer. Warmed liquid then goes through a 15 meters long insulated coiled pipeline (2) which causes the significant delay (20 – 200 s) in the system. The air-water heat exchanger (3) with two

cooling fans (4, 5) represents a heat-consuming appliance. The speed of the first fan can be continuously adjusted, whereas the second one is of on/off type. Input and output temperatures of the cooler are measured again by platinum thermometers as T_2, respective T_3. The platinum thermometer T_4 is dedicated for measurement of the outdoor-air temperature. The laboratory heat equipment is connected to a standard PC via technological multifunction I/O card MF 624. This card is designed for the need of connecting PC compatible computers to real world signals. The card is designed for standard data acquisition, control applications and optimized for use with Real Time Toolbox for SIMULINK. The MATLAB/SIMULINK environment was used for all monitoring and control functions.

3 Principle of MPC

Model Predictive Control attracts considerable research attention because of its unparalleled advantages. These include:

- Applicability to a broad class of systems and industrial applications.
- Computational feasibility.
- Systematic approach to obtain a closed-loop control and guaranteed stability.
- Ability to handle hard constraints on the control as well as the system states.
- Good tracking performance.
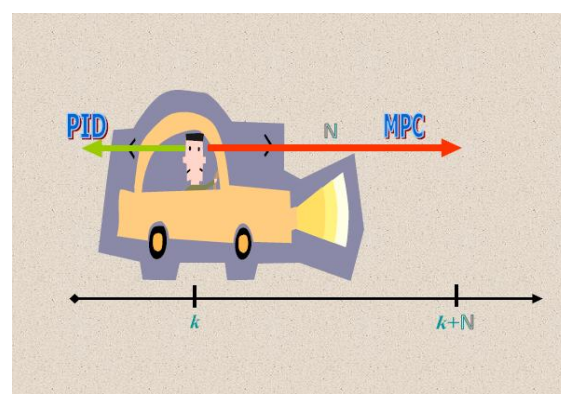- Robustness with respect to system modeling uncertainty as well as external disturbances.

Fig. 2. Difference between the MPC and PID control

The MPC strategy performs the optimization of a performance index with respect to some future control sequence, using predictions of the output signal based on a process model, coping with amplitude constraints on inputs, outputs and states.

For a quick comparison of MPC and traditional control scheme, such as PID control, Fig. 2 shows the difference between the MPC and PID control schemes in which "anticipating the future" is desirable while a PID controller only has capacity of reacting to the past behaviours. The MPC algorithm is very similar to the control strategy used in driving a car [23].

At current time k, the driver knows the desired reference trajectory for a finite control horizon, say $(k, k + N)$, and the taking into account the car characteristics to decide which control actions (accelerator, brakes, and steering) to take in order to follow the desired trajectory. Only the first control action is adopted as the current control law, and the procedure is then repeated over the next time horizon, say $(k + 1, k + 1 + N)$. The term "*receding horizon*" is introduced, since the horizon recedes as time proceeds.
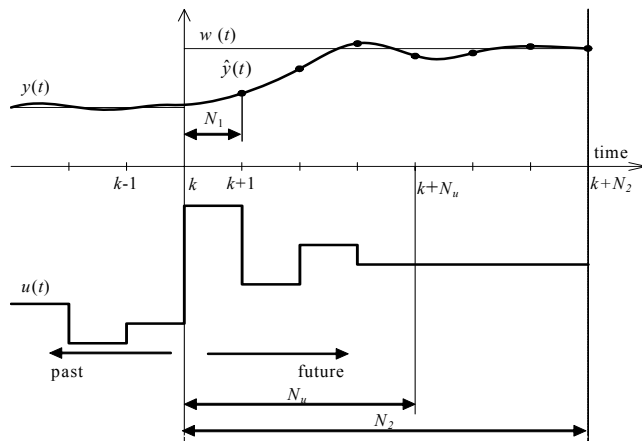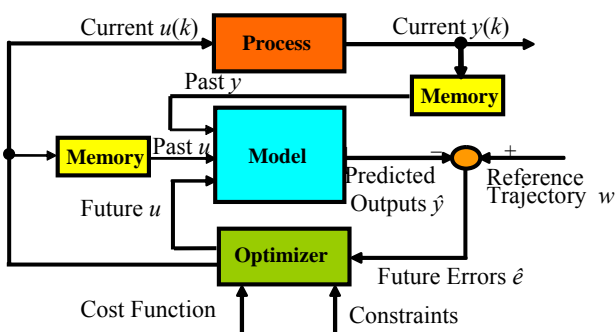

Fig. 3. Principle of MPC

Fig. 4. Block diagram of MPC

4 MPC Based on Minimization of Quadratic Criterion

The designed control algorithm is based on the GPC method. The standard cost function used in GPC contains quadratic terms of control error and control increments on a finite horizon into the future [20, 21]

$$J = \sum_{i=N_1}^{N_2} \left[\hat{y}(k+i) - w(k+i) \right]^2 + \sum_{i=1}^{N_u} \left[\lambda(i) \Delta u(k+i-1) \right]^2 \tag{1}$$

where $\hat{y}(k+i)$ is the process output of i steps in the future predicted on the base of information available upon the time k, $w(k+i)$ is the sequence of the reference signal and $\Delta u(k+i-1)$ is the sequence of the future increments of the manipulated variable that have to be calculated. Parameters N_1, N_2 and N_u are called minimum, maximum and control horizon. The parameter $\lambda(i)$ is a sequence which affects future behaviour of the controlled process. The output of the model (predictor) is computed as the sum of the free response y_0 and forced response y_n

$$\hat{y} = y_0 + y_n \tag{2}$$

The free response is that part of the prediction, which is determined by past values of the manipulated variable and past values of the systems output. The forced response is determined by future increments of the manipulated variable and is computed as the multiplication of the matrix G (Jacobian Matrix of the model) and the vector of future control increments Δu, which is generally a priori unknown

$$y_n = G\Delta u \tag{3}$$

where

$$G = \begin{bmatrix} g_1 & 0 & 0 & \cdots & 0 \\ g_2 & g_1 & 0 & \cdots & 0 \\ g_3 & g_2 & g_1 & \cdots & 0 \\ \vdots & \vdots & \vdots & \ddots & \vdots \\ g_{N_2} & g_{N_2-1} & g_{N_2-2} & \cdots & g_{N_2-N_u+1} \end{bmatrix} \tag{4}$$

is matrix containing values of the step sequence.

It follows from (2) and (3) that the predictor in a vector form is given by

$$\hat{y} = G\Delta u + y_0 \tag{5}$$

The cost function (1) can be modified to the form

$$J = (\hat{y} - w)^T (\hat{y} - w) + \lambda \Delta u^T \Delta u =$$
$$= (G\Delta u + y_0 - w)^T (G\Delta u + y_0 - w) + \lambda \Delta u^T \Delta u \tag{6}$$

Minimisation of the cost function (6) now becomes a direct problem of linear algebra. The solution in an unconstrained case can be found by setting partial derivative of J with respect to Δu as zero and yields

$$\Delta u = \left(G^T G + \lambda I \right)^{-1} G^T \left(w - y_0 \right) \qquad (7)$$

Equation (7) gives the whole trajectory of the future increments of the manipulated variable and such is an open-loop strategy. To close the loop, only the first element is applied to the system and the whole algorithm is recomputed at time $k+1$. If we denote the first row of the matrix $\left(G^T G + \lambda I \right)^{-1} G^T$ as K then the actual increment of the manipulated variable can be calculated as

$$\Delta u(k) = K \left(w - y_0 \right) \qquad (8)$$

5 Computation of Predictor

An important task is computation of predictions for arbitrary prediction and control horizons. Dynamics of most of processes requires horizons of length where it is not possible to compute predictions in a simple straightforward way. Recursive expressions for computation of the free response and the matrix G in each sampling period had to be derived. There are several different ways of deriving the prediction equations for transfer function models. Some papers make use of Diophantine equations to form the prediction equations [20]. In [19] matrix methods are used to compute predictions. We derived a method for recursive computation of both the free response and the matrix of the dynamics [24].

Computation of the predictor for the time-delay system can be obtained by modification of the predictor for the corresponding system without a time-delay. At first we will consider the second order system without time-delay and then we will modify the computation of predictions for the time-delay system.

5.1 Second Order System without Time-Delay

The deterministic model is described by the discrete transfer function

$$G\left(z^{-1}\right) = \frac{B\left(z^{-1}\right)}{A\left(z^{-1}\right)} = \frac{b_1 z^{-1} + b_2 z^{-2}}{1 + a_1 z^{-1} + a_2 z^{-2}} \qquad (9)$$

Model (10) can be also written in the form

$$A\left(z^{-1}\right) y(k) = B\left(z^{-1}\right) u(k) \qquad (10)$$

A widely used model in GPC is the CARIMA model which can be obtained from the nominal model (11) by adding a disturbance model

$$A\left(z^{-1}\right) y(k) = B\left(z^{-1}\right) u(k) + \frac{C\left(z^{-1}\right)}{\Delta} n_c(k) \qquad (11)$$

where $n_c(k)$ is a non-measurable random disturbance that is assumed to have zero mean value, constant covariance and $\Delta = 1 - z^{-1}$. Inverted Δ is then an integrator. The difference equation of the second order CARIMA model without the unknown term $n_c(k)$ can be expressed as

$$y(k) = \left(1 - a_1\right) y(k-1) + \left(a_1 - a_2\right) y(k-2)$$
$$+ a_2 y(k-3) + b_1 \Delta u(k-1) + b_2 \Delta u(k-2) \qquad (12)$$

It was necessary to compute three step-ahead predictions in straightforward way by establishing of lower predictions to higher predictions. The model order defines that computation of one step-ahead prediction is based on three past values of the system output. The three step-ahead predictions are in detail derived in [25] and their matrix equation is

$$
\begin{bmatrix} \hat{y}(k+1) \\ \hat{y}(k+2) \\ \hat{y}(k+3) \end{bmatrix}
=
\begin{bmatrix} g_1 & 0 \\ g_2 & g_1 \\ g_3 & g_2 \end{bmatrix}
\begin{bmatrix} \Delta u(k) \\ \Delta u(k+1) \end{bmatrix}
+
\begin{bmatrix} p_{11} & p_{12} & p_{13} & p_{14} \\ p_{21} & p_{22} & p_{23} & p_{24} \\ p_{31} & p_{32} & p_{33} & p_{34} \end{bmatrix}
\begin{bmatrix} y(k) \\ y(k-1) \\ y(k-2) \\ \Delta u(k-1) \end{bmatrix}
$$

$$
=
\begin{bmatrix} b_1 & 0 \\ b_1(1-a_1)+b_2 & b_1 \\ (a_1-a_2)b_1+(1-a_1)^2 b_1+(1-a_1)b_2 & b_1(1-a_1)+b_2 \end{bmatrix}
\begin{bmatrix} \Delta u(k) \\ \Delta u(k+1) \end{bmatrix}
$$

$$
+
\begin{bmatrix} (1-a_1) & (a_1-a_2) \\ (1-a_1)^2+(a_1-a_2) & (1-a_1)(a_1-a_2)+a_2 \\ (1-a_1)^3+2(1-a_1)(a_1-a_2)+a_2 & (1-a_1)^2(a_1-a_2)+a_2(1-a_1)+(a_1-a_2)^2 \end{bmatrix}
$$

$$
\left.
\begin{matrix} a_2 & b_2 \\ a_2(1-a_1) & b_2(1-a_1) \\ a_2(1-a_1)^2+(a_1-a_2)a_2 & b_2(1-a_1)^2+(a_1-a_2)b_2 \end{matrix}
\right]
\begin{bmatrix} y(k) \\ y(k-1) \\ y(k-2) \\ \Delta u(k-1) \end{bmatrix}
\qquad (13)
$$

It is possible to divide computation of the predictions to recursion of the free response and recursion of the matrix of the dynamics. Based on the three previous predictions it is repeatedly computed the next row of the free response matrix in the following way:

$$
\begin{aligned}
p_{41} &= \left(1 - a_1\right) p_{31} + \left(a_1 - a_2\right) p_{21} + a_2 p_{11} \\
p_{42} &= \left(1 - a_1\right) p_{32} + \left(a_1 - a_2\right) p_{22} + a_2 p_{12} \\
p_{43} &= \left(1 - a_1\right) p_{33} + \left(a_1 - a_2\right) p_{23} + a_2 p_{13} \\
p_{44} &= \left(1 - a_1\right) p_{34} + \left(a_1 - a_2\right) p_{24} + a_2 p_{14}
\end{aligned}
\qquad (14)
$$

The first row of the matrix is omitted in the next step and further prediction is computed based on the three last rows including the one computed in the previous step. This procedure is cyclically repeated. It is possible to compute an arbitrary number of rows of the matrix.

The recursion of the dynamics matrix is similar. The next element of the first column is repeatedly computed in the same way as in the previous case and the remaining columns are shifted to form a lower triangular matrix in the way which is obvious from the equation (14). This procedure is performed repeatedly until the prediction horizon is achieved. If the control horizon is lower than the prediction horizon a number of columns in the matrix is reduced. Computation of the new element is performed as follows:

$$g_4 = (1 - a_1) g_3 + (a_1 - a_2) g_2 + a_2 g_1 \qquad (15)$$

5.2 Second Order System with Time-Delay

The nominal second order model with d steps of time-delay is considered as

$$G(z^{-1}) = \frac{B(z^{-1})}{A(z^{-1})} z^{-d} = \frac{b_1 z^{-1} + b_2 z^{-2}}{1 + a_1 z^{-1} + a_2 z^{-2}} z^{-d} \qquad (16)$$

where d is a number of time-delay steps.

The CARIMA model for time-delay system without the unknown term $n_c(k)$ takes the form

$$\Delta A(z^{-1}) y(k) = z^{-d} B(z^{-1}) \Delta u(k) \qquad (17)$$

In order to compute the control action it is necessary to determine the predictions from $d+1$ to $d+N_2$. The predictor (13) is then modified for an arbitrary number of time delay steps to

$$
\begin{bmatrix} \hat{y}(k+3) \\ \hat{y}(k+4) \\ \hat{y}(k+5) \end{bmatrix} =
\begin{bmatrix} p_{(1+d)1} & p_{(1+d)2} & p_{(1+d)3} \\ p_{(2+d)1} & p_{(2+d)2} & p_{(2+d)3} \\ p_{(3+d)1} & p_{(3+d)2} & p_{(3+d)3} \end{bmatrix}
\begin{bmatrix} y(k) \\ y(k-1) \\ y(k-2) \end{bmatrix}
$$
$$
+ \begin{bmatrix} g_1 & 0 \\ g_2 & g_1 \\ g_3 & g_2 \end{bmatrix}
\begin{bmatrix} \Delta u(k) \\ \Delta u(k+1) \end{bmatrix} \qquad (18)
$$
$$
+ \begin{bmatrix} g_{1+d-1} & g_{2+d-1} & p_{(1+d)4} \\ g_{2+d-1} & g_{3+d-1} & p_{(2+d)4} \\ g_{3+d-1} & g_{4+d-1} & p_{(3+d)4} \end{bmatrix}
\begin{bmatrix} \Delta u(k-1) \\ \Delta u(k-2) \\ \Delta u(k-3) \end{bmatrix}
$$

Recursive computation of the matrices is analogical to the recursive computation described for the second order system without time-delay [26].

6 Identification of Heat Exchanger

The heat exchanger has been identified using off-line methods (for simulation verification of the GPC algorithms and determination of the initial model parameter estimates) and recursive (on-line) method which was used in the adaptive GPC. Static and dynamic models of the laboratory heat exchanger were obtained from input (the power of a flow heater P [W]) and output (the temperature T_2 [°C] of the cooler) data of the process (see Fig. 1).

6.1 Off-Line Process Identification

The number of time delay steps d is either approximately known on the basis of *a priori* information or it can be obtained by an off-line identification using the least squares method (LSM) [27]

$$\hat{\boldsymbol{\Theta}} = (\boldsymbol{F}^T \boldsymbol{F})^{-1} \boldsymbol{F}^T \boldsymbol{y} \qquad (19)$$

where

$$\hat{\boldsymbol{\Theta}}^T = \begin{bmatrix} \hat{a}_1 & \hat{a}_2 & \cdots & \hat{a}_n & \hat{b}_1 & \hat{b}_2 & \cdots & \hat{b}_n \end{bmatrix} \qquad (20)$$

is the vector of parameter model estimates of dimension ($2n$),

$$
\boldsymbol{F} = \begin{bmatrix}
-y(n+d) & -y(n+d-1) & \cdots & -y(d+1) \\
-y(n+d+1) & -y(n+d) & \cdots & -y(d+2) \\
\vdots & \vdots & \cdots & \vdots \\
-y(N-1) & -y(N-2) & \cdots & -y(N-n) \\
u(n) & u(n-1) & \cdots & u(1) \\
u(n+1) & u(n) & \cdots & u(2) \\
\vdots & \vdots & \cdots & \vdots \\
u(N-d-1) & u(N-d-2) & \cdots & u(N-d-n)
\end{bmatrix} \qquad (21)
$$

is the data matrix of dimension (N-n-d, $2n$) and

$$\boldsymbol{y}^T = \begin{bmatrix} y(n+d+1) & y(n+d+2) & \cdots & y(N) \end{bmatrix} \qquad (22)$$

is the output vector of dimension (N-n-d).). N is the number of samples of measured input and output data, n is the model order [12].

Consider that model (16) is the deterministic part of the stochastic process described by the ARX (regression) model

$$y(k) = -a_1 y(k-1) - a_2 y(k-2) +$$
$$+ b_1 y(k-1-d) + b_2 y(k-2-d) + n_c(k) \quad (23)$$

where $n_c(k)$ is the random non-measurable component. The vector of parameter model estimates is computed by solving equation (19)

$$\hat{\boldsymbol{\Theta}}^T(k) = \begin{bmatrix} \hat{a}_1 & \hat{a}_2 & \hat{b}_1 & \hat{b}_2 \end{bmatrix} \quad (24)$$

and is used for computation of the prediction output

$$\hat{y}(k) = -\hat{a}_1 y(k-1) - \hat{a}_2 y(k-2) +$$
$$\hat{b}_1 u(k-1-d) + \hat{b}_2 u(k-2-d) \quad (25)$$

The quality of identification can be considered according to error, i.e. the deviation

$$\hat{e}(k) = y(k) - \hat{y}(k) \quad (26)$$

In this paper, the error was used for suitable choice of the time-delay dT_0. The LSM algorithm (19) − (22) is computed for several time-delays dT_0 and the suitable time-delay is chosen according to quality of identification based on the prediction error (26).

Except LSM the MATLAB function from the Optimization Toolbox

$$x = \text{fminsearch}('name\_fce', x_0) \quad (27)$$

was also used for the off-line process identification. This function find minimum of an unconstrained multivariable function using derivative-free method. Algorithm "fminsearch" uses the simplex search method of [28]. This is a direct search method that does not use numerical or analytic gradients.

It is obvious that the quality of time-delay systems identification is very dependent on the choice of a suitable input exciting signal $u(k)$. Therefore the MATLAB function from the System Identification Toolbox

$$u = \text{idinput}(N, type, band, levels) \quad (28)$$

was used [29]. This MATLAB code generates input signals u of different kinds, which are typically used for identification purposes. N determines the number of generated input data. *Type* defines the type of input signal to be generated. This argument takes one of the following values:

type = 'rgs': Gives a random, Gaussian signal.
type = 'rbs': Gives a random, binary signal. This is the default.
type = 'prbs': Gives a pseudorandom, binary signal.

type = 'sine': Gives a signal that is a sum of sinusoids.

6.2 Recursive Identification Algorithm

The regression (ARX) model of the following form

$$y(k) = \boldsymbol{\Theta}^T(k) \boldsymbol{\Phi}(k) + n_c(k) \quad (29)$$

is used in the identification part of the designed controller algorithms, where

$$\boldsymbol{\Theta}^T(k) = \begin{bmatrix} a_1 & a_2 & b_1 & b_2 \end{bmatrix} \quad (30)$$

is the vector of model parameters and

$$\boldsymbol{\Phi}^T(k-1) = \begin{bmatrix} -y(k-1) & -y(k-2) & u(k-d-1) & u(k-d-2) \end{bmatrix} \quad (31)$$

is the regression vector. The non-measurable random component $n_c(k)$ is assumed to have zero mean value $E[n_c(k)] = 0$ and constant covariance (dispersion) $R = E[n_c^2(k)]$.

The digital adaptive GPC controller uses the algorithm of identification based on the Recursive Least Squares Method (RLSM) extended to include the technique of directional (adaptive) forgetting. Numerical stability is improved by means of the LD decomposition [30], [31]. This method is based on the idea of changing the influence of input-output data pairs to the current estimates. The weights are assigned according to amount of information carried by the data.

When using the adaptive principle, the model parameter estimates must approach the true values right from the start of the control. This means that as the self-tuning algorithm begins to operate, identification must be run from suitable conditions − the result of the possible *a priori* information. The role of suitable initial conditions in recursive identification is often underestimated.

6.3 Off-Line Identification of Laboratory Heat-Exchanger

The dynamic off-line model of the laboratory heat exchanger was obtained from processed input (the power of a flow heater P [W]) and output (the temperature of a T_2 [^{o}C] of the cooler) data (see Fig. 1). The input signal $u(k)$ was generated using the MATLAB function "idinput" and discrete parameter estimates of model (25) for sampling period $T_0 = 100$ s and time-delay $T_d = 200$ s were computed using off-line LSM and MATLAB function "fminsearch".

The graphical variable courses of individual identification experiments are shown in Figs. 5 − 7.
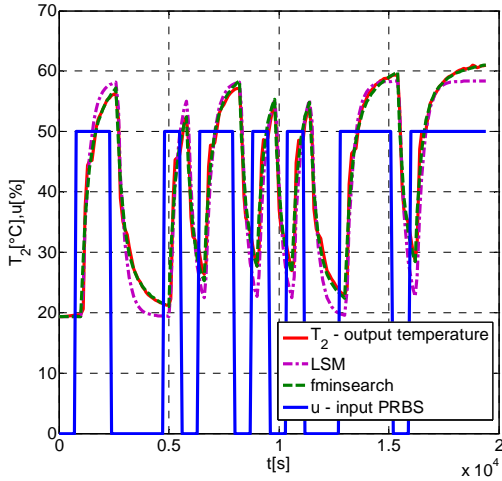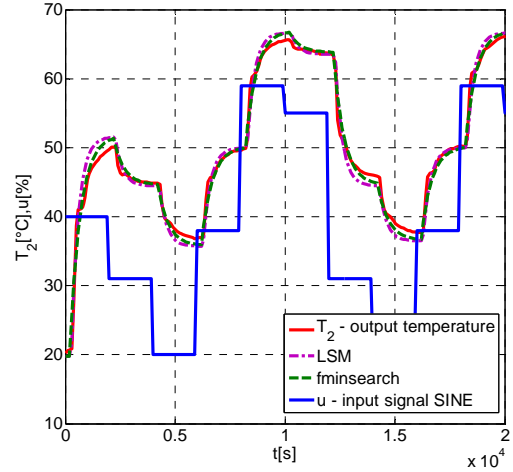
Fig. 5. Identification results: input PRBS

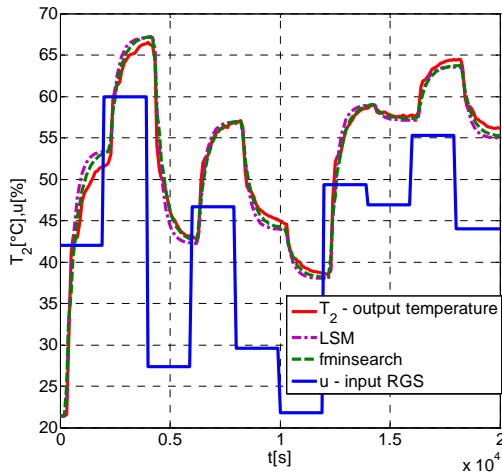Fig. 7. Identification results: input SINE

Six discrete models which were obtained from individual experiments and criterions of identification quality are presented in [32]. The real output variable T_2 and the modelled output variables of the individual models were compared using criterion of identification quality

$$S_y = \frac{1}{N} \sum_{k=1}^{N} \left[y(k) - \hat{y}(k) \right]^2 \qquad (32)$$

where $\hat{y}(k)$ is the predicted output and the estimate of static gain is

$$\hat{K}_g = \frac{\hat{b}_1 + \hat{b}_2}{1 + \hat{a}_1 + \hat{a}_2} \qquad (33)$$

Fig. 6. Identification results: input RGS
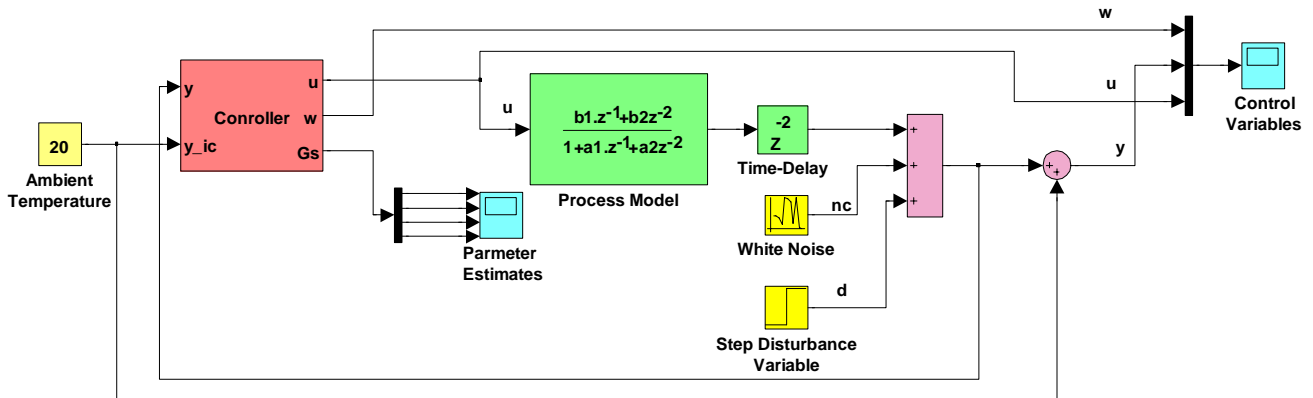
Fig. 8. General SIMULINK control scheme

7 Predictive Control of Heat Exchanger

On the basis of identification experiments, the discrete model in the form

$$G(z^{-1}) = \frac{0.1088 z^{-1} + 0.1964 z^{-2}}{1 - 0.0855 z^{-1} - 0.5157 z^{-2}} z^{-2} \qquad (34)$$

was used for simulation verification of the designed predictive algorithm. A typical
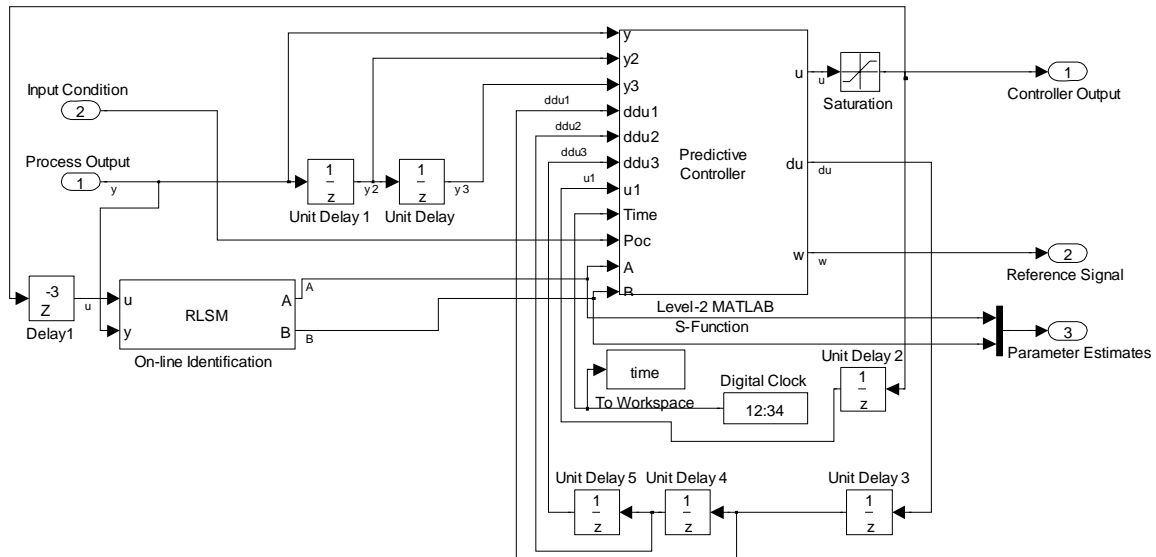
Fig. 9. SIMULINK scheme of subsystem Predictive Controller

SIMULINK scheme used for predictive control of second order systems with time-delay of two sample steps is depicted in Fig. 8. The general scheme consists of the constant block for setting of the Ambient Temperature, the Controller and Process Model with the Time-delay block. The SIMULINK scheme is completed by the White Noise Generator and the Step Disturbance. The main block Predictive Controller contains generating of the reference signal, the recursive identification part and own predictive controller (see SIMULINK scheme – Fig. 9). Following individual horizons were used:

$$N_1 = d + 1 = 3, N_2 = 30, N_u = N_2 - d = 28.$$

Two real-time control experiments for different values of the weighting factor λ were realized:

1) The model parameters of (32)

$$\hat{\boldsymbol{\Theta}}^T(0) = \begin{bmatrix} -0.0855 & -0.5157 & 0.1088 & 0.1964 \end{bmatrix}$$

were used as the initial model parameter estimates for the real-time control, it comes to this, that *a priori* information was used. Therefore elements of the main diagonal covariance matrix were chosen $C_{ii}(0) = 10^{-3}$ (an assumption, that the dispersions of the parameter estimates are in a narrow interval). The courses of the control variables are well including of the initial control interval – see Fig. 10. The evolution of the model parameter estimates in the individual sampling steps is shown in Fig. 11.

2) The model parameter estimates were chosen without *a priori* information

$$\hat{\boldsymbol{\Theta}}^T(0) = \begin{bmatrix} -0.0855 & 0.5157 & 0.1088 & 0.1964 \end{bmatrix}$$

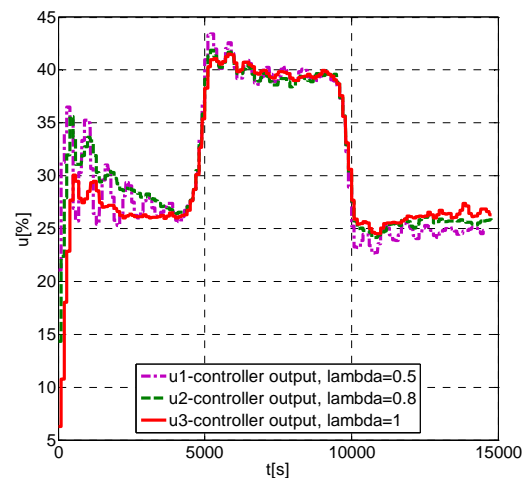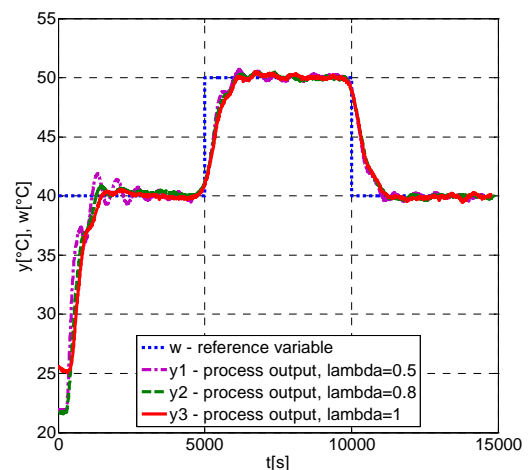

Fig. 10. Process control with *a priori* information

Fig. 11. Evolution of model parameter estimates,
$C_{ii}(0) = 10^{-3}$

Fig. 12. Process control without *a priori* information

(by parameter estimate $\hat{a}_2$ was changed polarity).
Therefore elements of the main diagonal covariance
matrix were chosen $C_{ii}(0) = 10^3$ (an assumption, that
the dispersions of the parameter estimates are in a

wide interval). The courses of the control variables
oscillate in the initial control interval, when the
model parameter estimates are converged, the
quality of the control process is very good – see Fig.
12. The evolution of the model parameter estimates
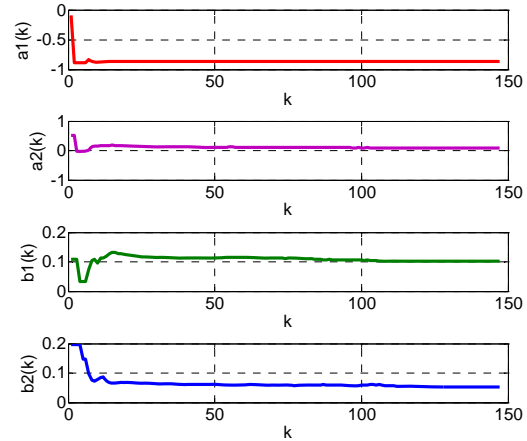in the individual sampling steps is shown in Fig. 13.

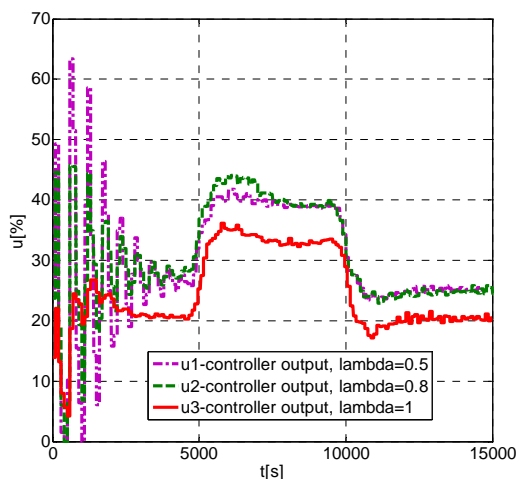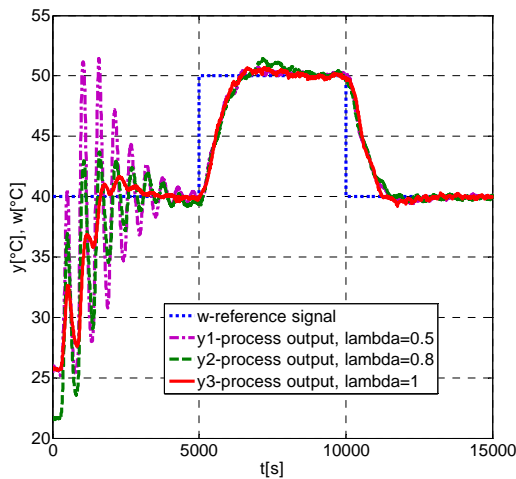Fig. 13. Evolution of model parameter estimates,
$C_{ii}(0) = 10^3$

The dependence of the process variables (process
and controller outputs) on the weighting factor λ is
obvious from Figs. 10 and 12. The experimental
control results were influenced by variation of the
outdoor temperature (see e.g. the courses of the
control variables for $\lambda = 1$ in Fig. 12, where the
experiment was realized for low outdoor
temperature).

Some journal or conference papers deal with
MPC of heat exchangers. Robust MPC of a heat
exchanger network is designed and verified by
simulation in [33]. The subject of paper [34] is a
design of the MPC for a shell and tube heat
exchanger. The designed MPC algorithm and its
comparison with PID cotroller were realized only in
simulation conditions. A cascade GPC for a heat
exchanger process is proposed in [35]. The result of
this paper is the simulation study of the effect of the
cascaded GPC and basic GPC control algorithms on
a model of heat exchangers. Adaptive GPC of a heat
exchanger pilot plant is designed in [36]. The
performance of the proposed controller is illustrated
by a simulation example of a heat exchanger pilot
plant.

From the above-mentioned citations it is obvious
that most authors deal only with verification of the
designed MPC algorithms by simulation and no by
real-time control of real heat exchangers. It is also
necessary to consider different structures of the
individual equipments. Therefore a comparison of
real-time control-loops is very problematic.

7 Conclusion

The contribution presents the adaptive predictive control applied to the time-delay process – the laboratory heat exchanger. The predictive controller is based on the recursive computation of predictions by direct use of the CARIMA model. The computation of predictions was extended for time-delay systems. A linear model with constant coefficients used in pure model predictive control can not describe the control system in all its modes. Therefore, an adaptive approach was applied. It consists of the recursive identification and the predictive controller. The model parameter estimates obtained from the identification procedure are used in the adaptive predictive controller. The GPC based on a minimisation of the quadratic criterion was derived and tested. For obtaining of a suitable model for simulation verification were used the experimental data measured on the laboratory heat exchanger system. This laboratory equipment was identified by combination of various input signals. Two off-line identification methods were used. The parameter estimates of one suitable discrete model from the point of view of quality identification were used in the initial part of the real-time control (the use *a priori* information). The designed adaptive GPC method was verified also in the case without *a priori* information. The real-time experiments confirmed that the predictive approach is able to cope with the given control problem. The real-time experiments demonstrated that the outdoor temperature has great influence up to dynamical behaviour of the laboratory heat exchanger. The following research will be directed to the extension of the designed predictive algorithm over the measurable disturbance.

Conclusion Remark:
This paper was included in the Special Issue on Multi-Models for Complex Technological Systems [37]. The Special Issues of the WSEAS Transactions on Systems [37] – [51] are very useful means for publication of monotematically focused contributions into an above mentioned journal. The Special Issues enable faster and easier access of interested academics and researches for the acquisition of partial necessary information in their research area.

References:
[1] R. Matušů, and R. Prokop, Control of Periodically Time-Varying Systems with Delay: An Algebraic Approach vs. Modified Smith Predictors, *WSEAS Transactions on Systems*, Vol. 9, No. 6, 2010, pp. 689-702.

[2] L. Pekar, A Ring for Description and Control of Time-Delay Systems, *WSEAS Transactions on Systems*, Vol. 11, No. 4, 2012, pp. 571-585.

[3] P. Dostál, V. Bobál and Z. Babík, Control of Unstable and Integrating Time Delay Systems, *WSEAS Transactions on Systems*, Vol. 11, No. 4, 2012, pp. 586-595.

[4] M. A. Pakzad, Kalman Filter Design for Time Delay Systems, *WSEAS Transactions on Systems*, Vol. 11, No. 4, 2012, pp. 551-560.

[5] M. A. Pakzad and S. Pakzad, Stability Map of Fractional Order Time-Delay Systems, *WSEAS Transactions on Systems*, Vol. 11, No. 4, 2012, pp. 541-550.

[6] R. Prokop, J. Korbel and R. Matušů, Auto-tuning Principles for Time-delay Systems, *WSEAS Transactions on Systems*, Vol. 11, No. 4, 2012, pp. 561-570.

[7] O. J. Smith, Closed Control of Loops, *Chem. Eng. Progress*, Vol. 53, 1957, pp. 217-219.

[8] Z. J. Palmor and Y. Halevi, Robustness Properties of Sampled-data Systems with Dead Time Compensators, *Automatica*, Vol. 26, 1990, pp. 637-640.

[9] B. C. Torrico, and J. E. Normey-Rico, 2DOF Discrete Dead-time Compensators for Stable and Integrative Processes with Dead-time, *Journal of Process Control*, Vol. 15, 2005 pp. 341-352.

[10] J. E. Normey-Rico and E. F. Camacho, *Control of Dead-time Processes*, Springer-Verlag, London, 2007.

[11] C. C. Hang, K. W. Lim and B. W. Chong, A Dual-rate Digital Smith Predictor, *Automatica*, Vol. 20, 1989, pp. 1-16.

[12] V. Bobál, P. Chalupa, P. Dostál and M. Kubalčík, Design and Simulation Verification of Self-tuning Smith Predictors, *International Journal of Mathematics and Computers in Simulations*, Vol. 5, No. 4, 2011, pp. 342-351.

[13] V. Bobál, P. Chalupa, J. Novák and P. Dostál, MATLAB Toolbox for CAD of Self-tuning of Time-delay Processes, In: *Proceedings of the International Workshop on Applied Modelling and Simulation*, Roma, 2012, pp. 44 – 49.

[14] V. Bobál, P. Chalupa, and J. Novák, Toolbox for CAD and Verfication of Digital Adaptive Control Time-Delay Systems. Tomas Bata University in Zlín, Faculty of Applied Informatics, 2011. Available from http://nod32.fai.utb.cz/promotion/Software_OBD/Time_Delay_Tool.zip.

[15] V. Bobál, P. Chalupa, M. Kubalčík and P. Dostál, Identification and Self-tuning Control of Time-delay Systems, *WSEAS Transactions on Systems*, Vol. 11, No. 4, 2012, pp. 598-606.

[16] D. W. Clarke, C. Mohtadi and P. S. Tuffs, Generalized Predictive Control, Part I: The Basic Algorithm, *Automatica*, Vol. 23, 1987, pp. 137-148.

[17] D. W. Clarke, C. Mohtadi and P. S. Tuffs, Generalized Predictive Control, Part II: Extensions and Interpretations, *Automatica*, Vol. 23, 1987, pp. 149-160.

[18] J. M. Maciejowski, *Predictive Control with Constraints*, Prentice Hall, London, 2002.

[19] J. A. Rossiter, Model Based Predictive Control: a Practical Approach, CRC Press, 2003.

[20] E. F. Camacho and C. Bordons, *Model Predictive Control*, Springer-Verlag, London, 2004.

[21] J. Mikleš and M. Fikar, *Process Modelling, Optimisation and Control*, Springer-Verlag, Berlin, 2008.

[22] L. Pekař, R. Prokop and P. Dostálek, Circuit Heating Plant Model with Internal Delays, *WSEAS Transactions on Systems and Control*, Vol. 8, No. 9, 2009, pp. 1093-1104.

[23] M. Ch. Li, *Delay Identification and Model Predictive Control of Time Delayed Systems*, Ph.D. Thesis, Mc Gill University, Montreal, Canada, 2008.

[24] M. Kubalčík and V. Bobál, Techniques for Predictor Design in Multivariable Predictive Control, *WSEAS Transactions on Systems and Control*, Vol. 6, No. 9, 2011, pp. 349-360.

[25] V. Bobál, P. Chalupa, P. Kubalčík and P. Dostál, Self-tuning Predictive Control of Non-linear Servomotor, *Journal of Electrical Engineering*, Vol. 61, No. 6, 2010, pp. 265-372.

[26] V. Bobál, M. Kubalčík, P. Dostá, and J. Matějíček, Adaptive Predictive Control of Time-delay systems, *Computers and Mathematics with Applications*, Vol. 66, 2013, pp. 165-176.

[27] L. Ljung, *System Identification: Theory for the User*, Englewood Cliffs, NJ, Prentice-Hall, 1987.

[28] L. Ljung, *System Identification ToolboxTM, User's Guide*, The MathWorks, Natick, MA, 2012.

[29] J. C Lagaris, J. A Reeds, M. H. Wright and P. E. Wright, Convergence Properties of the Nelder-Mead Simplex Method in Low Dimensions, *SIAM Journal of Optimization*, Vol. 9, No. 1, 1998, pp. 112-147.

[30] R. Kulhavý, Restricted Exponential Forgetting in Real Time identification, *Automatica*, Vol. 23, 1987, pp. 586-600.

[31] V. Bobál, J. Böhm, J. Fessl and J. Macháček, *Digital Self-tuning Controllers: Algorithms, Implementation and Applications*, Springer-Verlag, London, 2005.

[32] V. Bobál, P. Chalupa, M. Kubalčík and P. Dostál, Identification and Self-tuning Control of Time-delay Systems, *WSEAS Transactions on Systems*, Vol. 11, No. 10, 2012, pp. 596-608.

[33] M. Bakošová and J. Oravec, Robust Model Predictive Control of Heat Exchanger Network, *Chemical Engineering Transactions*, Vol. 35, 2013, pp. 241-246.

[34] V. Krishna, K. Ramkumar and V. Alagesan, Control of Heat Exchangers Using Model Predictive Controller, In: *Proceedings of the IEEE International Conference on Advances in Engineering, Science and Management*, Nagapttinam, India, 2012, pp. 242-146.

[35] R. D. Kokate and L. M. Waghmare, Cascade Generalized Predictive Control for Heat Exchanger Process, *International Journal of Signal System Control and Engineering Application*, Vol. 3, No. 2, 2010, pp. 13-27.

[36] Z. Zidane, M. A. Lafkih and M. Ramzi, Adaptive Predictive Control of Heat Exchanger, *Journal of Mechanical Engineering and Automation*, Vol. 2, No. 5, 2012, pp. 100-107.

[37] C. Ciufudean and F. Neri, Open research issues on Multi-Models for Complex Technological Systems, *WSEAS Transactions on Systems*, Vol. 13, 2014 (in press).

[38] A. V. Doroshin and F. Neri, Open research issues on Nonlinear Dynamics, Dynamical Systems and Processes, *WSEAS Transactions on Systems*, Vol. 13, 2014 (in press).

[39] F. Neri, Open research issues on Computational Techniques for Financial Applications, *WSEAS Transactions on Systems*, Vol. 13, 2014 (in press).

[40] P. Karthikeyan and F. Neri, Open research issues on Deregulated Electricity Market: Investigation and Solution Methodologies.

WSEAS Transactions on Systems, Vol. 13, 2014 (in press).

[41] M. Panoiu and F. Neri, Open research issues on Modeling, Simulation and Optimization in Electrical Systems. *WSEAS Transactions on Systems*, Vol. 13, 2014 (in press).

[42] F. Neri, Open research issues on Advanced Control Methods: Theory and Application, *WSEAS Transactions on Systems*, Vol. 13, 2014 (in press).

[43] P. Hájek and F. Neri, An introduction to the special issue on computational techniques for trading systems, time series forecasting, stock market modeling, financial assets modelling, *WSEAS Transactions on Business and Economics*, Vol. 10, No. 4, 2013, pp. 201-292.

[44] M. Azzouzi and F. Neri, An introduction to the special issue on advanced control of energy systems, *WSEAS Transactions on Power Systems*, Vol. 8, No. 3, 2013, p. 103.

[45] Z. Bojkovic and F. Neri, An introduction to the special issue on advances on interactive multimedia systems, *WSEAS Transactions on Systems*, Vol. 12 , No. 7, 2013, pp. 337-338.

[46] L. Pekař and F. Neri, An introduction to the special issue on advanced control methods: Theory and application, *WSEAS Transactions on Systems*, Vol. 12, No. 6, 2013, pp. 301-303.

[47] G. Guarnaccia and F. Neri, An introduction to the special issue on recent methods on physical polluting agents and environment modeling and simulation, *WSEAS Transactions on Systems*, Vol. 12, No. 2, 2013, pp. 53-54.

[48] F. Neri, An introduction to the special issue on computational techniques for trading systems, time series forecasting, stock market modeling, and financial assets modelling, *WSEAS Transactions on Systems*, Vol. 12, No. 12, 2013, pp. 659-660.

[49] M. Muntean and F. Neri, Foreword to the special issue on collaborative systems, *WSEAS Transactions on Systems*, Vol. 11, No. 11, 2012, p. 617.

[50] L. Pekař and F. Neri, An introduction to the special issue on time delay systems: Modelling, identification, stability, control and applications, *WSEAS Transactions on Systems*, Vol. 11, No. 10, 2012, pp. 539-540.

[51] C. Volos and F. Neri, An introduction to the special issue: Recent advances in defence systems: Applications, methodology, technology, *WSEAS Transactions on Systems*, Vol. 11, No. 9, 2012, pp. 477-478.

Specific problems on the operation of the automatic control system of temperature into an individual dwelling

DANIEL POPESCU

Department of Electrical Engineering for Civil Engineering and Building Services
Technical University of Civil Engineering Bucharest
Bd. Pache Protopopescu nr.66, 021414 Bucuresti Sector 2
ROMANIA
dpopescu@instal.utcb.ro

Abstract: The article makes an analysis of the functioning for the heating automation system with hot air blown into an individual dwelling. The structure of the automatic control system for indoor temperature in the dwelling is determined, in which the controller is a thermostat having feature type relay with hysteresis, the conditions related to the evolution of automatic control of the process are specified and the oscillation period of the control system is calculated.

The automatic temperature control system model in individual dwelling is established using Simulink and its functioning by simulation in different representative situations is checked. The results of the simulation are compared with those obtained by calculation or they are used to determine the performance of the automatic control system

Key-words: nonlinear automatic system, changeover controller, thermostat, relay with hysteresis, oscillation period of the control system, precision of the control, comfort in buildings, automation of heating installations.

1 Introduction

This article deals with ensuring indoor comfort in individual dwellings by using nonlinear automatic control systems of the type changeover [1,2,3,4,5]. Indoor temperature regulation is done by using a thermostat, placed in a room chosen as being representative. Heating is assured with blowing hot air at a constant temperature [6,7,8,9].

By comparison to the complex automatic control systems, using the thermostat temperature control device in individual dwellings [10] is a cheap and reliable solution, and automatic control system performance may be acceptable, if the right information about hysteresis loop that characterize bimetallic lamella of the thermostat, the function mode of the command cycle for the heating and thermal inertia of the house is used [11].

The changeover adjusting of the temperature with thermostat is the most used solution for individual dwellings.

Indoor thermal comfort is ensured in large buildings by implementing control structures with feed-forward loop, which controls the water temperature depending on the outside temperature (main disturbance which acts on the process of building heating) [12,13]. The adjusting structure may be used for individual dwellings if an automation device called "ambient probe" is used;

the device is placed in the reference room where the indoor temperature is measured and allows correction with $\pm 2.5\,^0C$ of the reference indoor temperature value set by the control cabinet of the heating plant.

Recent research on indoor temperature control in large buildings use control methods of heating taking into account the heat loss through the building envelope [14,15,16,17]. A perimetral monitoring system of the temperatures of the external surfaces of building provides infrared thermal map of these areas. The thermal map is processed in order to obtain an electrical signal used for driving the heating installation. The indoor temperature is maintained constant by regulating the temperature of the outer surface of the building.

2 Objectives of the paper

The paper presents the time domain analysis of the control system for the indoor temperature using differential equations. Using basic concepts from the theory of nonlinear automatic systems [18,19,20,21,22,23,24] the mathematical inequalities that must be satisfied between the outdoors temperature, hot air temperature, desired indoor temperature and the size of insensitivity domain of the hysteresis are specified, so that the

cycle of control of the heating process can evolve over time. It calculates the oscillation period of the automatic control system.

Using the mathematical model made in Simulink for automatic adjustment of the indoor temperature, it is analyzed its behavior in time, for different representative situations. Through analysis, it is checked:

- the precision for automatic control of the indoor temperature through stationary error evaluation;
- the oscillation domain of the controlled variable;
- the conditions for the cyclic operation of heating process;
- the coincidence between the values of oscillation periods obtained by calculation with those determined by computer simulation;
- the determination of a minimum acceptable value for the temperature interval Δ of the hysteresis of the thermostat.

3 Automatic indoor temperature control structure into individual dwelling

The room chosen as representative for individual dwelling is heated with hot air blowing at 40^0C. The indoor temperature is adjusted by successive actions start / stop for introducing hot air in the room, until they get to values as close as the temperature θ_{ref} set at 18^0C or 20^0C. Control of duty cycles is assured by a changeover controller (thermostat), appropriate located on a wall of the room, which has feature type relay with hysteresis (Figure 1).
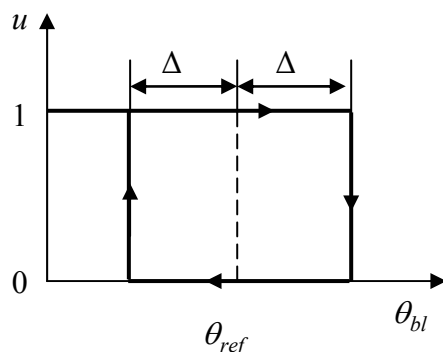

Fig. 1. Feature type relay with hysteresis.

Bimetallic lamella of the thermostat is deformed by heating / cooling and operates an electric switch used to control the introduction of hot air in the

house. The values of the temperatures at which is actioned the electrical contact are established as shown in figure 1, in which is highlight the cycle with hysteresis of the command u according to the temperature θ_{bl} of bimetallic lamella. The temperature interval corresponding to the hysteresis of the bimetallic lamella is denoted by Δ.

Bimetallic lamella temperature θ_{bl} depends on ambient temperature θ_{room} according to the relation

$$\theta_{bl}(s) = \left[\frac{1}{1 + \tau_{bl} \cdot s}\right] \cdot \theta_{room}(s), \qquad (1)$$

where τ_{bl} is the thermal inertia of bimetallic lamella.

Heated room behaves like a first-order inertial element with transfer function

$$H_2(s) = \frac{1}{1 + \tau_2 s}. \qquad (2)$$

The structure of the automatic adjustment system of indoor temperature is presented in figure 2.

4 Imposed conditions for the functioning of automatic control structure

It is noted in figure 2 that the command $u = 1$ the room temperature θ_{room} and bimetallic lamella temperature θ_{bl} is moving towards the value given by $\theta_{out} + K_1$; if the command $u = 0$, then the temperatures θ_{room} and θ_{bl} decrease toward the temperature θ_{out}. The operation of automatic adjustment structure is only possible if the limits within which varies the temperature of bimetallic lamella θ_{bl} are located outside the cycle with hysteresis; therefore, the relations of inequality that need to be fulfilled to generate the periodical commands that produce the heating of the room are:

$$\theta_{out} + K_1 > \theta_{ref} + \Delta, \quad \theta_{out} < \theta_{ref} - \Delta. \qquad (3)$$
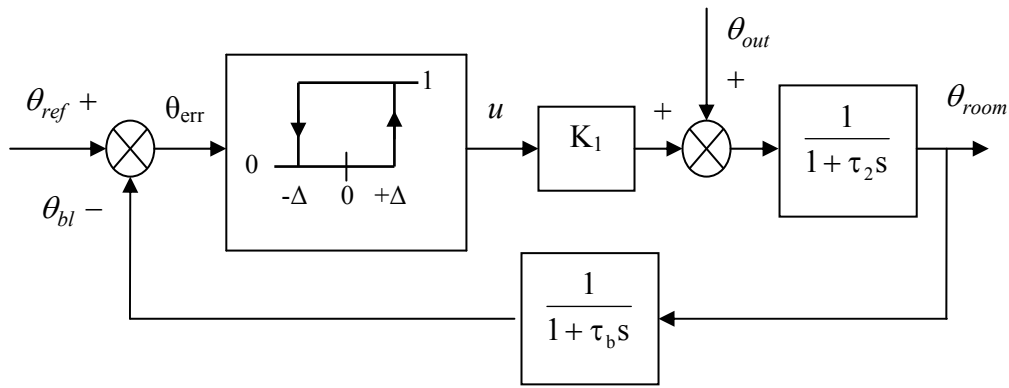
Fig. 2. The structure of the automatic adjustment system of indoor temperature.

5 Determination of the oscillation period of the automatic control system

Starting from the structure of the automatic control system shown in figure 2, the following differential equations can be written:

$$\tau_2 \frac{d\theta_{room}}{dt} + \theta_{room} = \theta_{out} + K_1 \cdot u \qquad (4)$$

$$\tau_{bl} \frac{d\theta_{bl}}{dt} + \theta_{bl} = \theta_{room} . \qquad (5)$$

Substituting θ_{room} from equation (5) into equation (4) it obtain

$$\tau_2 \tau_{bl} \frac{d^2\theta_{bl}}{dt^2} + (\tau_2 + \tau_{bl}) \frac{d\theta_{bl}}{dt} + \theta_{bl} = \\ = \theta_{out} + K_1 \cdot u \qquad (6)$$

Since the time constant τ_2 is much bigger than τ_{bl}, then equation (6) is reduced to an equation of the first order

$$\tau_c \frac{d\theta_{bl}}{dt} + \theta_{bl} = \theta_{out} + K_1 \cdot u , \qquad (7)$$

having the time constant $\tau_c = \tau_2 + \tau_{bl} = 480s$.

For performing calculations and simulation of system model the following numerical values are selected: $K_1 = 40^0 C$, $\tau_2 = 450s$, $\tau_{bl} = 30s$, $\Delta = 1,5^0 C$; the simplifying hypothesis is used, in which the outside temperature has a constant value $\theta_{out} = 5^0 C$.

The oscillation period T is composed by two time intervals: first interval $[0, t_0]$, when $u = 1$ and the second interval $(T - t_0)$, when $u = 0$. These time intervals are calculated by solving the equation (7), taking into account the characteristic of the bimetallic lamella shown in figure 1.

$[0, t_0]$, $\theta_{bl}(0) = \theta_{ref} - \Delta$:

$$\tau_c \frac{d\theta_{bl}}{dt} + \theta_{bl} = \theta_{out} + K_1 \qquad (8)$$

$[t_0, T]$, $\theta_{bl}(t_0) = \theta_{ref} + \Delta$:

$$\tau_c \frac{d\theta_{bl}}{dt} + \theta_{bl} = \theta_{out} \qquad (9)$$

The differential equation (7), in the time interval $[0, t_0]$, has the solution

$$\theta_{bl} = \theta_{out} + K_1 + [\theta_{ref} - \Delta - \theta_{out} - K_1] \cdot e^{-\frac{t}{\tau_c}} \qquad (10)$$

which for $t = t_0$, moment in which $\theta_{bl}(t_0) = \theta_{ref} + \Delta$, allow the calculation of the value t₀ thus:

$$t_0 = \tau_c \cdot \ln\left[\frac{\theta_{out} + K_1 + \Delta - \theta_{ref}}{\theta_{out} + K_1 - \Delta - \theta_{ref}}\right] = 53,4s . \qquad (11)$$

For the time interval $[t_0, T]$ the solution of differential equation (7) is

$$\theta_{bl} = \theta_{out} + [\theta_{ref} + \Delta - \theta_{out}] \cdot e^{-(t-t_0)/\tau_c} , \qquad (12)$$

which for $t = T$ (moment in which $\theta_{bl}(T) = \theta_{ref} - \Delta$), we can calculate the oscillation period T as follows:

$$T = t_0 + \tau_c \cdot \ln\left(\frac{\theta_{ref} + \Delta - \theta_{out}}{\theta_{ref} - \Delta - \theta_{out}}\right) = 164,6s . \quad (13)$$

If it calculates t_0 and T for $\theta_{ref} = 20^0$C, $\theta_{out} = -10^0$C, $\Delta = 1^0C$, $K_1 = 40^0 C$, $\tau_2 = 450s$, $\tau_{bl} = 30s$, $\tau_c = \tau_2 + \tau_{bl} = 480s$, then we obtain:

$$t_0 = \tau_c \cdot \ln\left[\frac{\theta_{out} + K_1 + \Delta - \theta_{ref}}{\theta_{out} + K_1 - \Delta - \theta_{ref}}\right] = \quad (14)$$

$$= 450 \cdot \ln\left[\frac{-10 + 40 + 1 - 20}{-10 + 40 - 1 - 20}\right] = 90,3s$$

$$T = t_0 + \tau_c \cdot \ln\left(\frac{\theta_{ref} + \Delta - \theta_{out}}{\theta_{ref} - \Delta - \theta_{out}}\right) = \quad (15)$$

$$= 90,3 + 450 \cdot \ln\left[\frac{20 + 1 + 10}{20 - 1 + 10}\right] = 120,31s$$

6 The model of automatic temperature control system in individual housing

The model of automatic temperature control system is done using Simulink, in two variants, which differ by the way they act the main disturbance (outdoor temperature):

- variant 1, in which outdoor temperature has a constant value, that temperature is the average diurnal (figure 3);
- variant 2, in which the outdoor temperature varies sinusoidal form day to night, with a given amplitude to an average diurnal value (figure 4).

7 Analysis of the functioning of automatic heating system model of individual housing

A. Shall be checked by simulation using the model developed in variant 1 (figure 3), the fact that the command u is launched periodically for heating of the house and evaluate the precision of the temperature adjustment in the house with θ_{room} and θ_{bl} (figure 5).

The simulation is done for $\theta_{ref} = 18^0$C, $\theta_{out} = 5^0$C, $\Delta = 1,5^0 C$, $K_1 = 40^0 C$, $\tau_2 = 450s$, $\tau_{bl} = 30s$, $\tau_c = \tau_2 + \tau_{bl} = 480s$, identical to the values entered in the relations (11) for t_0 and (13) for T.

Analyzing the graphs obtained by simulation, it is found that the room temperature is regulated around average value of 18^0C, equal to that required by θ_{ref} and the periodical evolution of commands applied to the automated heating process for which shall be determined from graphs $t_0 \cong 55s$ and $T \cong 160s$. The size of oscillation domain for adjusted parameter θ_{room}, determined by graph, has the approximate value of 3^0C, that which was expected because $\Delta = 1,5^0 C$.
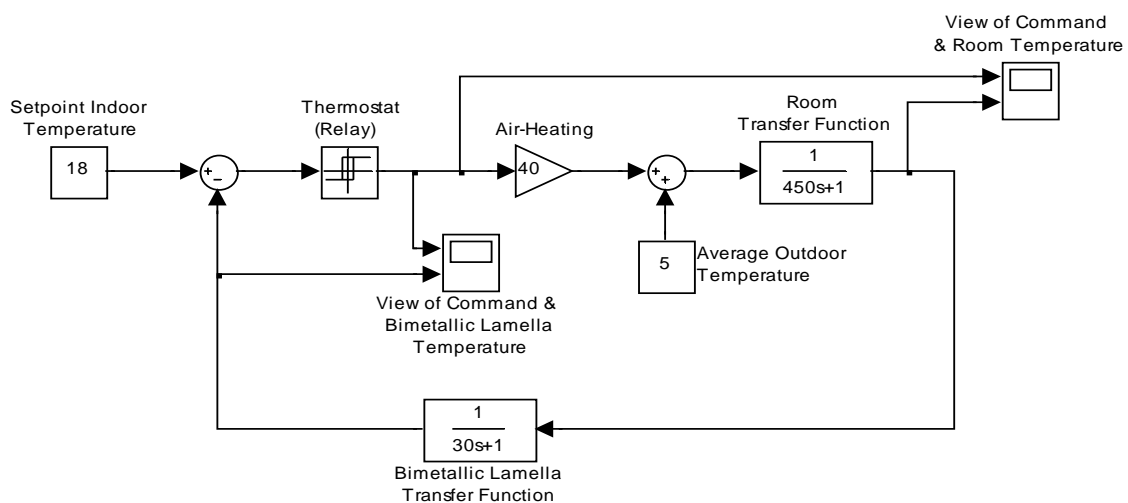

Fig. 3. The model of automatic temperature control system in which outdoor temperature has a constant value.
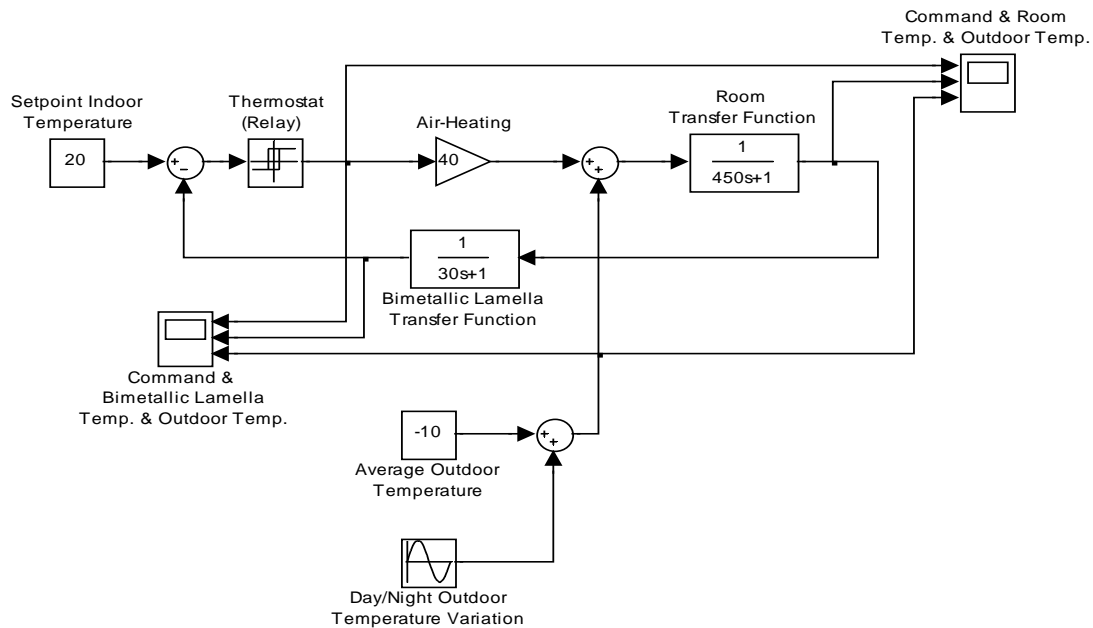
Fig. 4. The model of automatic temperature control system in which the outdoor temperature varies sinusoidally.

B. The simulation is done for θ_{ref} = 20^{0}C, θ_{out} = -10^{0}C, $\Delta = 1^0 C$, $K_1 = 40^0 C$, $\tau_2 = 450s$, $\tau_{bl} = 30s$, $\tau_c = \tau_2 + \tau_{bl} = 480s$, identical to the values entered in the relations (14) for t_0 and (15) for T. The simulation results are presented in figure 6.

It is found through simulation that the regulation of room temperature is around average value of 20^{0}C, equal to that imposed by θ_{ref} and that is taking place the periodically evolution of commands applied at the automated heating process; using the graphs it determine $t_0 \cong 88s$ and $T \cong 122s$. The size of oscillation domain for adjusted parameter θ_{room}, determined by graph, has the approximate value of 2^{0}C, that which was expected because $\Delta = 1^0 C$.

C. Simulation is done using the model developed in Simulink, version 2 from figure 4, in which numerical values entered are the following: θ_{ref} = 20^{0}C, $\Delta = 1^0 C$, $K_1 = 40^0 C$, $\tau_2 = 450s$, $\tau_{bl} = 30s$; the outdoor temperature has the average value θ_{out} = -10^{0}C, over which are

overlapping variations from day to night with sinusoidal form and amplitude 8^{0}C.

The graph obtained for the indoor temperature θ_{room} during the day when the outside temperature achieve the highest value θ_{out} = -2^{0}C, is shown in figure 7, and the graph obtained for θ_{room} during the night, when the outside temperature achieves the lowest value θ_{out} = -18^{0}C, is shown in figure 8.

It is noted the evolution of the temperature adjustment cycles in the room by repeating the command u for heating and, as expected, the time interval [0, t$_0$] when the command $u = 1$, is higher in the case when θ_{out} = -18^{0}C than if θ_{out} = -2^{0}C.

The value $\Delta = 1^0 C$ chosen for the characteristic of the thermostat ensure the adequate precision for the indoor temperature in the house. A decrease of the value Δ at thermostat would enhance the precision of the adjustment, but it would force too much the actuator of the control system by decreasing the oscillation period T.
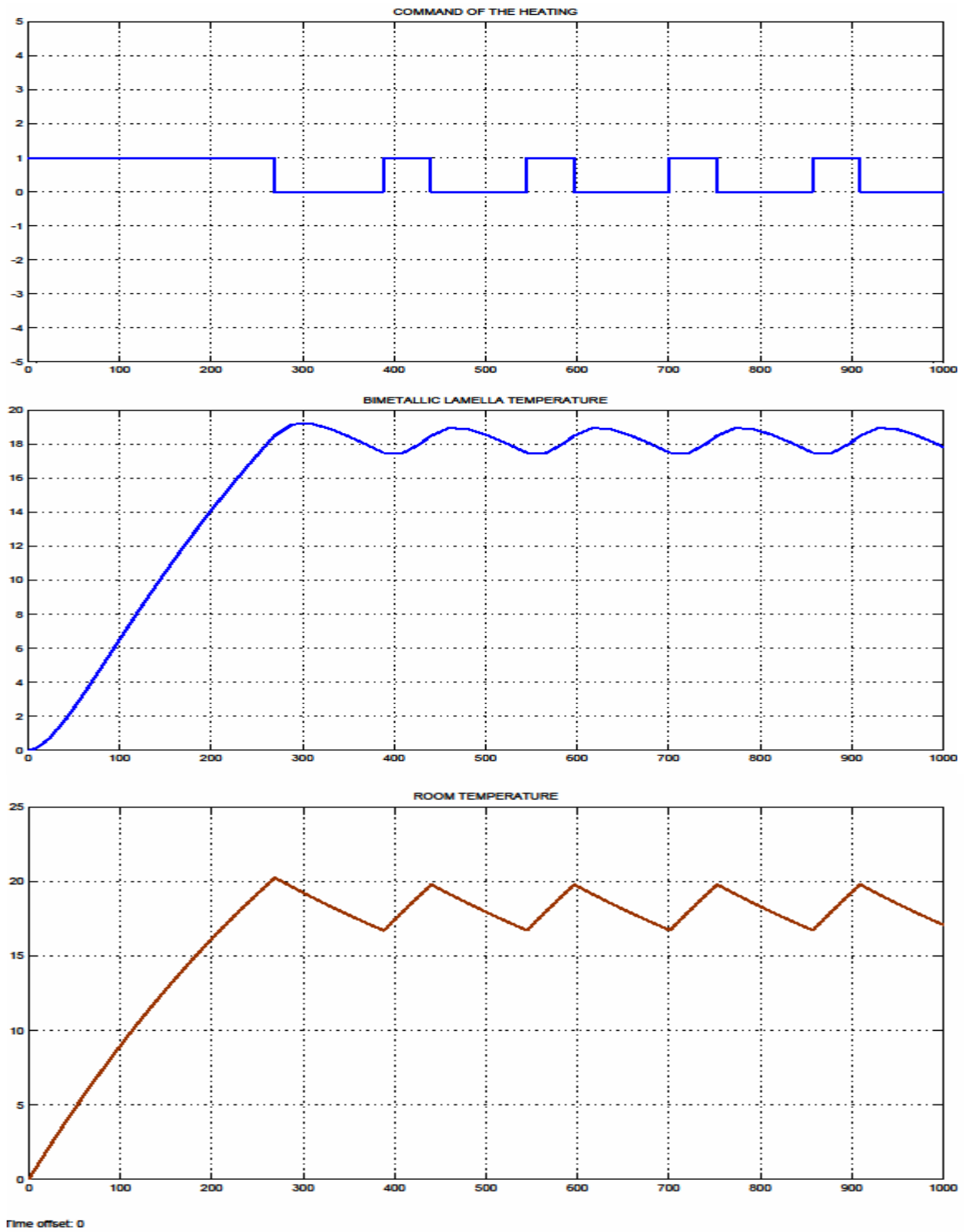
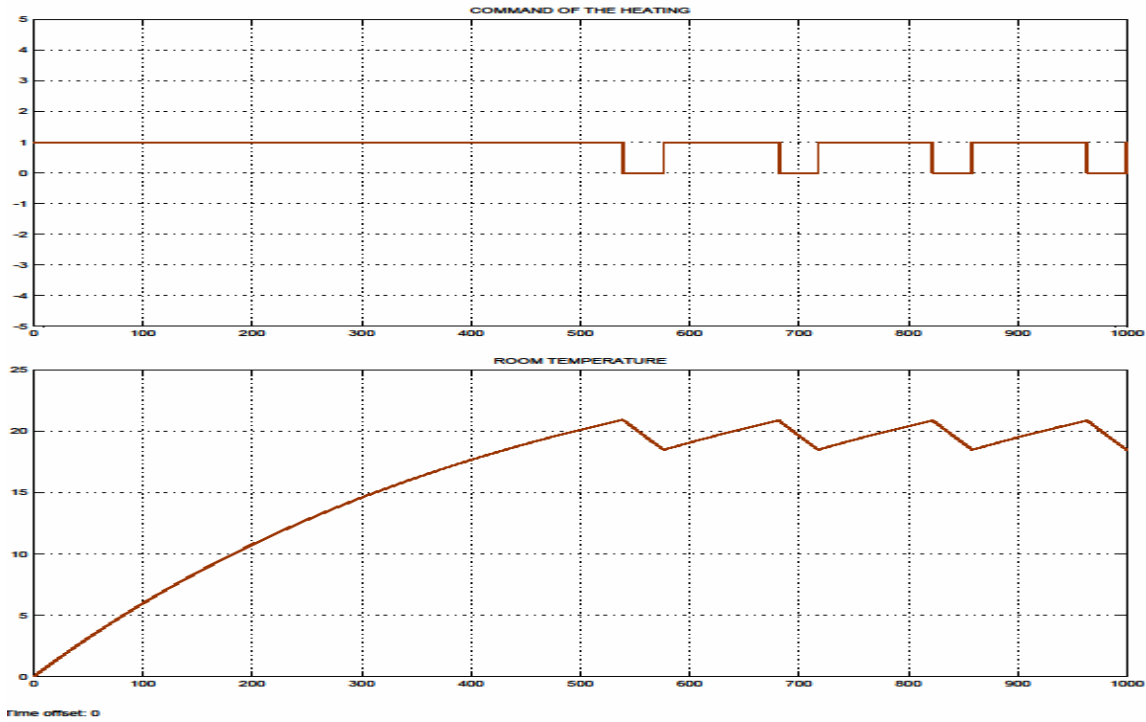Fig. 5. Model simulation results in which outdoor temperature has a constant value.

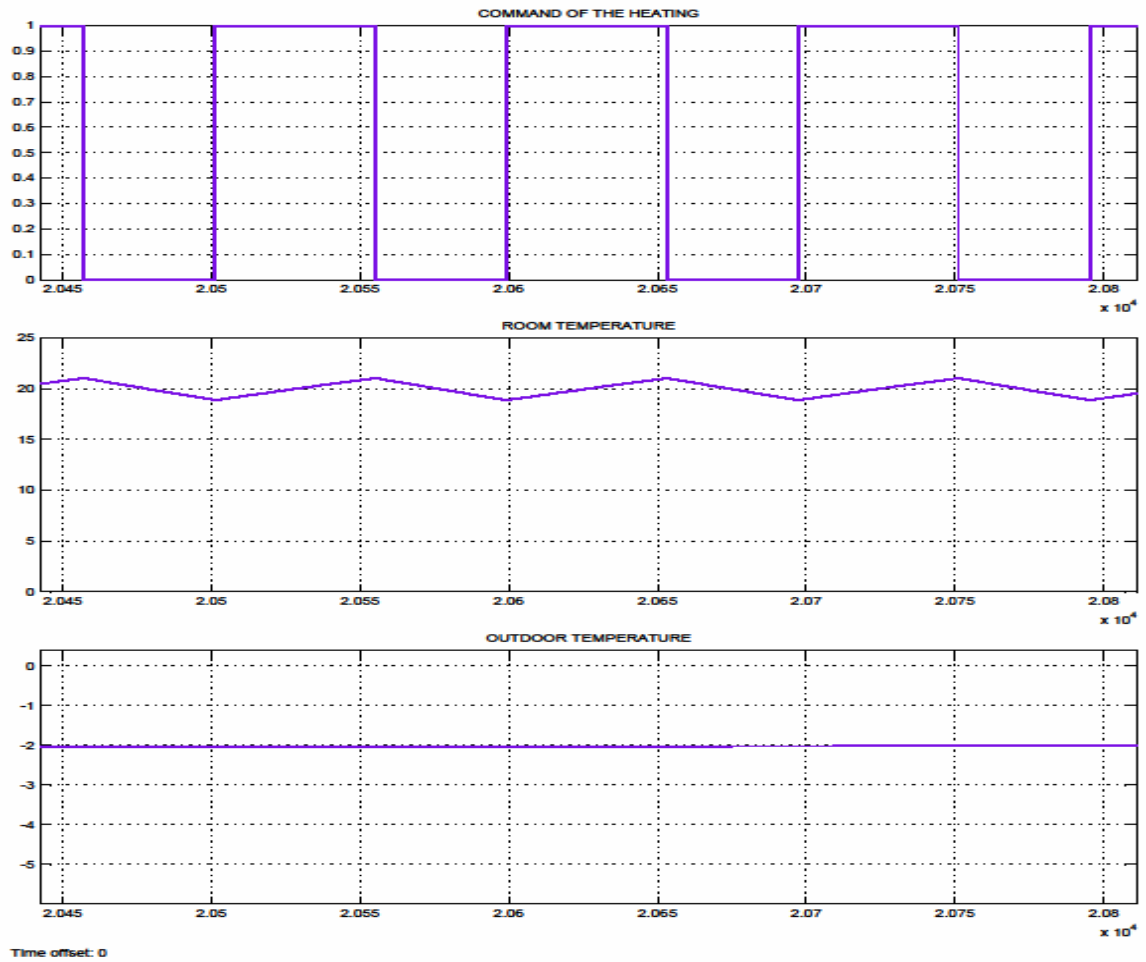Fig. 6. Model simulation results in which the outdoor temperature varies sinusoidally.

Fig. 7. The graph obtained for the indoor temperature when the outside temperature achieve the highest value.
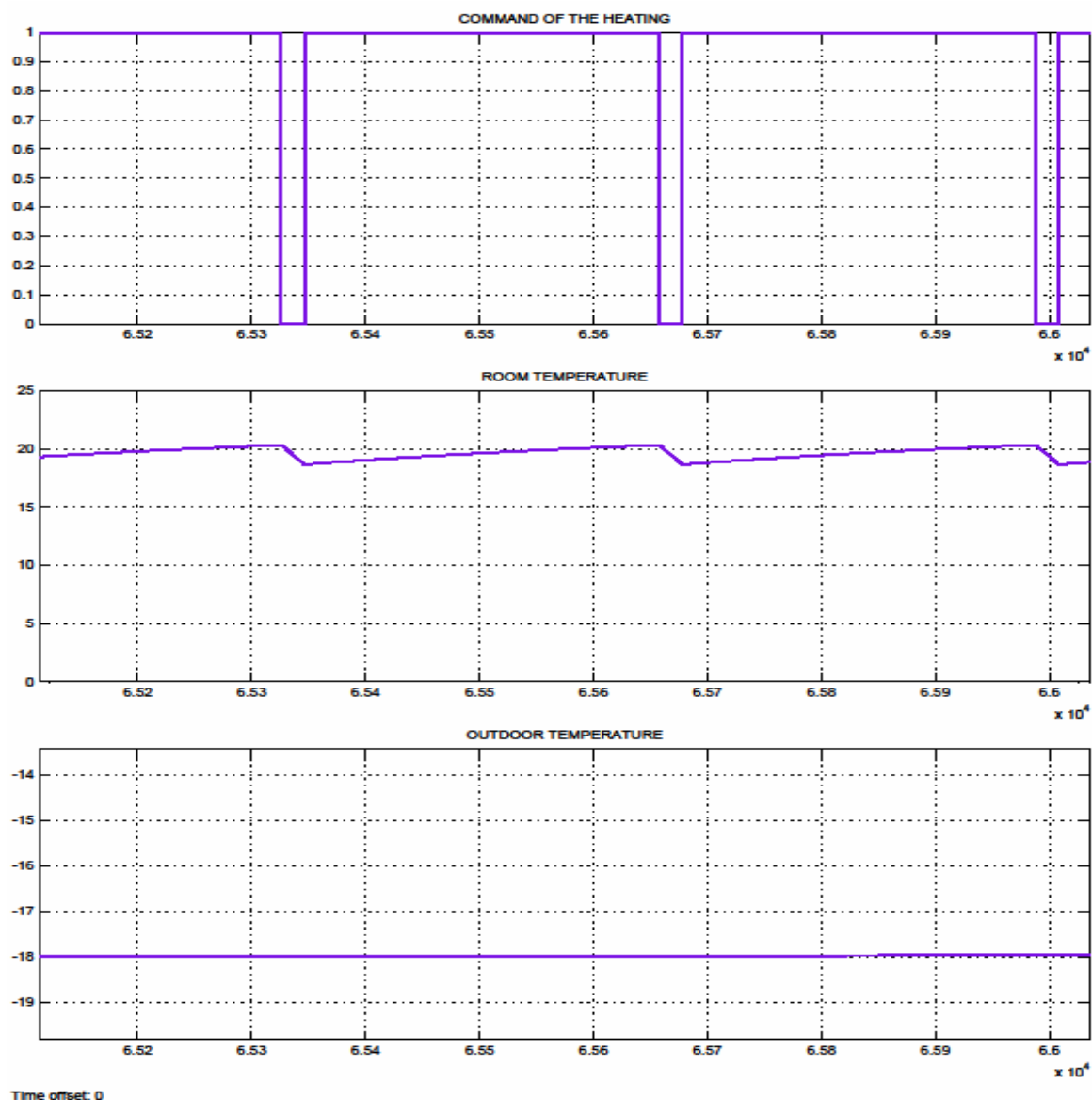
Fig. 8. The graph obtained for the indoor temperature when the outside temperature achieves the lowest value.

8 Conclusions

It is found that are satisfied the conditions (3) for the automatic control system, in all situations analyzed by simulation.

The approaching between numerical values obtained for t_0 and T by calculation in paragraph 5 and by simulation in paragraph 7 variants A and B, validates the correctness of the two approaches in this paper.

The analysis perform in paragraph 7, in the variants of point C, corresponds quite well the real situation of a cold winter day in Romania.

The decreasing values chosen for the temperature domain Δ, corresponding to the hysteresis of thermostat (figure 1), increase the control precision of indoor temperature, but would extra force the actuator that controls the introduction of warm air in the home, by increasing the switching frequency.

The way in which was made the analyze of the automatic control system for indoor temperature into an individual housing when using the hot air heating, can be applied in the case when using a similar structure of the automatic control, for heating with radiators through which circulate heat transfer medium heated to a constant temperature.

The automation solution with changeover regulator (thermostat) placed in a room chosen as reference, can not be applied for automatic control of the indoor temperature in the great buildings.

References:

[1] Belea, C., (1983) *Automatică neliniară*, Editura Tehnică, Bucureşti.

[2] Doroshin, A. V., Neri, F. (2014) *Open research issues on Nonlinear Dynamics, Dynamical Systems and Processes*. WSEAS Transactions on Systems, 13, in press.

[3] Ciufudean, C., Neri, F. (2014) *Open research issues on Multi-Models for Complex Technological Systems*. WSEAS Transactions on Systems, 13, in press.

[4] Neri, F. (2014) *Open research issues on Advanced Control Methods: Theory and Application*. WSEAS Transactions on Systems, 13, in press.

[5] Pekař, L., Neri, F. (2013) *An introduction to the special issue on advanced control methods: Theory and application* (2013) WSEAS Transactions on Systems, 12 (6), pp. 301-303.

[6] Mira, N., (coordinator) (2010) *Enciclopedia tehnică de instalaţii,* vol. 1, Instalaţii de încălzire, ISBN 978-973-85936-5-7, Editura ARTECNO Bucureşti.

[7] Karthikeyan, P., Neri, F. (2014) *Open research issues on Deregulated Electricity Market: Investigation and Solution Methodologies*. WSEAS Transactions on Systems, 13, in press.

[8] Panoiu, M., Neri, F. (2014) *Open research issues on Modeling, Simulation and Optimization in Electrical Systems*. WSEAS Transactions on Systems, 13, in press.

[9] Azzouzi, M., Neri, F. (2013) *An introduction to the special issue on advanced control of energy systems* (2013) WSEAS Transactions on Power Systems, 8 (3), p. 103.

[10] Iordache, F., Popescu, D. (2005) *Aspecte privind automatizarea funcţionării unor instalaţii de încălzire centrală de tip individual*, Instalatorul, No. 6, pp. 10-15, ISSN 1223-7418, Editura ARTECNO Bucureşti.

[11] Pekař, L., Neri, F. (2012) *An introduction to the special issue on time delay systems: Modelling, identification, stability, control and applications* WSEAS Transactions on Systems, 11 (10), pp. 539-540.

[12] Popescu, D., Ionescu, D., Iliescu, M. (2009) *Conducerea automată a instalaţiilor de încălzire din clădirile mari – aspecte privind realizarea practică*. Instalatorul, No. 4, pp. 24-26, ISSN 1223-7418, Editura ARTECNO Bucureşti.

[13] Popescu, D., Ionescu, D., Iliescu, M. (2008) *Aspecte privind comportarea părţii fixate a sistemelor de automatizare din instalaţiile de încălzire ale clădirilor mari*, A 43-a Conferinţă Naţională de Instalaţii, pp. 31-36, ISBN 978-973-755-406-2, Sinaia, October 15-18, 2008.

[14] Popescu, D., Ciufudean, C. (2008) *Automatic Control System for Heating Systems in Buildings Based on Measuring the Heat Exchange through Outer Surfaces,* Proceedings of the 8th WSEAS International Conference on Simulation, Modelling and Optimization (SMO'08), pp. 117-121, ISBN 978-960-474-007-9, ISSN 1790-2769, Santander, Cantabria, Spain, September 23-25, 2008.

[15] Popescu, D., (2008) *A New Solution for Automatic Control of Heating Systems in Buildings Based on Measuring Heat Transfer Through Outer Surfaces*, Proceedings of the 10th WSEAS International Conference on Automatic Control, Modeling and Simulation (ACMOS'08)*,* pp. 206-209, ISBN 978-960-6766-63-3, ISSN 1790-5117, Istanbul, Turkey, May 27-30, 2008.

[16] Popescu, D., Ciufudean, C., Ghiauş, A. (2009) *Specific Aspects of Design of the Automated System for Heating Control that Accounts for Heat Losses Through the Building's Envelope*. Proceedings of the 13th WSEAS International Conference on Systems (part of the 13th WSEAS CSCC Multiconference –CSCC'09- Circuits, Systems, Communications and Computers), pp. 352 – 356, ISSN 1790-2768, ISBN 978-960-474-097-0, Rodos, Greece, July 22-24, 2009.

[17] Popescu, D., Ciufudean, C., Ionescu, D. (2009) *Experimental Analysis of the Automated System for Heating Control based on Heat Losses through Building's Envelope*. 9th WSEAS International Conference on Simulation, Modelling and Optimization (SMO'09*),* pp. 160 – 166, ISSN 1790-2769, ISBN 978-960-474-113-7, Budapest Tech University, Hungary, September 3-5, 2009.

[18] Neri, F. (2014) *Open research issues on Computational Techniques for Financial Applications*. WSEAS Transactions on Systems, 13, in press.

[19] Hájek, P., Neri, F. (2013) *An introduction to the special issue on computational techniques for trading systems, time series forecasting, stock market modeling, financial assets modeling* WSEAS Transactions on Business and Economics, 10 (4), pp. 201-292.

[20] Bojkovic, Z., Neri, F. (2013) *An introduction to the special issue on advances on interactive multimedia systems* WSEAS Transactions on Systems, 12 (7), pp. 337-338.

[21] Guarnaccia, C., Neri, F. (2013) *An introduction to the special issue on recent methods on physical polluting agents and environment modeling and simulation* WSEAS Transactions on Systems, 12 (2), pp. 53-54.

[22] Neri, F. (2012) *An introduction to the special issue on computational techniques for trading systems, time series forecasting, stock market modeling, and financial assets modeling* WSEAS Transactions on Systems, 11 (12), pp. 659-660.

[23] Muntean, M., Neri, F. (2012) *Foreword to the special issue on collaborative systems* WSEAS Transactions on Systems, 11 (11), p. 617.

[24] Volos, C., Neri, F. (2012) *An introduction to the special issue: Recent advances in defense systems: Applications, methodology, technology* WSEAS Transactions on Systems, 11 (9), pp. 477-478.

Aggregation modeling of large wind farms using an improved *K*-means algorithm

Jian-ping Zhang, Hao-zhong Cheng, Shu-xin Tian and Ding Yan
Key Laboratory of Control of Power Transmission and Conversion, Ministry of Education
Department of Electrical Engineering
Shanghai Jiao Tong University
800 Dongchuan Rd., Shanghai 200240 China
Email   zjp42132@139.com; hzcheng@sjtu.edu.cn; tsx396@163.com; 15821801855@163.com

Abstract: - Large wind farms require modeling and simulation in their planning and construction process to provide a basis for grid planning. As a large wind farm is comprised of hundreds or even thousands of wind generators, the detailed-model building of wind farms is difficult, which are associated with slow simulation speeds and heavy workloads. In this paper, an improved *K*-means algorithm-based aggregation modeling method is proposed for large wind farms. A model is built for a typical 300 MW wind farm of the northern Jiangsu Province in China and its simulations are performed. The results based on a comparison between a single-fan aggregation model and a multi-fan aggregation model are obtained. The aggregation method proposed in this paper proves to be accurate and fast, which is able to meet the requirements for output simulation.

Key-words: - wind farm, power grid, wind generator, aggregation modeling, output simulation, *K*-means clustering algorithm.

1 Introduction

With the development of wind-power technology, large wind farms are continuously being connected into the power grid. The volatility of these plants affects the quality, reliability, and stability of the power grid [1,2]. To study the operational characteristics of a wind farm, it is necessary to plan and construct the grid structure, as well as accurately built equivalent model and predict the output of the wind farm before large-scale wind power penetration.

The wake effect of a fan directly influences the output of a wind farm [3]. At the same time, due to the differences in the locations of the distributed fans and randomness in the wind speed, the disparate wind speeds incident on each fan increases the complexity of the modeling. In addition, the planning and application of a real power grid calls for simple models and fast simulation speeds. Therefore, an effective aggregation modeling

method is needed to complete the work introduced above [4-6]. In similar work [7-9], single-fan equivalent models are built based on the operation data of detailed –model for wind farm. Owing to large distributional regions of wind farm and the impacts of wake effect and geomorphic feature, the single–fan model is only applied to some studies with low simulation accuracy. So an equivalent modeling method with the high simulation accuracy and parameters optimization model of a wind farm are proposed by using the operational data of a DFIG wind farm with the detailed models Regarding DFIGs with different parameters the dynamic and transient performances are simulated and analyzed The results are also compared with those by using the detailed model and the capacity weighted equivalent model of the DFIG wind farm The results show that the proposed wind farm equivalent model has the same wind farm operation characteristics with the detailed model and it has better representation of the

dynamic and transient performances of the wind farms.

2 Fan aggregation modeling using single-fan characterization

Single-fan characterization method is one of the commonest methods of aggregation modeling used for the fans in wind farms at present. In this method, the wind farm is deemed to be equivalent to a wind turbine and an generator. The main features of the aggregation method are as indicated below [10]:

(1) Determine the rated capacity of the wind turbine.

(2) Determine the corresponding capacity increment of booster transformer.

(3) Determine the short-circuit capacity of the infinite system.

(4) Determine the value of the overcurrent protection setting of the rotor.

(5) Determine the shafting parameter of the fan set.

(6) Determine the reference value of the power measurement module in the power frequency conversion control system of the rotor.

(7) Determine the average air density on the premise of a constant blowing area of the wind wheel.

The single-fan equivalence method is suitable for aggregation modeling of small wind farms due to its simple and efficient calculation process. However, its accuracy is not satisfactory when applied to large wind farms considering the influence of geographical conditions and the wake effect of the fans.

3 Fan aggregation modeling using multi-fan characterization

3.1 Basic principles

In order to accurately characterize the output properties of a large wind farm, simplify the aggregation model, and shorten the model's simulation time, this paper proposes a multi-fan characterized aggregation model for wind farm. In this model, the fans in the large wind farm are classified according to their operation characteristics. The fans on adjacent operation points are classified as a single class. Moreover, fans of the same class are aggregated into one fan.

3.2 Classification indices for fans

To reasonably and objectively classify the large number of fans in the wind farm, a classification index is required to accurately reflect the operation point of the fans [11-15].

This study investigates the output of the wind farm in the steady state. Due to the differences of the input wind speeds, the fans in the wind farm are placed in different locations. As the wind speed set in the simulation is the mean wind speed, there is no need to take into account the storage and release of the fan rotator energy induced by wind speed fluctuation. Therefore, wind speed can be used as the classification index for the fans.

3.3 Fan classification using the K-means clustering algorithm

In statistics, the K-means algorithm is one of widely used clustering algorithms. The key feature of the algorithm is that N sample points are classified into K clusters based on the principle of minimizing a standard measurement function. Sample points in the same cluster have a high degree of similarity, while those in different clusters show lower degrees of similarity. Different methods of selecting the initial center value used for clustering lead to the K-means algorithm showing disparate clustering accuracy and convergence degrees [16-24]. Generally the K-means algorithm is carried out according to the following steps:

(1) Randomly select K sample points to act as

the initial cluster centers.

(2) Allocate the residual N – K sample points to their nearest clusters according to the distance between the sample point and each cluster center.

(3) Calculate the sample mean of each cluster m and the value expressions of the standard measurement function E are given by

$$m_i = \frac{1}{N_i} \sum_{\tau \in Ci} \tau \ , \ E = \sum_{i=1}^{K} \sum_{\tau \in Ci} |\tau - m_i|^2 \qquad (1)$$

where m_i is the mean of sample cluster i, τ is a sample point, C_i is the set of sample points in cluster i, and N_i is the number of sample points in cluster i.

(4) Substitute the initial cluster center with the sample means from each cluster and repeat steps (2)–(4) until the standard measurement function converges.

It can be seen from the steps above that the algorithm is heuristic, i.e. the convergence of the K-means algorithm is greatly affected by the initial values selected. Therefore, there is no guarantee that the final convergence results represent the optimum solution desired. This problem is solved by repeating the calculation multiple times. The initial values in each set of calculations are randomly selected and are different each time. Finally, the results obtained from each set of calculations are compared to determine the solution with the minimum measurement function. This is taken to be the optimum solution desired.

In this study, the wind speed including the wind wake effect is used for the clustering index of the fan. As the fans are distributed according to a certain law, when initial wind speed is constant, the wind speeds among the fans are similar to each other and show a decreasing order. Therefore, the initial clustering centers selected for the K-means algorithm are K-2 points between the maximum and minimum wind speeds, as well as the minimum and maximum wind speeds themselves.

In the standard K-means algorithm, K is given a constant value. In this study, K is merely given the

initial value K_0 and an upper limiting value of K_{max}, and K is allowed to increase from K_0 to K_{max}. Generally, the larger the value of K, the smaller the value of measurement function, and the more accurate the model. As the value of K increases, the value of measurement function is smaller than a certain given value, the circulation is terminated. The value of K here is the final value. Under the special condition that $n_0 < K_{max}$, where n_0 is the number of kinds of wind speed, the measurement function is zero when $K = n_0$ and fan clustering has achieved the optimum state.

3.4 Aggregation modeling

After the clustering calculation on the fans has finished according to the steps above, the fans in the same cluster can be parameterized and aggregated using the single-fan equivalent method. As the fans in the same cluster are highly similar, the aggregated model is more accurate [25]. After aggregation, the input wind speed of each equivalent fan is set to the mean wind speed of corresponding fan cluster.

4 Fan aggregation modeling of a typical wind farm in northern Jiangsu

4.1 Detail model of wind farm

A 300 MW wind farm in northern Jiangsu Province was chosen for analysis. Fig.1 shows the fan layout in this wind farm. The fans used in this plant are SL3000/113 doubly-fed induction generators (DFIGs) [26]. Each fan has a unit capacity of 3 MW, impeller diameter of 113 m, hub height of 90 m, cut-in wind speed of 3 m/s, cut-out wind speed of 25 m/s, and a rated wind speed of 11.6 m/s [27].
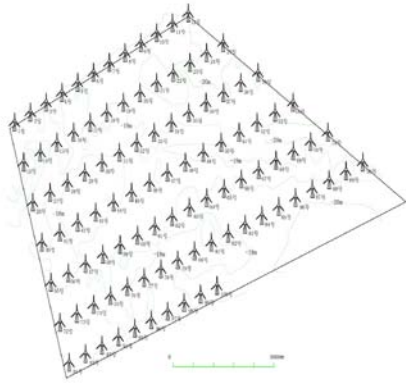
Fig.1. The wind farm in northern Jiangsu

The direction that is vertical to the first row of fans from the inside out is taken to be the positive direction. To compare the output under different wind speeds, four typical simulation scenarios are introduced in this study: (1) 11.6 m/s in the positive direction at an angle of incidence of 0° (i.e. the rated conditions); (2) 15 m/s in the positive direction at 30°; (3) 9 m/s in the positive direction at 60°; (4) 11.6 m/s in the positive direction at 90° (the worst case scenario). Appendix Table 1 lists the equivalent input wind speeds of each fan under the different conditions.

A simplified DFIG model was used for the single-fan model. Then, by adjusting the parameters in this simplified model, a single-fan simplified model of a 3 MW fan in this plant was obtained. Finally, a detailed model of the wind farm (100 fans) was established.

Fans with exactly the same input speed were simplified as multiple identical fans in parallel and expressed as one fan multiplied by the number of fans based on DIgSILENT software. As there were 19 different kinds of wind speed in the wind farm (see appendix Table 1), the wind farm can be represented by 19 sets of parallel fans. Fig.2 shows the detailed model.
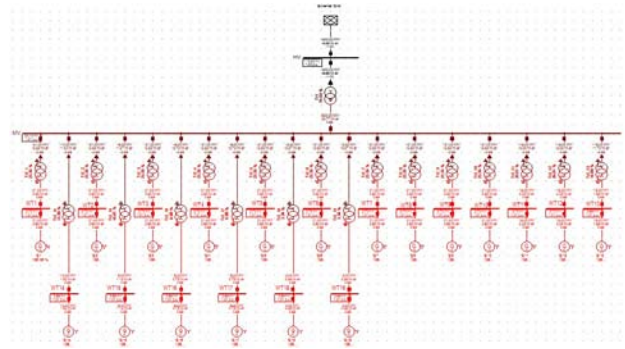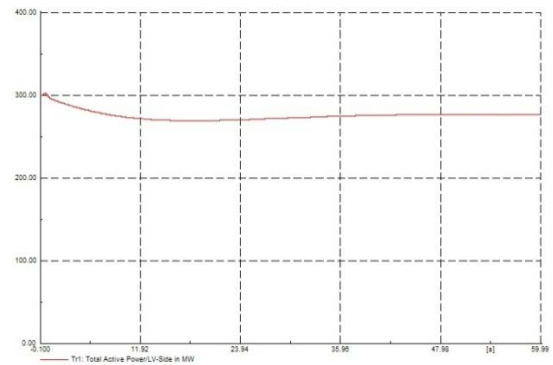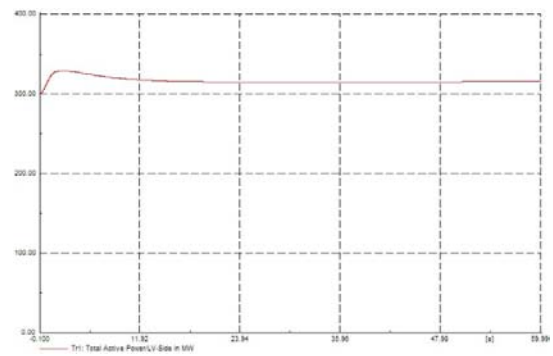

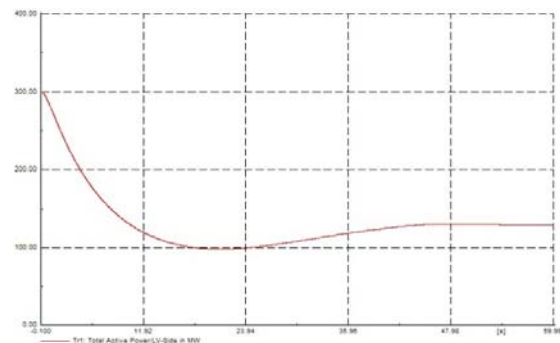Fig.2. The detailed model of the wind farm

Fig.3 illustrates the output results from simulations using the detailed model of the wind farm in the four scenarios.
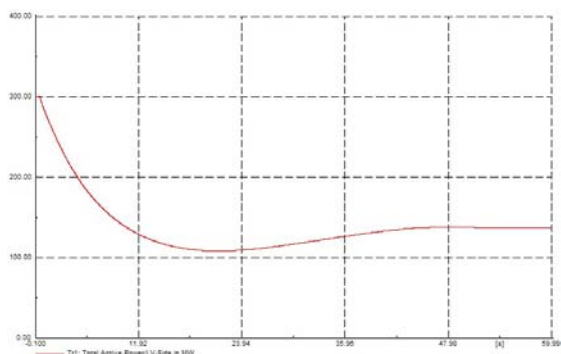

(a) Wind speed of +11.6 m/s, angle = 0°

(b) Wind speed of +15 m/s, angle =30°

(c) Wind speed of +9 m/s, angle =60°

(d) Wind speed of +11.6 m/s, angle =90°
Fig.3. Output of simulations based on the detailed
model of wind farm in the four scenarios

As shown in Fig.3(a), at the rated wind speed, the real output of the 300 MW wind farm is 277 MW due to the wake effect. In Fig.3(b), although the wake effect has attenuated the output, the effective input wind speeds of all fans are still higher than the rated wind speed as the input wind speed is much higher than the rated wind speed. Therefore, by controlling the pitch angle, the output of the fans is ultimately slightly higher than the rated output value. In Fig.3(c), as the wind speed is lower than the rated wind speed, the output from the plant is further weakened after attenuation by the wake effect. In Fig.3(d), the intercepted wind energy from the fans is greatly reduced compared with the rated case in Fig.3(a) due to the extreme conditions (i.e. the wind direction is parallel with the row of fans). The actual output from the wind farm is only 137 MW even though the installed capacity is 300 MW. Generally, the front of the row of fans is set towards the dominant wind direction in the region during the establishment of the wind farm, just as in Fig.3(a). Thus, the condition shown in Fig.3(d) is commonly impossible in practice. For some regions in which the variation in the regularity of the wind direction is not obvious, the distance between the fans in the same row can be increased during establishment of the wind farm to reduce the wake effect.

4.2 Aggregation model of the wind farm

using the single-fan equivalent method

An aggregation model of the wind farm was built using the single-fan equivalent method. The one hundred DFIGs are taken to be equivalent to one fan with large capacity. Table 1 shows the modifications made to the parameters of the DFIG model before and after aggregation.

Fig.4 lists the output results of wind power at the four scenarios given in Section 4.1 using the single-fan aggregation model.

(a) Wind speed of +11.6 m/s, angle = 90°

(b) Wind speed of +15 m/s, angle = 30°
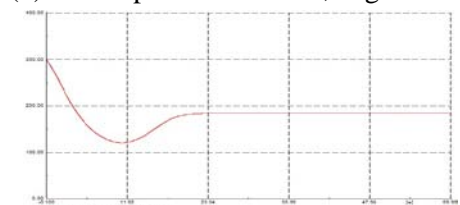
(c) Wind speed of +9 m/s, angle =60°

(d) Wind speed of +11.6 m/s, angle = 90°
Fig.4. Output of the simulations based on the
single-fan equivalent model in the four scenarios

Fig. 4 suggests that for the different given wind speeds, some differences between the output results from the single-fan equivalent model and detailed model are small while others are larger. When the

wind speed approaches the dominant wind speed in wind farm, the output from wind farm is more accurately reflected by the single-fan equivalent model. Otherwise, the simulation results are seriously inconsistent with the actual situation, as shown in Fig.4(d). In Fig.4(a), at the rated wind speed, the single-fan equivalent model suggests a higher output value than that in the detailed model due to the neglect of attenuation by the wake effect. Comparison of Figs.3(a) and 4(a) implies that, at the rated wind speed, the differences under these conditions are about 7.7% or so. Thus, this figure represents the proportion of the wind energy lost in actual wind farms because of the wake effect.

4.3 Fan aggregation modeling based on multi-fan characterization

The models of four scenarios in Section 4.1 were built using multi-fan characterization. The classification index employed in the K-means clustering algorithm was the equivalent input wind speed of each fan, as shown in appendix Table 1. In the K-means clustering model, we set $K_0=4$, $K_{max}=10$, and $\lambda=0.5$, i.e. the wind speed was classified into at least four but no more than ten clusters at most. A measurement function smaller than 0.5 was considered to meet accuracy requirement. Thus the calculation can be terminated. Table 2 shows the equivalent parameters of the multi-fan characterization model for the four scenarios.

Using the data in Table 2, the fan clusters were equivalently aggregated. Fig.5 shows the corresponding simulation results in the four scenarios.
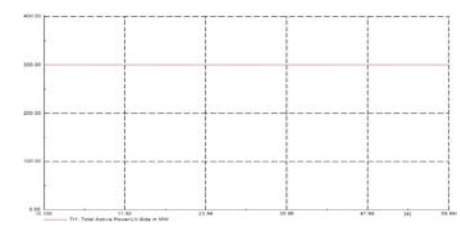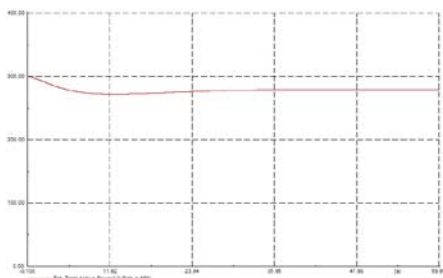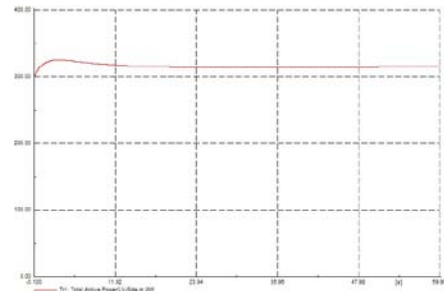

(a) Wind speed of +11.6 m/s, angle = 0°.

(b) Wind speed of +15 m/s, angle = 30° .
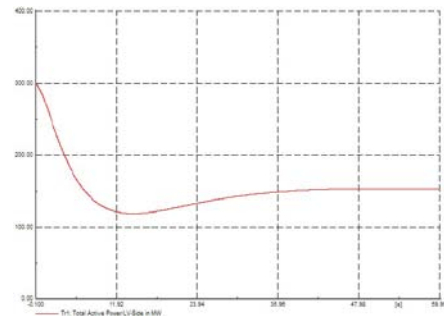
(c) Wind speed of +9 m/s, angle = 60°.
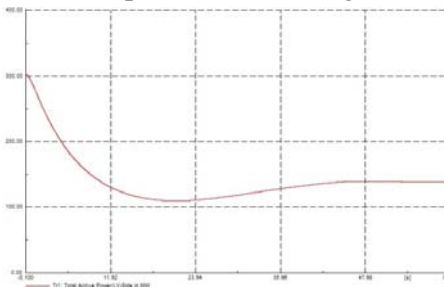
(d) Wind speed of +11.6 m/s, angle = 90°.
Fig.5. Output from the simulations based on the multi-fan characterization in the four scenarios

The multi-fan characterization model is closer to the real condition reflected by the detailed model than the single-fan characterization model shown in Fig.3–Fig.5. Table 3 shows the steady output of the multi-fan aggregation model after simulation for 1 minute. Based on the table 3, the multi-fan aggregation model presents an output phase closer to that of the detailed model than the single-fan equivalent model, especially for the second and third scenario. The error in the second scenario decreased from 32.4% (single-fan aggregation model) to 4.3% (multi-fan aggregation model), while that in the third scenario dropped from 43.9% to 6.0%.

Table 1. Equivalent parameters in the single-fan aggregation model

Index	Single-fan model, before aggregation	Equivalent fan model of the plant after aggregation	Expansion multiple
Rated capacity of the fan set (MVA)	3	300	100
Capacity of the medium voltage step-up transformer (MVA)	3.75	375	100
Capacity of the high voltage step-up transformer (MVA)	4	400	100
Short-circuit capacity of the infinite bus system (MVA)	300	30000	100
Average air density (kg/m^3)	0.0021042	0.443765	210.895
Rotating inertia of the doubly-fed generator (kg·m^2)	6.03	603	100
Shaft elasticity coefficient	120.405	1240.5	100
Output reference value of the fan (MW)	2.25	225	100
Output reference value of the wind motor (MW)	1.970627	197.0627	100
Mutual damping coefficient between the low speed shaft of wind wheel and the high speed shaft of the doubly-fed machine	2.25	225	100
Measurement module reference value of the frequency converter on the rotor side	3	300	100
Rotor overcurrent protection value	2.25	225	100

Table 2. Calculation parameters from the K-means clustering model based on multi-fan characterization

Wind speed of +11.6 m/s, angle = 0°	Equivalent fan number	4			
	Equivalent wind speed of each fan (m/s)	10.7158	10.9476	11.1619	11.6
	Aggregated fan number of each fan	18	15	30	37
Wind speed of +15 m/s, angle = 30°	Equivalent fan number	4			
	Equivalent wind speed of each fan (m/s)	14.0386	14.2777	14.5248	14.9159
	Aggregated fan number of each fan	11	14	16	59
Wind speed of +9 m/s, angle = 60°	Equivalent fan number	4			
	Equivalent wind speed of each fan (m/s)	8.0651	8.3013	8.6219	9
	Aggregated fan number of each fan	12	18	34	36
Wind speed of +11.6 m/s,	Equivalent fan number	8			

angle = 90°	Equivalent wind speed of each fan (m/s)	7.9607	8.1608	8.4018	8.6883
	Aggregated fan number of each fan	13	24	21	14
	Equivalent wind speed of each fan (m/s)	8.9611	9.2487	9.7225	11.6
	Aggregated fan number of each fan	7	7	7	7

Table 3. Simulation results of the models after 1 minute of simulation

Simulation condition	Detailed model (MW)	Single-fan equivalent aggregation model (MW)	Error in the single-fan equivalent aggregation model (%)	Multi-fan equivalent aggregation model (MW)	Error in the multi-fan equivalent aggregation model (%)	Detailed model (MW)
Wind speed of +11.6 m/s, angle = 0°	277	300	8.3	280	1.1	277
Wind speed of +15 m/s, angle = 30°	315	316	0.3	315	0	315
Wind speed of +9 m/s, angle = 60°	139	184	32.4	145	4.3	139
Wind speed of +11.6 m/s, angle = 90°	134	300	43.9	142	6.0	134

5 Conclusions

In this paper, a model of 300 MW wind farm in northern Jiangzu Province was built to study the benefits of aggregation modeling for large wind farms considering wake effects. The wind farm was simulated using a detailed model, a single-fan aggregation model, and multi-fan aggregation model respectively. The detailed model accurately reflected the output of the wind farm. However, this model involves a complex modeling process and has a slow simulation speed. The single-fan characterization method is a simple, convenient, and commonly used aggregation method. Unfortunately, it is prone to generate large errors since it ignores the wind energy loss caused by the wake effect. The improved K-means-based multi-fan characterization method put forward in this paper is flexible, accurate, and produces results rapidly when used to build the model of wind farm. The effectiveness and feasibility of the method proposed are verified by taking a 300 MW wind farm in northern Jiangsu Province as computational examples.

References:
[1] Wang Zhen-hao, Liu Jin-long, Li Guoqing, et al, Power and voltage regulation of wind farm based on EDLC energy storage, *Electric Power Automation Equipment*, Vol.31, No.3, 2011, pp. 113-116.
[2] Bai Hong-bin, Wang rui-hong, Influence of the grid connected wind farm on power quality, *Proceedings of the Chinese Society of Universities for Electric Power System and its Automation*, Vol.24, No.1, 2012, pp. 120-124.
[3] Chen Shu-yong, Dai Hui-zhu, Bai Xiao-min, et al, Impact of wind turbine wake on wind power output, *Electric Power*, Vol.31, No.11, 1998, pp. 28-31.
[4] Huang Mei, Wan Hang-yu, Simplification of

wind farm model for dynamic simulation, *Transactions of China Electrotechnical Society*, Vol.24, No.9, 2009, pp. 147-152.

[5] J. Usaola, P. Ledesma, J. M. Rodriguez, et al, Transient stability studies in grid with great wind power generation: Modelling issues and operation requirements, *IEEE Power Engineering Society General Meeting*, Vol.3, 2003, pp. 1534-1541.

[6] L. M. Fernandez, C. A. Garcia, F. Jurado, et al, Aggregation of doubly fed induction generators wind turbines under different incoming wind speeds, *Power Tech IEEE Russia*, 2005, pp. 1-6.

[7] Li Hui, Wang He-sheng, Shi Xu-yang, et al, Study on equivalent model of wind farms based on genetic algorithm, *Power System Protection and Control*, Vol.39, No.11, 2011, pp. 1-8.

[8] Slootweg J G, Kling W L, Modeling of large wind farms in power system simulations, *Proceedings of the IEEE PES Summer Meeting*, 2002, pp. 25-29.

[9] Miguel Garcia-Gracia, Paz Comech M, Jesus Sallan, et al, Modelling wind farms for grid disturbance studies. *Renewable Energy*, Vol.33, No.9, 2008, pp. 2109-2121.

[10] R. M. G., Castro, J. M., Ferreira de Jesus, An aggregated wind park model, *Proceedings of the 13th Power Systems Computation Conference*, 1999, pp. 1-5.

[11] Mi Zeng-qiang, Su Xun-wen, Yang Qi-xun, et al, Multi-machine representation method for dynamic equivalent model of wind farms, *Transactions of China Electrotechnical Society*, Vol.25, No.5, 2010, pp. 162-169.

[12] Yang Shan-lin, Li Yong-sen, Hu Xiao-xuan, et al, Optimization Study on k Value of K-means Algorithm, *Systems Engineering-theory & Practice*, Vol.26, No.2, 2006, pp. 96-101.

[13] Gao Feng, Zhao Dong-lai, Zhou Xiao-xin, et al, Dynamic equivalent algorithm for wind farm composed of direct-drive wind turbines, *Power System Technology*, Vol.36, No.12, 2012, pp. 222-227.

[14] Fu Rong, Xie Jun, Wang Bao-yun, Study on dynamic equivalence model of wind farms with DFIG under wind turbulence, *Power System Protection and Control*, Vol.40, No.15, 2012, pp. 1-6.

[15] Yan Hui-min, Study on plan and policy of wind power development in Jiangsu, *Jiangsu Electrical Engineering*, Vol.24, No.1, 2005, pp. 8-10.

[16] Hájek, P., Neri, F., An introduction to the special issue on computional techniques for trading systems, time series forecasting, stock market modeling, financial assets modeling, *WSEAS Transactions on Business and Economics*,

Vol.10, No.4, 2013, pp. 201-292.

[17] Azzouzi, M., Neri, F., An introduction to the special issue on advanced control of energy systems, *WSEAS Transactions on Power Systems*, Vol.8, No.3, 2013, pp. 103.

[18] Bojkovic, Z., Neri, F., An introduction to the special issue on advances on interactive multimedia systems, *WSEAS Transactions on Systems*, Vol.12, No.7, 2013, pp. 337-338.

[19] Pekař, L., Neri, F., An introduction to the special issue on advanced control methods: Theory and application, *WSEAS Transactions on Systems*, Vol.12, No.6, 2013, pp. 301-303.

[20] Guarnaccia, C., Neri, F., An introduction to the special issue on recent methods on physical polluting agents and environment modeling and simulation, *WSEAS Transactions on Systems*, Vol.12, No.2, 2013, pp. 53-54.

[21] Neri, F., An introduction to the special issue on computational techniques for trading systems, time series forecasting, stock market modeling, and financial assets modeling, *WSEAS Transactions on Systems*, Vol.11, No.12, 2012, pp. 659-660.

[22] Muntean, M., Neri, F., Foreword to the special issue on collaborative systems, *WSEAS Transactions on Systems*, Vol.11, No.11, 2012, pp. 617.

[23] Pekař, L., Neri, F. (2012) An introduction to the special issue on time delay systems: Modelling, identification, stability, control and applications, *WSEAS Transactions on Systems*, Vol.11, No.10, 2012, pp. 539-540.

[24] Volos, C., Neri, F., An introduction to the special issue: Recent advances in defense systems: Applications, methodology, technology, *WSEAS Transactions on Systems*, Vol.11, No.9, 2012, pp. 477-478.

[25] ZHANG Jian-ping , Zhang Li-bo CHENG Hao-zhong, et al, Evaluation of Probabilistic Load Flow Based on Improved Latin Hypercube Sampling, *East China Electic Power*, Vol.41, No.10, 2013, pp. 2028-2034.

[26] ZHANG Jian-ping ZHANG Xiang CHENG Hao-zhong, et al, Production Simulation of Power System with Wind Farms Considering EPP Influence, *East China Electic Power*, Vol.41, No.9, 2013, pp. 1804-1807.

[27] ZHANG Jian-ping LIU Jie-feng CHENG Hao-zhong, et al, Saturated Load Forecasting Based on Per Capita Electricity Consumption and Per Capita Electricity Load, *East China Electic Power*, Vol.42, No.4, 2014, pp. 661-664.

Appendix

Appendix Table 1. Equivalent wind speed calculation results for a typical 300MW wind farm in northern Jiangsu Province.

(a) Wind speed of 11.6 m/s, with an angle of 0° in the positive direction									
11.60	11.60	11.60	11.60	11.60	11.60	11.60	11.60	11.60	11.60
11.60	11.60	11.60	11.60	11.60	11.60	11.60	11.60	11.60	11.60
11.60	11.60	11.60	11.60	11.60	11.60	11.16	11.16	11.16	11.16
11.16	11.16	11.16	11.16	11.16	11.16	11.16	11.16	11.60	11.60
11.16	11.16	11.16	11.16	11.16	11.16	11.16	11.16	11.16	11.16
11.16	11.16	11.16	11.60	11.60	11.16	10.97	10.97	10.97	10.97
10.97	10.97	10.97	10.97	10.97	10.97	10.97	10.97	11.16	11.60
11.60	11.60	11.16	10.87	10.76	10.76	10.76	10.76	10.76	10.76
10.76	10.76	10.76	10.76	10.76	10.87	11.16	11.60	11.60	11.60
11.60	11.16	10.87	10.64	10.64	10.64	10.64	10.64	10.64	10.64

(b) Wind speed of 15 m/s, with an angle of 30° in the positive direction									
15.00	15.00	15.00	15.00	15.00	15.00	15.00	15.00	14.86	15.00
14.86	15.00	15.00	14.86	15.00	15.00	14.86	14.86	15.00	14.86
14.86	15.00	15.00	14.86	14.86	15.00	15.00	14.86	14.86	14.86
14.86	14.86	14.86	15.00	14.86	14.86	14.86	15.00	14.86	14.86
14.52	14.86	14.86	14.86	14.52	14.86	15.00	14.86	14.52	14.86
15.00	14.86	14.52	14.52	14.86	14.86	14.52	14.52	14.86	15.00
14.86	14.52	14.29	14.86	15.00	14.52	14.29	14.52	14.86	14.52
14.29	14.52	14.86	14.52	14.29	14.29	14.86	14.52	14.29	14.23
14.52	14.29	14.04	14.52	14.29	14.04	14.29	14.29	14.04	14.23
14.29	14.04	14.04	14.29	14.04	14.04	14.04	14.04	14.04	14.04

(c) Wind speed of 7 m/s, with an angle of 60° in the positive direction									
7.00	7.00	7.00	7.00	7.00	7.00	7.00	7.00	7.00	7.00
7.00	7.00	7.00	7.00	7.00	7.00	7.00	7.00	7.00	7.00
7.00	6.72	7.00	7.00	7.00	7.00	6.72	7.00	6.72	7.00
7.00	6.72	7.00	6.72	7.00	6.72	6.72	7.00	6.72	7.00
6.72	6.72	6.72	6.72	7.00	6.72	6.72	6.72	6.72	6.72
6.72	7.00	6.72	6.72	6.60	6.72	6.72	6.72	7.00	6.60
6.72	6.47	6.72	6.72	6.60	7.00	6.47	6.72	6.47	6.60
6.72	6.47	6.47	6.60	6.47	6.47	6.72	6.47	6.47	6.47
6.47	6.47	6.47	6.39	6.47	6.47	6.39	6.32	6.39	6.32
6.30	6.32	6.30	6.30	6.30	6.30	6.24	6.24	6.19	6.13

(d) Wind speed of 11.6 m/s, with an angle of 90° in the positive direction									
11.60	11.60	11.60	9.72	11.60	9.72	11.60	9.72	9.25	11.60

9.72	9.25	11.60	9.72	9.25	8.96	9.72	9.25	8.96	9.72
9.25	8.96	8.76	9.25	8.96	8.76	9.25	8.96	8.76	8.61
8.96	8.76	8.61	8.96	8.76	8.61	8.49	8.76	8.61	8.49
8.76	8.61	8.49	8.40	8.61	8.49	8.40	8.61	8.49	8.40
8.31	8.49	8.40	8.31	8.49	8.40	8.31	8.24	8.40	8.31
8.24	8.40	8.31	8.24	8.31	8.24	8.18	8.31	8.24	8.18
8.24	8.18	8.12	8.24	8.18	8.12	8.18	8.12	8.07	8.18
8.12	8.07	8.12	8.07	8.03	8.12	8.07	8.03	8.07	8.03
7.98	8.03	7.98	7.98	7.95	7.95	7.91	7.91	7.88	7.85

An Approach to Developing Power Grid Control Systems with IEC 61850, IEC 61499 and Holonic Control

VALENTIN VLAD, CORNELIU BUZDUGA, CALIN CIUFUDEAN
Electrical Engineering and Computer Science Department
Ştefan cel Mare University of Suceava
Str. Universităţii, 13
ROMANIA
{vladv | cbuzduga | calin }@eed.usv.ro

Abstract: - This paper presents some models and concepts for developing smart power grid control systems based on holonic concepts and the open standards IEC 61850, IEC 61499. Along with the proposed holonic models for different levels of control, we present a simple fault protection application illustrating how the IEC 61499 artifacts can be used for modeling and implementation of IEC 61850 compliant applications.

Key-Words: power grid, holonic control, IEC 61499, IEC 61850

1 Introduction

In the last years an increase in the degree of automation and intelligence of power grids can be observed, the future trends being on developing the so called "smart grid", which should allow a more efficient management of energy consumption, a more robust behavior in case of perturbations (e.g. equipment failures or fluctuations in energy production or consumption) and the facile integration of renewable energy sources [1].

The complexity of the decision process in the smart grid imposes its distribution to the low levels of measuring and automation devices rather than being realized in a centralized form as in the majority of the actual distribution networks. Consequently, on the information and communication technology (ICT) side the focus of current research is on developing distributed control architectures based on open standards like FIPA (Foundation for Intelligent Physical Agents), IEC 61850 and IEC 61499, with a view to support the decision-making process and to allow the effective integration and interaction between different automation devices [2]-[16].

2 IEC 61850

IEC 61850 is an important new international standard for substation automation, considered to have a significant impact on how electric power systems are designed and built for many years to come [17]. Focused on communications between automation devices, the standard deals not only with the specification of protocol elements (like legacy communication protocols) but also with the internal organization of data in devices, which allows for a better interoperability and easier configuration of devices [18].

The standard adopts a model-driven approach by standardizing device, object and service models. The control logic resides in microprocessor-based devices named *intelligent electronic devices (IED)*, equipped with one or more microprocessors, memory, and communication interfaces (e.g. serial ports, Ethernet interfaces), like the everyday used computers. IEDs can be classified by their functions, common types including relay devices, circuit breaker controllers, recloser controllers, voltage regulators, etc. One IED can perform more than one function, given its general-purpose microprocessors [19].

An IED is defined by its network address and may contain one or more *logical devices*. Each logical device contains one or more *logical nodes* (LN), which are named grouping of data and associated services, logically related to some power system function. There are logical nodes for automatic control, for metering and measurement, for supervisory control, protection, switchgears, etc. Each logical node contains one or more elements of Data each with a unique standard name. Each element of data within the logical node conforms to the specification of a common data class (CDC), describing the type and structure of the data.

The abstract model of the device is mapped to a specific communication protocol stack based on MMS (Manufacturing Messaging Specification – ISO 9506), TCP/IP, and Ethernet [20]. In this mapping, the standard specifies a method of transforming the model information into a named

MMS variable object that allows the unique identification of each element of data in the model. The communication services defined by the Abstract Communication Service Interface (ACSI) are also mapped to MMS Services.

In addition to the MMS mapping, the standard defines profiles also for other type of communication, as depicted in Fig. 1: the Sampled Values and GOOSE (Generic Object Oriented Substation Events) applications map directly into the Ethernet data frame thereby eliminating processing of any middle layers; the Generic Substation Status Event (GSSE) is the identical implementation as the UCA (Utility Communication Architecture) GOOSE and operates over connectionless ISO services; TimeSync messages use the UDP/IP protocol.

Fig. 2 illustrates the substation architecture defined by the standard IEC 61850. The monitor and control equipment is placed on three levels, namely process, bay and substation level.

The process level is related to gathering information, such as voltage, current, and status information from the transformers and transducers connected to the primary power system equipment. This information is digitized by Merging Units and transmitted to the upper level through a "process bus", realized as a high bandwidth Ethernet network.
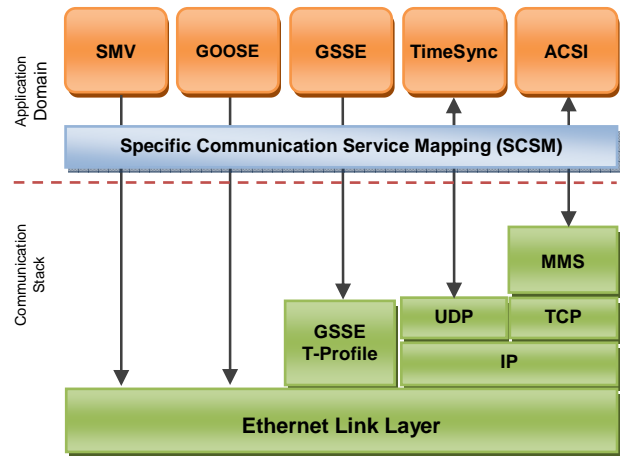

Fig. 1. IEC 61850 communication profiles [17]

The bay level includes Intelligent Electronic Devices (IEDs) running applications for protection and control, and communicating with each other through a "station bus". The substation bus is realized as a medium bandwidth Ethernet network, which carries all ACSI requests/responses and generic substation events messages (including GOOSE and GSSE). A substation usually has only one global substation bus but multiple process buses, one for each bay. On *the station level* there are applications for monitoring and control of the whole station. Remote network access is supported through a secure gateway.
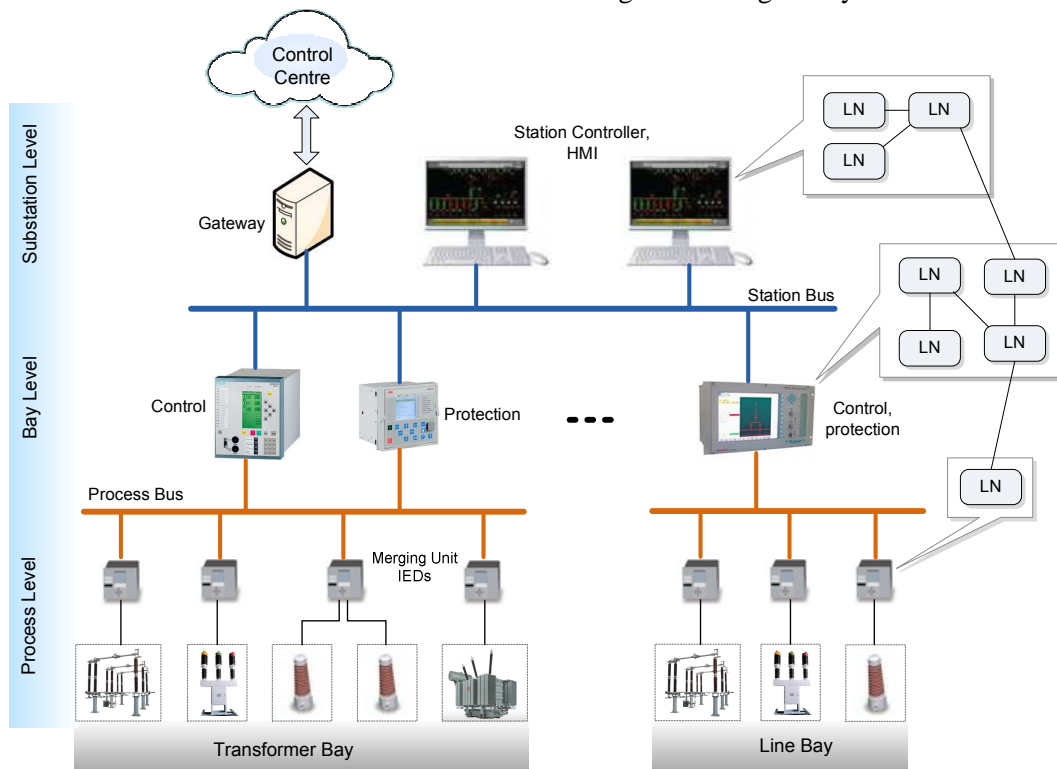

Fig. 2. Substation architecture according to IEC 61850

3 IEC 61499 standard and holonic concepts

3.1 IEC 61499

The IEC 61499 standard defines an open architecture for distributed control and automation. The programming unit of the IEC 61499 is the function block. There are three types of function blocks: basic function blocks, composite function blocks and service interface function blocks. A basic function block executes an elemental control function, such as reading a sensor or setting the state of an actuator, and contains algorithms and an execution control chart (ECC). Basic function blocks may be combined together in a composite function block, to encapsulate a higher-level control function. The service interface function blocks have the role to abstract the specific functions of a hardware platform, allowing the application developer to focus on the application logic. A common example of service interface function blocks is represented by those for communication services [21].

Other key elements of distributed control architecture under IEC 61499 are application, device and resource. An application is a related set of functions that must talk to each other to fulfill a control task. A device is a control unit having one or more processors. It interfaces to the physical I/O and also communicates with other devices on the network. A resource is essentially a processor on which part of a distributed application will run.

3.2 Holonic concepts

Holonic concepts originate in the observations of writer Arthur Koestler about the way biological systems and social organizations are constructed. Koestler introduces in 1969 the term „holon", as a combination of two words from the Greek "holos", meaning "whole" and "on", meaning "particle", to describe the idea that components within a complex system behave both as a whole which can be divided into subcomponents and as a component which belongs to a greater whole [22].

The holons are characterized by autonomy and cooperation, and collaborate in order to accomplish the global objectives of the system. Holons are organized in dynamical hierarchies, called holarchies. Holarchies are recursive in the sense that a holon in a holarchy can in itself be an entire holarchy of other holons. Holons on the lowest level, which do not include other holons, are called simple holons (or elementary holons), while the holons representing holarchies of holons are called complex holons.

Different research works for applying holonic concepts in modeling the power distribution grid are reported by the scientific literature, e.g.[23], [24].

4 Holonic models for power grid control systems

The power distribution systems include a large and diversified range of equipment, from equipment within power substations to the domestic renewable energy sources and smart appliances. In defining the architecture of holons we focused on the area of power substations, but the proposed models can easily be extended to other areas.

A holon is an intelligent entity with decision-making capabilities, which can interact with other holons to collect information for his decisions or provide information to them.

In structuring the control of the power stations according to the holonic principles, we tried to keep the architecture and models defined by the IEC 61850 specifications. As showed in Figure 1, the standard groups control functions and data in logical nodes (LN) placed on different control levels (process, bay, and station) and distributed among several Intelligent Electronic Devices (IEDs). The process level is dedicated mainly to the acquisition of data from the primary equipment, transmission of this data to the devices on the upper levels, and execution of the received control commands. The devices on the bay level include logical nodes for protection and control of the primary equipment, which in some cases collect information from other bays for their decisions. Due to these control responsibilities, we decided to define the simple holons at the bay level. A simple holon will include in this case the primary equipment of a bay, the modules for acquisition and transmission of data, the IEC 61850 logical nodes for protection and control of the bay, and an intelligent component for local decision and interaction with other holons. Fig. 3 depicts the proposed general architecture of a simple holon.
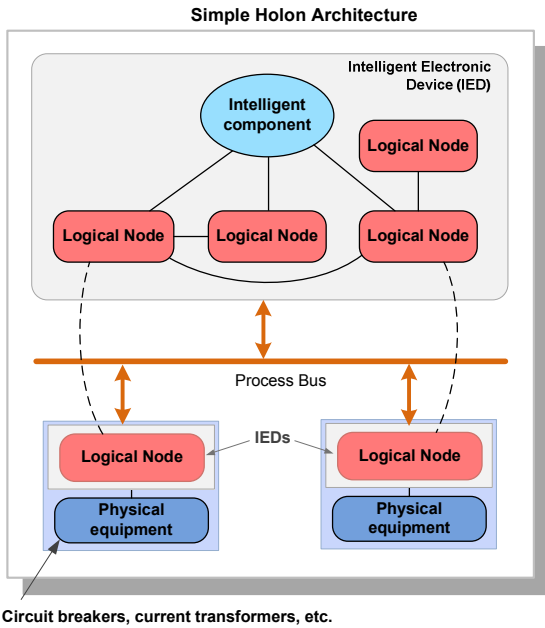
Simple Holon Architecture

Fig. 3. Architecture of a simple holon

Fig. 4. Example of a simple holon for a transformer bay
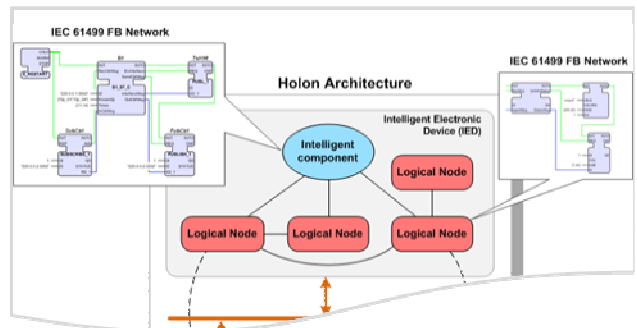
Fig. 5. Implementation of the control logic through IEC 61499 models

Figure 4 contains the example of a simple holon modelling a transformer bay. The meanings of the acronyms for the IEC 61850 logical nodes are given bellow.

XSWI	Circuit switch
XCBR	Circuit breaker
TCTR	Current transformer
YLTC	Tap changer
CSWI	Switch controller
CILO	Interlocking
MMXU	Measurement
PTOC	Protection Time Overcurrent
ATCC	Automatic tap changer controller

For the implementation of the control logic we chose the specifications of the IEC 61499 standard, both for the IEC 61850 logical nodes and the intelligent component of the holon, as illustrated in Figure 5.

The simple bay holons can be grouped along with station-level control components in a complex holon, representing the whole substation. The communication between the bay holons is done through the station bus, as illustrated in Figure 6.

Different substation holons in a region can be further grouped in a complex holon with high-level goals such as optimizing the distribution of energy in that region and reducing the effects of perturbations.
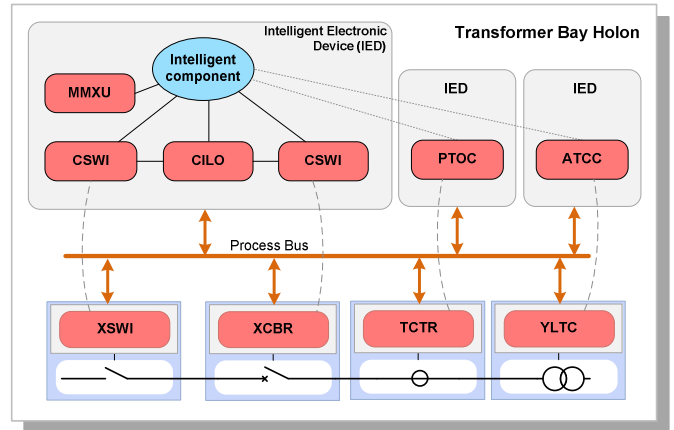
The holonic concepts and models developed can be used beyond the area of power substations, wherever there is an opportunity for operation efficiency improvement through smart control. Examples on the customer side include smart appliances, electric vehicles and micro-CHP units.

5 Example of protection application with IEC 61499 function blocks and GOOSE messages

This section presents a minimal protection application, modeled and implemented with IEC 61499 artifacts. The fault protection scenario, which is illustrated in Fig. 7, involves the transmission of GOOSE messages between several IEC 61850 logical nodes for tripping the circuit breaker and for publishing its new position.
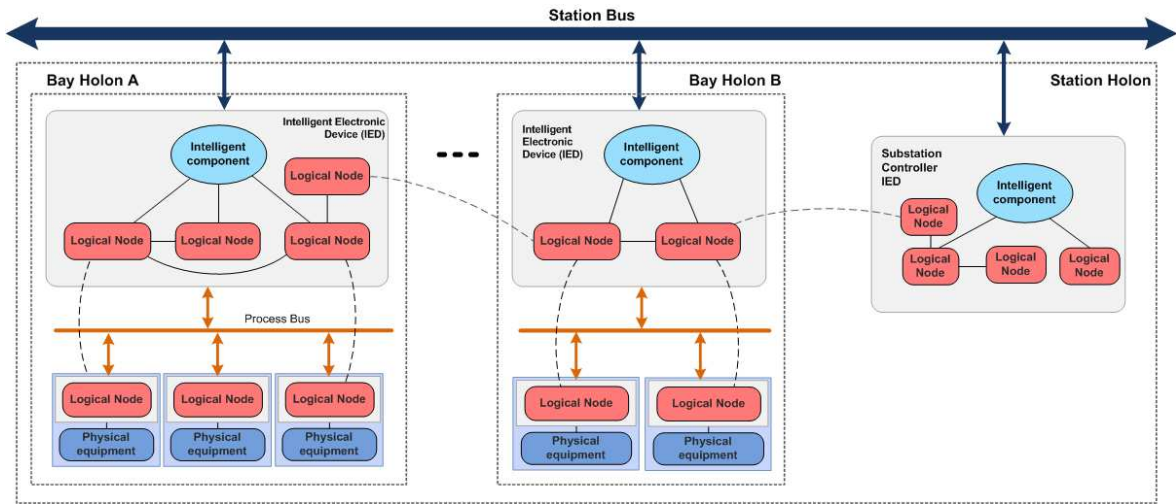
Fig. 6. Simple bay holons grouped in a complex station holon

The values measured by the current transformer (CT) are transmitted to a PTOC logical node. When an overcurrent is detected, PTOC communicates the anomalous condition to the PTRC (Protection trip conditioning) LN, which issues a *trip* command (in form of a GOOSE message) to the XCBR LN. As a result the circuit breaker (CB) is open and the new status is transmitted (also through GOOSE messages) to the PTRC and RREC (Auto-reclosing) logical nodes. After a short time, RREC issues a *reclose* command to the XCBR LN, which closes the circuit breaker and publishes its new status.

As shown in Fig. 8, the IEC 61499 system modeling the fault protection application includes three IEC 61499 devices: *BreakerIED*, *ProtectionIED* and *DISPLAY*. The BreakerIED device contains the XCBR logical node (modeled as a service interface function block), while the

ProtectionIED encapsulate the protection and autoreclosing logical nodes. The DISPLAY device includes two function blocks for modeling and visualization of the physical equipment, i.e. the circuit breaker and the current transformer.

Fig. 9 presents the visualization display and the function blocks behind it. The user is able to set the value of the feeder current between two limits with a slider. The set values are transmitted continuously to the PTOC logical node through IEC 61499 publish/subscribe communication services. When the values exceed a certain threshold (e.g. 20 units), the logical nodes undertake the protection scenario presented in Fig. 7. The opening of the circuit breaker will set the slider at the zero value, while the reclosing will set it at a non-zero low value (e.g. 10 units).
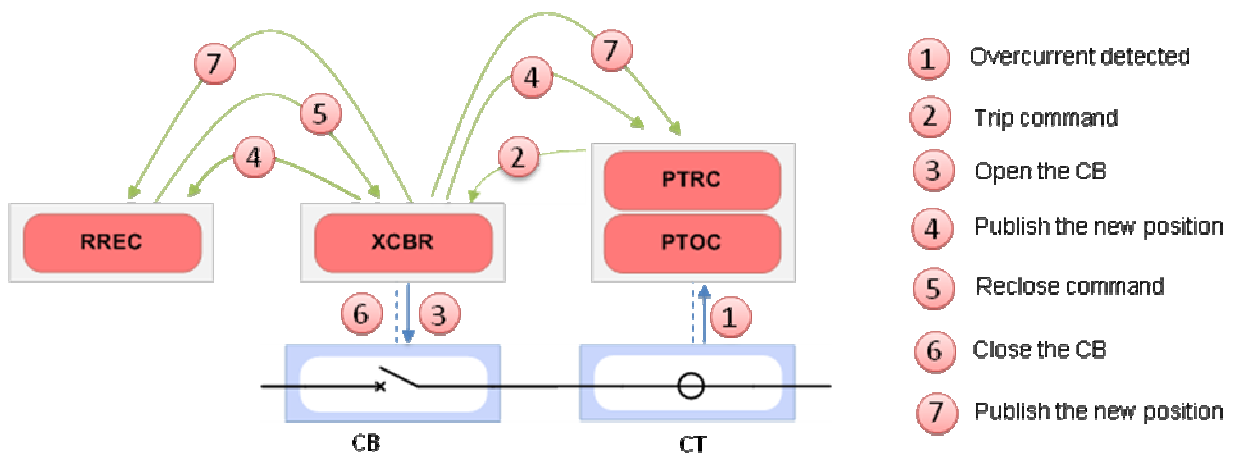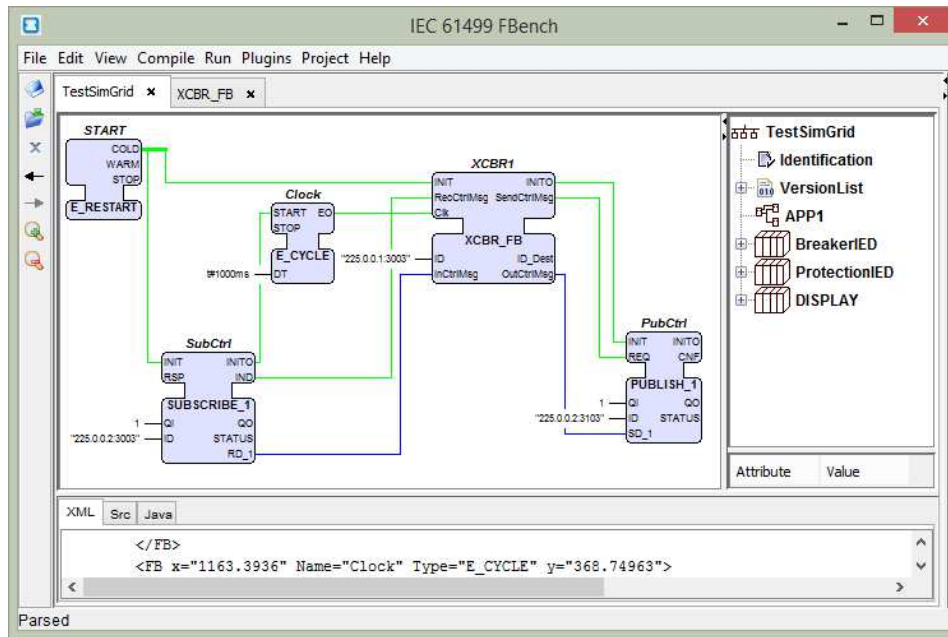

Fig. 7. Fault protection scenario

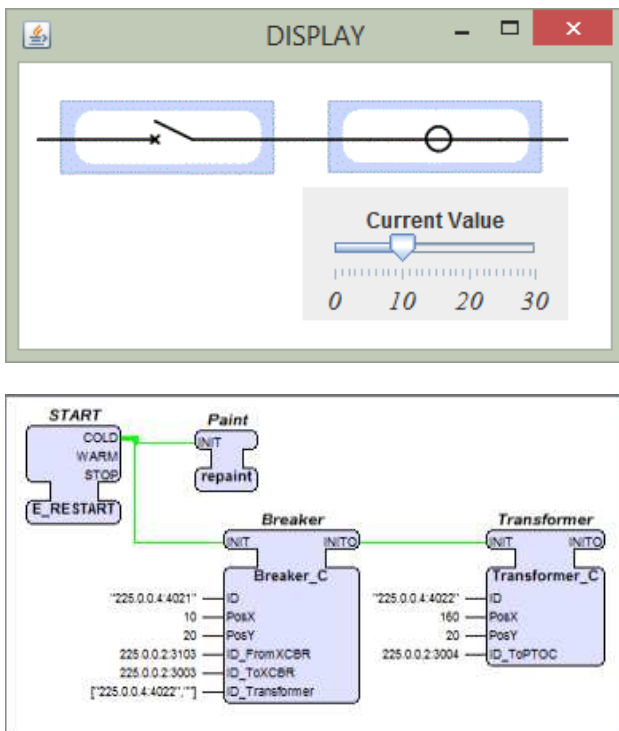Fig. 8. The IEC 61499 system modeling the fault protection application

Fig. 9. The visualization display and the corresponding function blocks

References:

[1] J. Moonjong, B.N. Ha, S.W. Lee, D.Y. Seo, The Study on the Construction of the Smart Grid Test Plant and the Integration of the Heterogeneous Systems, *WSEAS Transactions on Power Systems,* Vol. 8(2), 2013, pp. 95-101.

[2] M. Azzouzi, F. Neri, An introduction to the special issue on advanced control of energy systems, *WSEAS Transactions on Power Systems*, 8 (3), 2013, p. 103.

[3] P. Karthikeyan, F. Neri, Open research issues on Deregulated Electricity Market: Investigation and Solution Methodologies. *WSEAS Transactions on Systems*, 13, in press.

[4] M. Panoiu, F. Neri, Open research issues on Modeling, Simulation and Optimization in Electrical Systems. *WSEAS Transactions on Systems*, 13, in press.

[5] C. Guarnaccia, F. Neri, An introduction to the special issue on recent methods on physical polluting agents and environment modeling and simulation. *WSEAS Transactions on Systems*, 12 (2), pp. 53-54.

[6] A.V. Doroshin, F. Neri, Open research issues on Nonlinear Dynamics, Dynamical Systems and Processes. *WSEAS Transactions on Systems*, 13, 2014, in press.

[7] C. Ciufudean, F. Neri, Open research issues on Multi-Models for Complex Technological Systems. *WSEAS Transactions on Systems*, 13, 2014, in press.

[8] F. Neri. Open research issues on Computational Techniques for Financial Applications. *WSEAS Transactions on Systems*, 13, 2014, in press.

[9] F. Neri, Open research issues on Advanced Control Methods: Theory and Application.

WSEAS Transactions on Systems, 13, 2014, in press.

[10] P. Hájek, F. Neri, F. An introduction to the special issue on computational techniques for trading systems, time series forecasting, stock market modeling, financial assets modeling, *WSEAS Transactions on Business and Economics*, 10 (4), 2013, pp. 201-292.

[11] Z. Bojkovic, F. Neri, An introduction to the special issue on advances on interactive multimedia systems, *WSEAS Transactions on Systems*, 12 (7), 2013, pp. 337-338.

[12] L. Pekař, F. Neri, An introduction to the special issue on advanced control methods: Theory and application, *WSEAS Transactions on Systems*, 12 (6), 2013, pp. 301-303.

[13] F. Neri, An introduction to the special issue on computational techniques for trading systems, time series forecasting, stock market modeling, and financial assets modeling, *WSEAS Transactions on Systems*, 11 (12), 2012, pp. 659-660.

[14] M. Muntean, F. Neri, Foreword to the special issue on collaborative systems, *WSEAS Transactions on Systems*, 11 (11), 2012, p. 617.

[15] L. Pekař, F. Neri, An introduction to the special issue on time delay systems: Modelling, identification, stability, control and applications, *WSEAS Transactions on Systems*, 11 (10), 2012, pp. 539-540.

[16] C. Volos, F. Neri, An introduction to the special issue: Recent advances in defense systems: Applications, methodology, technology, *WSEAS Transactions on Systems*, 11 (9), 2012, pp. 477-478.

[17] R. E. Mackiewicz, "Overview of IEC 61850 and Benefits", *Power Engineering Society General Meeting*, 2006, pp. 8.

[18] H. Ito, K. Kaneda, K. Hamamatsu, T. Tanaka, K. Nara, Improvements in Dependability and Usability fora Substation Automation System with Redundancy, *WSEAS Transactions on Systems*, Vol. 7 (10), 2008, pp. 1104 – 1116.

[19] S. Aggarwal, Security Hub Architecture Support for IEC61850 Information Exchange Protocols, *2012 IEEE PES Innovative Smart Grid Technologies Conference*, 16-20 January, Washington, SUA.

[20] *IEC 61850 Communication Networks and Systems in Substations*, IEC 61850, 2004.

[21] V. Vyatkin, IEC 61499 Function Blocks for Embedded and Distributed Control Systems Design, *Instrumentation Society of America*, 2007, USA.

[22] A. Koestler, The Ghost in the Machine, *Arkana Books*, London, 1969.

[23] E. Negeri, N. Baken, M. Popov, Holonic Architecture of the Smart Grid, *Smart Grid and Renewable Energy*, Vol.4, 2013, pp. 202-212.

[24] A. Pahwa et al. Holonic Multi-agent Control of Power Distribution Systems of the Future, *Cigre Grid of the Future Symposium*, 2012, Kansas City, Missouri - United States of America.

CAM-based Digital Image Watermarking Revisited

Mohamed Tahar Ben Othman, Senior Member, IEEE
Computer Science Dept., College of Computer,
Qassim University,
KINGDOM of SAUDI ARABIA
Emails: maathaman@qu.edu.sa; mtothman@gmail.com

Abstract: The Content Addressable Method (CAM) is used in a new RGB image watermarking system. The image is divided into clusters indexed by CAM technique. Each cluster holds part of the watermark in sequence. A cluster is segmented into equal portions each of them is used to duplicate a number of bits of the watermark. These portions are numerated by a counter added to some LSB bits of the pixels. We used two techniques for this segmentation. In the first technique, the cluster's pixels are allocated to a portion in a first visited first allocated FVFA way. The counter is added to portions in sequence. In second technique, a Content Based Counter CBC is used to allocate pixels to the portion and a uniform redistribution is made for each cluster. The redistribution is done in a way to minimize the modifications in counter space. Both techniques show robustness resisting to rotation attacks. The CBC performs better as it minimizes the Number of Bit Change Rate (NBCR) in the counter field. Using CBC our watermarking system resists better to cropping attacks.

Key-Words: watermarking, image rotation, clustering, color images, Content Addressable Method, Content Based Counter.

1 Introduction

Several watermarking systems have been proposed for digital image protection. On the other hand, the large number of attacks which appear as fast as new algorithms are proposed emphasizes the limits of these latter. The need of image watermarking is growing for different aspects among which: data privacy, image integrity, authenticity, tamper detection and image correction, and confidentiality. Images can be tampered either by accidental or intentional attacks. To preserve the aforementioned aspects, intensive researches were conducted in the last decade. Image watermark is widely used for such purpose.

Digital image watermarking is different from steganography which in its turn different from Cryptography. Cryptography is defined as the art and science of secret writing. The word comes from Greek where the words kruptos and graphen mean secret and writing, respectively. The focus in cryptography is to protect the content of the message and to keep it secure from unintended audiences. On the other hand, steganography is the art and science of hiding information in ways that prevent the detection of hidden messages.

Steganography literally means "covered writing" and is usually interpreted to mean hiding information in other information. Comparing it to cryptography, steganography has its advantage because the message itself will not attract the audiences, as the very nature of a steganography system is to hide the message in an imperceptible manner. Watermarking is the process of embedding a message on a host signal. Watermarking, as opposed to steganography, has the additional requirement of robustness against possible attacks. Fig. 1 presents the general watermarking system.

i: original image.
w: watermark.
wi: watermarked image.
awi: attacked watermarked image.
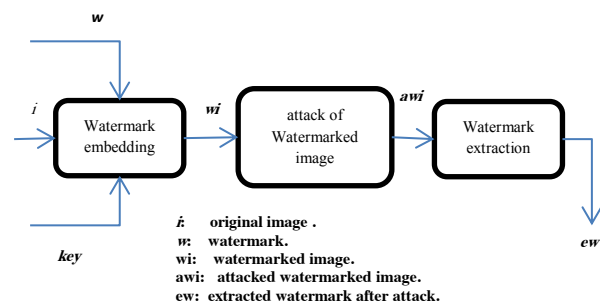ew: extracted watermark after attack.

Fig. 1: General watermarking system

There are two main watermarking domains namely spatial and frequency domain [14]. In spatial domain

techniques the watermark is embedded directly into the pixel data. In frequency domain techniques a transformation of the image to the frequency domain is made first using transforms such as SVD, DCT, DFT, or DWT. The watermark is embedded to the frequency domain coefficients and then the inverse transform is performed to restore the watermarked image. Several techniques were used for image watermarking and used to maintain a certain level of some aspects mentioned above among these techniques are: Matrix Norm Quantization [1,2], Hamming Codes [3], Singular Value Decomposition watermarking [4,5], DFT [5,6], Arnold Scrambling [7], Dual-Tree wavelet transform (DWT) [5,8], Discrete Cosine Transform (DCT) [8]. Some solutions mixed both spatial and frequency domains [16] to get better results. Several papers discussed the open research issues like in [17-31]. Our work is spatial watermarking technique based on image clustering using the Content Addressable Method (CAM). Each cluster contains all pixels of the image which have the same content address provided by the CAM technique.

The rest of this paper will be as follows: A review of the related works is presented in Section 2. Introduction to watermarking domains is presented in Section 3. The proposed System is given in Section 4. Section 5 shows the different experiments results, followed by a conclusion and future directions in Section 6.

2 Related works

In this section, we will give a brief study of some researches that used clustering in their watermark system. Lingling *et al* used in [9] the Statistical Quantity Histogram (SQH) shifting and clustering to construct a new watermark system for good robustness and low run-time complexity. They obtained comprehensive performance in terms of reversibility and robustness. Their work focused mainly on different masking models for various kinds of attacks. In [10], Yan Haowen proposed a watermarking technique by shuffling the cover image, extracting the feature points of the data which are grouped as clusters and then the watermark is embedded in the LSBs. This system is proposed mainly to protect copyrights. No intensive experiments were conducted which gives the main drawback of this technique. An enhancement of a watermarking algorithm based on kernel fuzzy clustering and singular value decomposition in the complex wavelet transform domain is proposed in [11]. The host image, also referred to as cover image,

is decomposed by complex wavelet transform. Then, the singular value of the low-frequency coefficients is selected as an embedded object. Finally, image low-frequency background and high-frequency texture features are used as fuzzy clustering feature vectors to determine the different embedding strength. The results show that the proposed system performs well against different kinds of attacks. Against image rotation (5°, 15°) the Normalized Correlation (NC) is going from 0.93 to 0.98 depending on images. Duc-Hung Le *et al* proposed in [12] a new watermarking extraction based on Content Addressing Memory FPGA. They implemented their system on hardware using FPGA to fast watermarking extraction from 2-dimension (2-D) data. The aim of this research was mainly to minimize the data extraction time without taking into account the possibility of attacks which main corrupt these data. In this paper we are proposing a new approach of image clustering which is called Content Addressing Method (CAM) for color images. Using the defined clusters, watermarks are embedded and extracted. The aim of this paper is to show the robustness of this system against image rotation attacks.

3 Watermarking domains
3.1 Spatial vs. frequency domains
The spatial domain techniques are based on direct modification of the values of the image pixels. The watermark is embedded by modifying these pixels. These techniques are simple and computationally efficient, because they modify the color, luminance or brightness values of a digital image pixels, therefore their application is done very easily, and requires minimal computational power [16]. The techniques are generally used with color images.

The Frequency (transform) domain techniques are based on a transformation of the cover image using a reversible transformation. Commonly used frequency-domain transforms include the Discrete Wavelet Transform (DWT), the Discrete Cosine Transform (DCT) and Discrete Fourier Transform (DFT). However, DWT has been used in digital image watermarking more frequently due to its excellent spatial localization and multi-resolution characteristics, which are similar to the theoretical models of the human visual system. The watermark is embedded by the modification of the resulting transformation's coefficients. After which, the inverse transformation produces the watermarked image. This approach distributes irregularly the watermark over the image pixels after the inverse transform, thus making detection or manipulation of the watermark more difficult [16].

The watermark is usually embedded in the middle frequencies of the image, avoiding in one side the most important parts of the image (low frequencies) to not disturb the image visualization and avoiding in the other side the parts presented by high frequencies, which are easily destroyed by a compression or a scaling operation.

Compared to spatial domain techniques, the works done using frequency-domain watermarking techniques demonstrates that these techniques proved to be more effective with respect to achieving the imperceptibility and robustness requirements of digital watermarking algorithms. On the other hand, the frequency based techniques are more complicated and require more computational power than spatial techniques.

Other works combine two or more techniques to further performance improvements. Some use combination between frequency-domain techniques and some use combination between frequency and spatial domain techniques in order to compensate for the drawbacks introduced by each.

Our proposed system (scheme) is a spatial-domain watermarking technique. We demonstrate that using our CAM-based algorithm the proposed system resists better to rotation attacks than frequency-based techniques.

3.2   Watermarking properties
There are several properties that researchers are looking to meet at a certain level among which:
1) Robustness: A digital watermark is called robust (vs. fragile/semi-fragile) if it resists a designated class of transformations.
2) Perceptibility: the hidden watermark should not deteriorate too much the perceived quality of the medium.
3) Capacity: how much information can reliably be hidden in the cover image is very important to users especially when the system gives them the ability to change this amount.
4) Complexity: some applications like in telemedicine require real time embedding and/or detection.

A compromise should be set between these properties as they cannot be all met at a high level in the same time.

4 Proposed System
4.1 Watermark Scheme algorithm
Our watermarking scheme proposed in [13] is shown in Fig. 2. It consists of five steps: 1) the cover image is divided into clusters, 2) the watermark image is imbedded into the cover image using clusters, 3) attack the watermarked image, 4) run clustering method again for result image, and 5) extract watermark from the attacked image using clusters.

1. cover image clustering
2. imbed watermark image into cover image using clusters
3. attack watermarked image
4. attacked watermarked image clustering
5. extract watermark from attacked image

Fig. 2: Watermark Scheme Algorithm

4.2   Image Clustering
The clustering method is shown in Fig. 3. The upper 4 bits for each RGB component are used as arguments for a function to produce a value used as address regrouping all entries sharing the same feature. In this paper, this function is taken as simple as concatenating three bits from each. This yields to an address of 9 bits which gives a maximum of 2^9=512 entries in each cluster.

The clustering function $f(x,y,z)$ should be chosen so that the distribution goes uniform as much as possible.
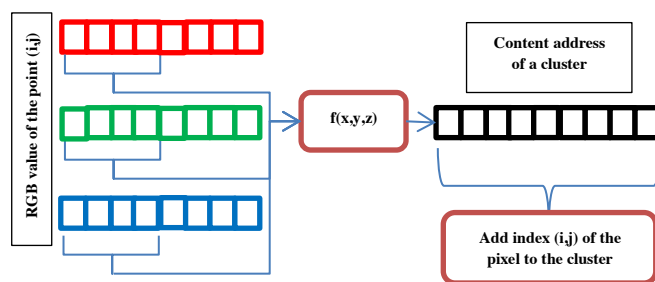

Fig. 3: Clustering Method

The clustering algorithm is going through all cover image pixels and including each pixel indexes in its cluster as shown in Fig. 4.

4.3   Embedding Process
The cover image is scanned using the clusters indexing instead of its own indexing as in Fig. 4. The pixels in each cluster are divided into a number of portions (or sub-cluster), we are using 64, depending on the number of bits that are used to maintain the

sequence number of the portion in the cluster (we are using 6 bits). Into each portion are duplicated one to three bits from the watermark image. These settings are parameters that should be chosen according to the number of clusters and the size of the watermark image. The maximum size of the watermark portion embedded in a full cluster is described in Table 1.

The three bits of the watermark image are embedded into 3 of the 4 LSB bits of one of RGB values (say R). The fourth bit is used as parity bit (for error detection). A portion sequence number (counter) is maintained to distinguish between the embedded data and to maintain their sequencing. This counter is written in 3-6 of the LSB bits of the remaining RGB values. A parity bit is also maintained in the fourth bit of each for error detection. The 3 bits extension of

the counter is taken from the parity bit protection of the four MSB of RGB values used in [13]. The reason we took out this protection comes from the fact that an image with a certain level of visualization cannot be impacted a lot in its MSB part.

Table 1: Embedded data size per cluster

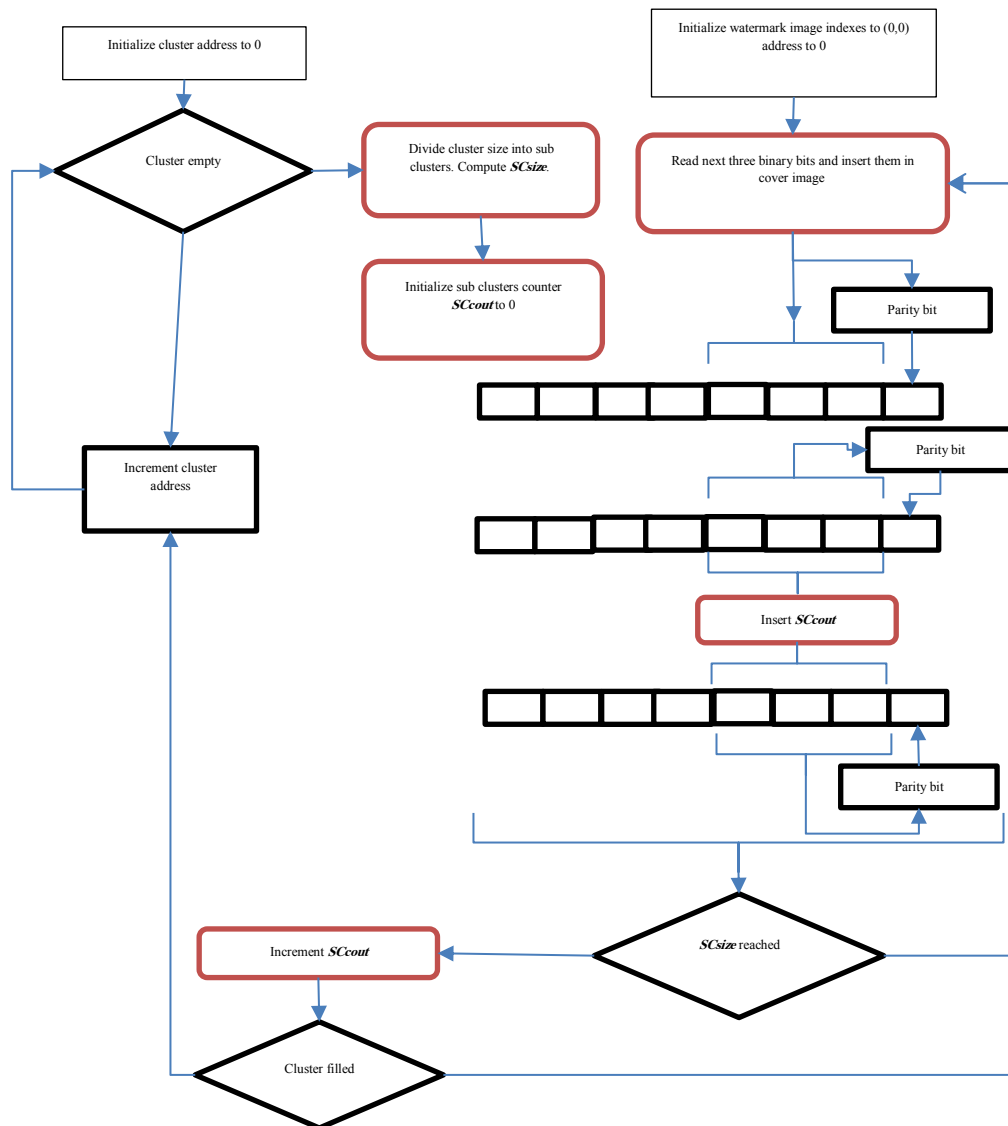| data_size/counter_size (bits)	Embedded Watermark size per cluster (bits)
3/6	192
2/7	256
1/8	256

Fig. 4: Embedding Process

4.4 Extracting Process

Fig. 5 is describing the Extracting process algorithm. Before executing the extracting phase, a new clustering process should take place. Again the image should be scanned using the clustering indexing. The watermark should be found in sequence from the first cluster until the last cluster. If the cluster is not empty, all pixels in this cluster are checked, parity bits are verified and a decision table is built as in Fig.5.
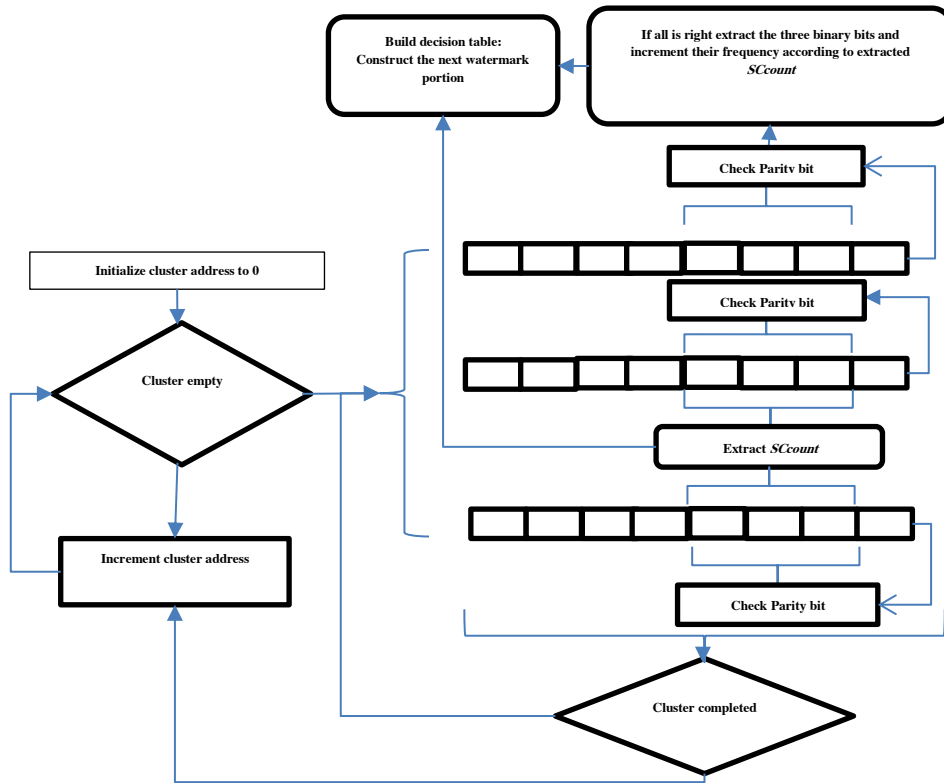

Fig. 5: Extracting process

A decision table is built for the data extracted from each cluster. Fig. 6 presents the decision table. A cluster contains 8x3 bits of watermark data. If a pixel is included in the current cluster and in case all parity bits are checked with no error detection, the counter and the watermark data are extracted and used as indexes to the decision table.

The entry is then incremented giving the number of times the data was found under the same counter without error detection. The column index of the entry with the highest counter gives the data. The order of the 8x3 bits is given by the counter: the first row contains the first three bits etc…

The drawback of this method is caused by the non-detected errors which are represented here by multiple non-zero entries in the same row. The difficulty of the decision is increased when more than one entry with high values close to each other. This problem is reduced when using big clusters sizes.
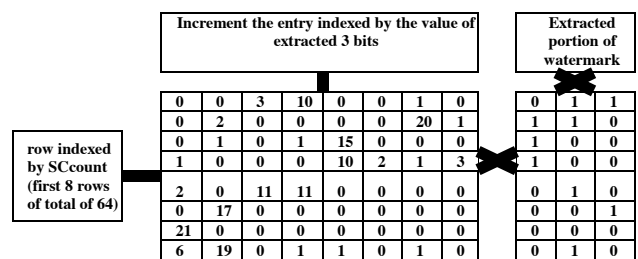

Increment the entry indexed by the value of extracted 3 bits								Extracted portion of watermark		
0	0	3	10	0	0	1	0	0	1	1
0	2	0	0	0	0	20	1	1	1	0
0	1	0	1	15	0	0	0	1	0	0
1	0	0	0	10	2	1	3	1	0	0
2	0	11	11	0	0	0	0	0	1	0
0	17	0	0	0	0	0	0	0	0	1
21	0	0	0	0	0	0	0	0	0	0
6	19	0	1	1	0	1	0	0	1	0

row indexed by SCcount (first 8 rows of total of 64)

Fig. 6: Building Decision Table for watermark extraction

4.5 Content based counter

Content Based Counter (CBC) is used to reduce the impact of using a portion sequence counter in a cluster. The algorithm has two phases as shown in Fig. 7:

```
Phase 1: CBC segmentation
for each cluster:
  for each pixel:
    pc=extractCounter();
    addPixel(portion[pc]);
  endfor
endfor
Phase 2: Uniform distribution
numberOfPortions=min(counterSize, clusterSize/minPortionSize)
portionAvgSize= clusterSize/numberOfPortions
for 1 until numberOfPortions
  dist=1 // 1 bit difference between entries
  while sizeCurrentPortion < portionAvgSize
    for each Entry e having distance dist with currentEntry
      if size(e)> portionAvgSize
        pixNbr=min(portionAvgSize- sizeCurrentPortion,
              size(e)- portionAvgSize);
        move pixNbr from e to CurrentPortion
      endif
    endfor
    dist = dist+1
  endwhile
endfor
```

Fig. 7: Content Based Counter Algorithm

The first phase is a cluster segmentation in portion based on the value in the counter space. This technique is used mainly to not modify the counter location as much as possible and then get better PSNR. Whereas, the second phase consists of redistribute uniformly the pixels within the portions and build consecutive portions sequence. To minimize the modifications, the latter is done using the minimum possible distance between source and destination. The distance is calculated as:

$$\text{distance}(C_s, C_d) = \sum_{bit0}^{Csize} xor(C_s, C_d) \quad (1)$$

Where C_s and C_d are source and destination counters respectively and C_{size} is the counter size in bits. The complexity of this algorithm is at most *O(MxN)* where *MxN* is the size of the image because it is bounded by visiting all pixels.

5 Experimental Results and Analysis

We used 512×512×3 color images as a host carrier signal, and 64×64 binary image as the watermark signal, as shown in Fig. 8 and Fig. 9. The correlation coefficient (NC) in Equation (2) is used for measuring the quantitative similarity between the extracted and embedded watermarking:

$$NC = \frac{\sum_x \sum_y i(x,y) w(x,y)}{\sum_x \sum_y i^2(x,y)} \quad (2)$$

Where *i* denotes the embedded original watermark and *w* denotes the extracted watermark.

The difference between watermarked image and original host image is evaluated using the Peak

Signal to Noise Ratio (*PSNR*). The *PSNR* formula is giving in the Equation (3):

$$PSNR = 10\log(\frac{\max(i^2(x,y))}{\frac{1}{MxN}\sum_{y=1}^{M}\sum_{x=1}^{N}(i(x,y)-w(x,y))^2}) \quad (3)$$
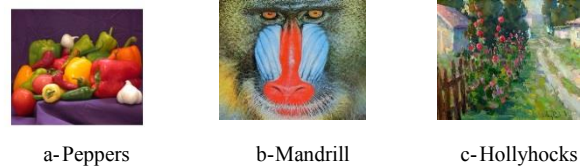

a- Peppers   b-Mandrill   c-Hollyhocks

**Fig. 8: Host carrier signal images**

Copyright image

Fig. 9: Watermark signal image

The proposed solution does not affect the normal visualization of the cover image as it is proved by the PSNR presented in Table 2. On the other hand, taking into account the CBC always improves the PSNR.

Table 2: PSNR of cover image

	Peppers	Mandrill	Hollyhocks
Complex Wavelet Transform Domain	45.11	44.83	NA
Our solution without CBC	41.56	44.68	44.00
Our solution with CBC	42.90	45.95	46.18

Fig. 10 gives the result of using CBC technique in different clusters for the different images. Phase 1 in the left column of the figure presents the cluster segmentation based on counter field content and the right column shows the result of the uniform redistribution with minimum cost of pixels.
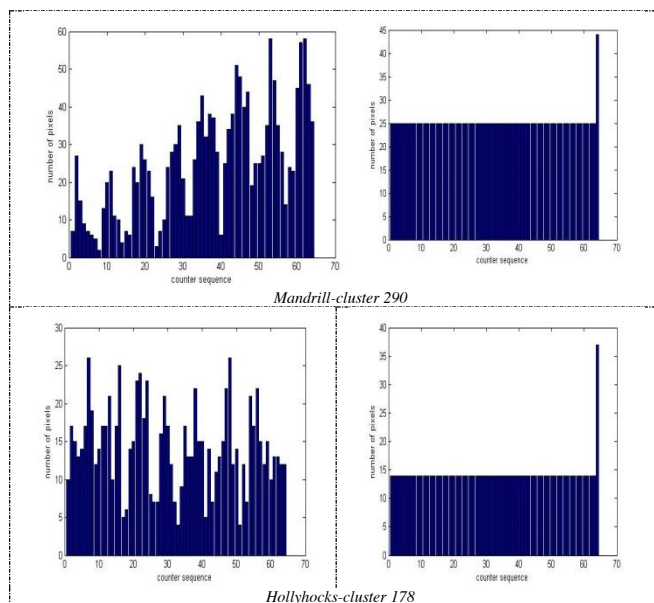
Mandrill-cluster 290

Hollyhocks-cluster 178
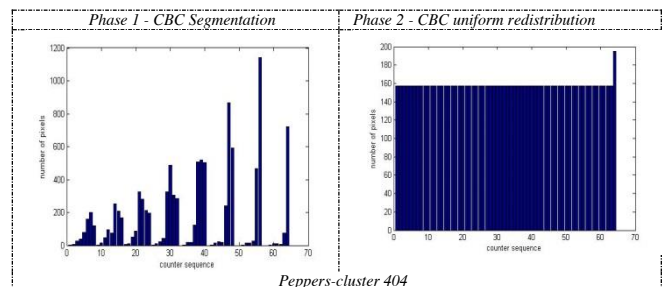
Fig. 10: Content Base Counter Algorithm

Table 3: NBCR of the watermark image(%)

	without CBC	*with CBC*
peppers	3.861	1.492
mandrill	1.962	0.666
Hollyhocks	2.315	0.519

The Number of Bit Change Rate (*NBCR*) given by table 3 confirms the results of *PSNR* improvement given in table 2 by introducing the content based counter. The formula of *NBCR* is given by the Equation 4 where, using a *MxN* image, *Csize* is the counter size and $C_b^{i,j}$ and $C_a^{i,j}$ is the counter value in the pixel *(i,j)* before and after modification respectively.

$$NBCR = \frac{(\sum_{i=1}^{M}\sum_{j=1}^{N}\sum_{bit0}^{Csize} xor(C_b^{i,j},C_a^{i,j}))x100\%}{MxNxCsize} \quad (4)$$

We compared our results with the results provided in [11] under the same environment. Table 4 shows that our system, under rotation attacks for 5° and 15°, the watermark is completely extracted without any distortion (*NC*=1). Fig. 11 shows that under any rotation attack the NC is always equal 1 which proves the robustness of the proposed system against rotation attacks.

Table 4: NC of the watermark image

		Rotation 5°	Rotation 15°
Spatial domain	peppers	0.927	0.885
	mandrill	0.918	0.869
Wavelet domain	peppers	0.945	0.913
	mandrill	0.937	0.896
Complex Wavelet Transform Domain [11]	peppers	0.981	0.946
	mandrill	0.966	0.930
Our solution	peppers	1.000	1.000
	mandrill	1.000	1.000
	Hollyhocks	1.000	1.000

Fig. 12 shows that the new portion allocation technique gives us better results against cropping attacks which was not possible using the First Visited First Allocated *(FVFA)* technique. This is due to the fact that some portions (sub-clusters) completely located on the boundary of the image which, if they are touched by the cropping attack, may impact the embedded watermark. Future work will be concentrated to the way of better distribute the allocation of the sub-clusters.

Looking at the watermarking properties mentioned earlier, our proposed system met them at a certain level as follows:

1) Robustness: we can consider our system more robust against rotation attacks than frequency domain watermarking.

2) Perceptibility: the PSNR of the watermarked image is always above 40 and with the improvement introduced by using CBC technique it reached better than other systems that used the frequency domain.

3) Capacity: as most of the research papers we checked used 64x64 bits watermark size, all our measurements used the same size. On the other hand, by reducing the size of the hidden information per sub-cluster and filling all clusters in the cover image we can reach a size of 256x256.

4) Complexity: the main goal of using spatial domain is to look for better results in terms of robustness remaining in a low complexity level.

6 Conclusion

In this paper we proposed a new watermark system for color images which uses the Content Addressable Method. The cover image is divided into a set of clusters which are built using Content Addressable Method. Each cluster is segmented in its turn into a number of portions. In all pixels of a portion a number of bits (3 bits in our study) of the watermark are duplicated. The robustness of our system comes from the fact that it resists to image rotation attacks. The results show that a rotation of any degree does not have any effect on the embedded watermark which can be extracted without any distortion. Two pixel-to-portion allocation techniques were used. In the first technique, the cluster's pixels are allocated to a portion in a First Visited First Allocated *(FVFA)* way. The counter providing the portion number is added to portions in sequence. In the second technique, a Content Based Counter CBC is used to allocate pixels to the portion and a uniform redistribution is made for each cluster. The redistribution is done in a way to minimize the modifications in counter space. Both techniques show high robustness resisting to rotation attacks. The CBC performs better in terms of Number of Bit Change Rate *(NBCR)* in the counter field. Future work will be concentrated on pushing more experiments on other geometric attacks like cropping as well as JPEG compression and LSBs attacks.

References:
[1] L. Xin, L. Xiaoqi , W. Ying, A Semi-Fragile Digital Watermarking Algorithm Based on Integer Wavelet Matrix Norm Quantization for Medical Images, *The 2nd International Conference on Bioinformatics and Biomedical Engineering, 2008. ICBBE 2008.* DOI: 10.1109/ICBBE.2008.189, Publication Year: 2008 , pp. 776–779.

[2] L. Xin, L. Xiaoqi, L. Qiang, Protect Digital Medical Images Based on Matrix Norm Quantization of Digital Watermarking Algorithm, *4th International Conference on Bioinformatics and Biomedical Engineering (iCBBE), 2010,*

DOI: 10.1109/ICBBE.2010.5516746, Publication Year: 2010, pp. 1–4.

[3] M.H. Lee, M.F. Horng , B.C. Chang, A DC-based Approach to Robust Watermarking with Hamming-Code, *Third International Conference on Intelligent Information Hiding and Multimedia Signal Processing, 2007.* IIHMSP 2007, Vol.2, DOI: 10.1109/IIH-MSP.2007.10, Publication Year: 2007, pp. 369 – 372.

[4] S. Laha, J. Chowdhury, A. Khan, S.K. Sarkar, A watermarking scheme based on Singular Value Decomposition and Particle Swarm Optimization, *IEEE 3rd International Advance Computing Conference (IACC), 2013,* DOI: 10.1109/IAdCC.2013.6514344, Publication Year: 2013 , pp. 888–892.

[5] R. Ansari, M.M. Devanalamath, K. Manikantan, S. Ramachandran, Robust Digital image Watermarking Algorithm in DWT-DFT-SVD domain for color images, *International Conference on Communication, Information & Computing Technology (ICCICT), 2012* DOI: 10.1109/ICCICT.2012.6398160, Year: 2012 , pp. 1-6.

[6] H. Zhang, J. Li, C. Dong, Multiple video Zero-Watermarking based on 3D DFT to resist geometric attacks, *2nd International Conference on Consumer Electronics, Communications and Networks (CECNet),* DOI: 10.1109/CECNet.2012.6201983, Year: 2012, pp. 1141–1144.

[7] V.K. Veena, G.J. Lal, S.V. Prabhu, S.S. Kumar, K.P. Soman, A robust watermarking method based on Compressed Sensing and Arnold scrambling, *International Conference on Machine Vision and Image Processing (MVIP), 2012,* DOI: 10.1109/MVIP.2012.6428771, Year: 2012 , pp. 105-108.

[8] A. Mairgiotis, L. Kondi, Y. Yang, Locally optimum detection for additive watermarking in the DCT and DWT domains through non-Gaussian distributions, *18th International Conference on Digital Signal Processing (DSP), 2013,* DOI: 10.1109/ICDSP.2013.6622794, Publication Year: 2013, pp. 1–6.

[9] L. An, X. Gao, X. Li, D. Tao, C. Deng, J. Li, Robust Reversible Watermarking via Clustering and Enhanced Pixel-Wise Masking, *IEEE Transactions on Image Processing*, Vol.21 , Issue: 8, DOI: 10.1109/TIP.2012.2191564, Publication Year: 2012, pp. 3598-3611.

[10] Y. Haowen , Watermarking Algorithm for Vector Point Clusters, *7th International Conference on Wireless Communications, Networking and Mobile Computing (WiCOM), 2011*, DOI: 10.1109/wicom.2011.6040148, Publication Year: 2011, pp. 1–4.

[11] J. Fan, Y. Wu, Watermarking Algorithm Based on Kernel Fuzzy Clustering and Singular Value Decomposition in the Complex Wavelet Transform Domain, *International Conference on Information Technology, Computer Engineering and Management Sciences (ICM), 2011*, Vol.3, DOI: 10.1109/ICM.2011.121, Publication Year: 2011, pp. 42–46.

[12] D.H. Le, T.B.T. Cao, K. Inoue, C.K. Pham, A fast CAM-based Watermarking extraction on FPGA, *International Conference on IC Design & Technology (ICICDT), Italy, 2013* DOI: 10.1109/ICICDT.2013.6563338, Year: 2013, pp. 207-210.

[13] M.T. Ben Othman, New Image Watermarking Scheme based on Image Content Addressing Method, accepted in *13th WSEAS International Conference on Applied Computer and Applied Computational Science ACACOS'14*, Kuala Lumpur, Malaysia, April 23-25, 2014.

[14] J.A. Hussein, Spatial Domain Watermarking Scheme for Colored Images Based on Log-average Luminance, *Journal of Computing*, vol. 2, No. 1, 2010, pp. 100-103.

[15] J. Manoharan, C.Vijila and A.Sathesh, Performance Analysis of Spatial and Frequency Domain Multiple Data Embedding Techniques towards Geometric Attacks, *International Journal of Security (IJS)*, Vol. 4, No. 3, 2010, pp. 28-37.

[16] D. Asatryan and N. Asatryan, Combined spatial and frequency domain watermarking, *in Proceedings of the 7th International Conference on Computer Science and Information Technologies*, pp. 323-326, 2009.

[17] Doroshin, A. V., Neri, F. (2014) Open research issues on Nonlinear Dynamics, Dynamical Systems and Processes. WSEAS Transactions on Systems, 13, in press.
[18] Ciufudean, C., Neri, F. (2014) Open research issues on Multi-Models for Complex Technological Systems. WSEAS Transactions on Systems, 13, in press.
[19] Neri, F. (2014) Open research issues on Computational Techniques for Financial Applications. WSEAS Transactions on Systems, 13, in press.
[20] Karthikeyan, P., Neri, F. (2014) Open research issues on Deregulated Electricity Market: Investigation and Solution Methodologies. WSEAS Transactions on Systems, 13, in press.
[21] Panoiu, M., Neri, F. (2014) Open research issues on Modeling, Simulation and Optimization in Electrical Systems. WSEAS Transactions on Systems, 13, in press.
[22] Neri, F. (2014) Open research issues on Advanced Control Methods: Theory and Application. WSEAS Transactions on Systems, 13, in press.
[23] Hájek, P., Neri, F. (2013) An introduction to the special issue on computational techniques for trading systems, time series forecasting, stock market modeling, financial assets modeling WSEAS Transactions on Business and Economics, 10 (4), pp. 201-292.
[24] Azzouzi, M., Neri, F. (2013) An introduction to the special issue on advanced control of energy systems (2013) WSEAS Transactions on Power Systems, 8 (3), p. 103.
[25] Bojkovic, Z., Neri, F.(2013) An introduction to the special issue on advances on interactive multimedia systems WSEAS Transactions on Systems, 12 (7), pp. 337-338.
[26] Pekař, L., Neri, F. (2013) An introduction to the special issue on advanced control methods: Theory and application (2013) WSEAS Transactions on Systems, 12 (6), pp. 301-303.
[27] Guarnaccia, C., Neri, F. (2013) An introduction to the special issue on recent methods on physical polluting agents and environment modeling and

simulation WSEAS Transactions on Systems, 12 (2), pp. 53-54.

[28] Neri, F. (2012) An introduction to the special issue on computational techniques for trading systems, time series forecasting, stock market modeling, and financial assets modeling WSEAS Transactions on Systems, 11 (12), pp. 659-660.

[29] Muntean, M., Neri, F. (2012) Foreword to the special issue on collaborative systems WSEAS Transactions on Systems, 11 (11), p. 617.

[30] Pekař, L., Neri, F. (2012) An introduction to the special issue on time delay systems: Modelling, identification, stability, control and applications WSEAS Transactions on Systems, 11 (10), pp. 539-540.

[31] Volos, C., Neri, F. (2012) An introduction to the special issue: Recent advances in defense systems: Applications, methodology, technology WSEAS Transactions on Systems, 11 (9), pp. 477-478.
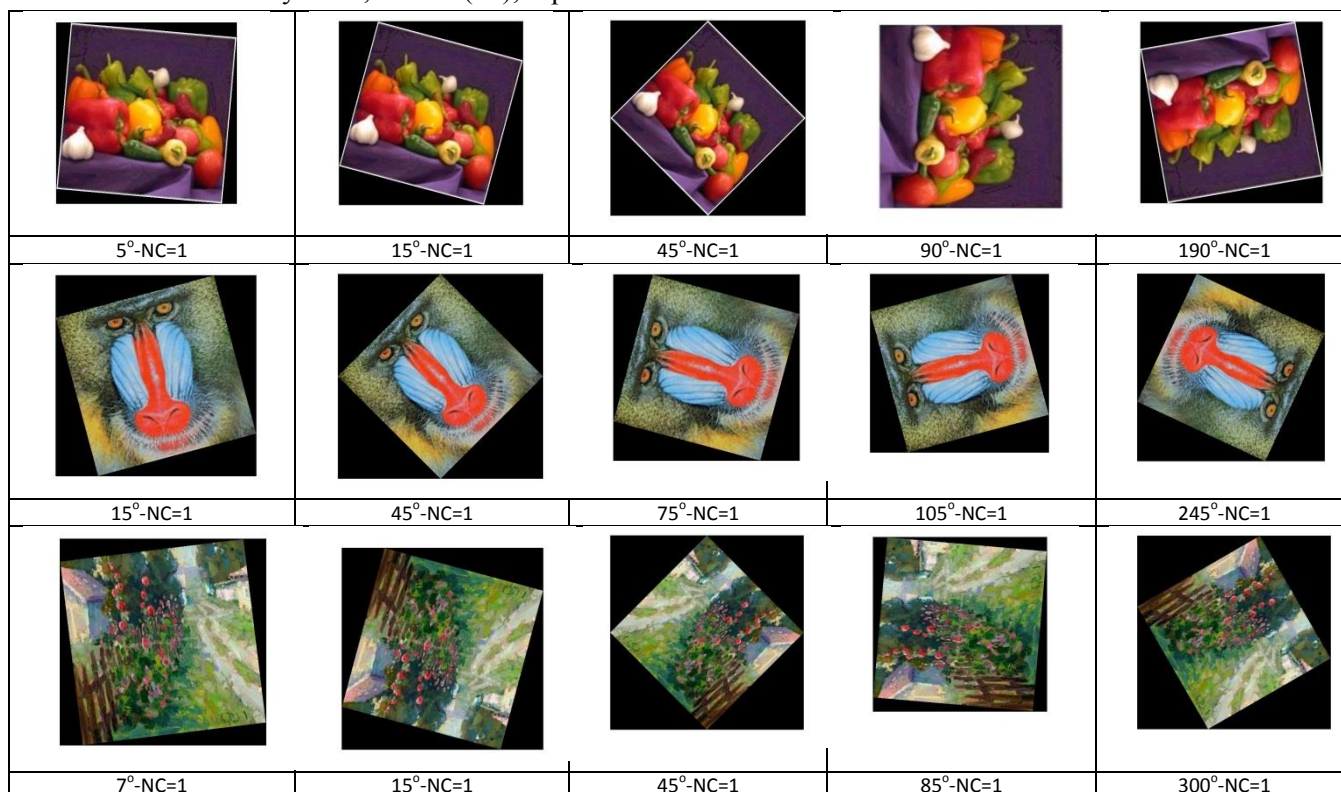
5°-NC=1	15°-NC=1	45°-NC=1	90°-NC=1	190°-NC=1
15°-NC=1	45°-NC=1	75°-NC=1	105°-NC=1	245°-NC=1
7°-NC=1	15°-NC=1	45°-NC=1	85°-NC=1	300°-NC=1

Fig. 11: Different rotation attacks with NC=1

Cropping Peppers to [1,75,440,400]

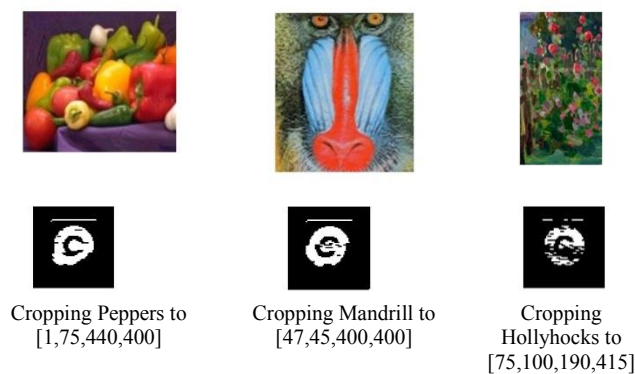Cropping Mandrill to [47,45,400,400]

Cropping Hollyhocks to [75,100,190,415]

Fig. 12: Extracted watermark after cropping attacks